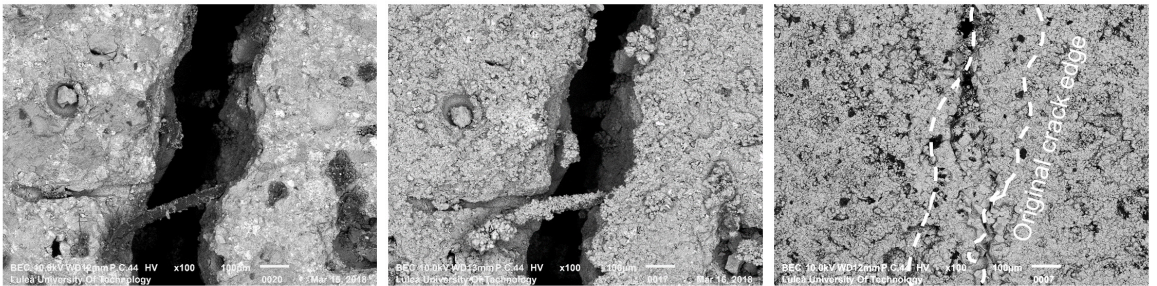


Self-Healing Concrete



Magdalena Rajczakowska

Building Materials



Self-Healing Concrete

Magdalena Rajczakowska

Luleå, December 2019

Building Materials
Department of Civil, Environmental and Natural Resources Engineering
Luleå University of Technology
SE-97187 Luleå, Sweden

The cover photo shows a compilation of scanning electron microscope images of the self-healing of an ultra-high-performance concrete crack. From the left: the crack before healing, the same crack after 1 day of healing, the same crack after 21 days of healing.

Printed by Luleå University of Technology, Graphic Production 2019

ISSN 1402-1757

ISBN 978-91-7790-490-8 (print)

ISBN 978-91-7790-491-5 (pdf)

Luleå 2019

www.ltu.se

Academic thesis

For the Degree of Licentiate (Tech. Lic) in building materials, which by due of the Technical Faculty Board at Luleå University of Technology will be publicly defended on:

Thursday, December 12th, 2019, 08:00 am
Room C305, Luleå University of Technology

Discussion leader:	Prof. Erik SCHLANGEN, Delft University of Technology
Principal supervisor:	Prof. Andrzej CWIRZEN, Luleå University of Technology
Assistant supervisors:	Dr. Tech. Karin HABERMEHL-CWIRZEN, Luleå University of Technology Adj. Prof. Hans HEDLUND, Luleå University of Technology

ACKNOWLEDGEMENTS

This Licentiate thesis summarizes the findings of the first 2.5 years of the PhD project on Self-healing Concrete at Luleå University of Technology. The work was conducted in the Building Materials research group. I would like to acknowledge the Swedish Transport Administration (Trafikverket), Development Fund of the Swedish Construction Industry (SBUF) and Skanska, for providing the financial support for my research.

Even though this thesis is only a small milestone towards the doctorate, it would not have been accomplished without many people who helped me along the way.

Above all, I would like to thank my supervisor, Prof. Andrzej Cwirzen. He is my true Mentor in the purest sense of this word. Thank you for your scientific guidance in this work, for countless checks of my publications, for always finding time for me, and for long conversations when I felt sad and frustrated.

I would like to express my deepest gratitude to my co-supervisors, Dr. Karin Habermehl-Cwirzen and Prof. Hans Hedlund. Thank you for your support and valuable comments. I would also like to acknowledge Prof. Mats Emborg as well as Katja Fridh and Magnus Åhs from Lund University. Thank you for all the productive discussions which helped me to start with the project.

I would like to thank my colleagues, especially Ilda, Ankit, Ploy, Faez, Abeer and Vasiola for enormous support during the last, very exciting, but complicated year. To Katalin and Carina, thank you for introducing me to LTU when I felt really scared of what is ahead of me. I am also grateful to my friends in Poland: Mima and Justyna, for mental support, and Damian – for showing me this opportunity.

To my parents, I don't think I can ever repay you. *Mamo, Tato, dziękuję Wam za nieustanną wiarę we mnie, za cierpliwe słuchanie w momentach zwątpienia oraz ciągle motywowanie do stawiania sobie nowych wyzwań.*

Special thanks to my daughter Julia, who closely cooperated with me on conducting most of the testing included in this thesis (without being fully aware of it) and, afterwards, was kind enough to sleep through the nights, giving me space to write. I hope your first word will be: “concrete”.

Last but not least, I would like to thank my husband, Andrés. Without his huge support, sometimes even against my will, I would probably not even be in Luleå. This thesis was written only thanks to his selfless commitment and unconditional love. I hope you have some deposits of patience still hidden in you because we are now on our journey to PhD.

Magdalena Rajczakowska

Luleå, December 2019

SUMMARY

Concrete is a brittle material prone to cracking due to its low tensile strength. Crack repairs are not only expensive and time-consuming but also increase the carbon footprint. Designing a novel concrete material possessing the ability to self-repair cracks would enhance its sustainability. Self-healing can be defined as a material's ability to repair inner damage without any external intervention. In the case of concrete, the process can be autogenous, based on an optimized mix composition, or autonomous, when additional capsules containing some healing agent and/or bacteria spores are incorporated into the binder matrix. The first process uses unhydrated cement particles as the healing material while the other utilizes a synthetic material or bacteria precipitating calcite which are released into the crack from a broken capsule or activated by access to water and oxygen. The main disadvantages of the autonomous method are the loss of the fresh concrete workability, worsened mechanical properties, low efficiency, low survivability of the capsules and bacteria during mixing and the very high price. On the other hand, the autogenous self-healing was found to be more efficient, more cost effective, safer, and easier to implement in full-scale applications. Knowledge related to mechanisms and key factors controlling the autogenous self-healing is rather limited. Therefore, the aim of this research work was to better understand the autogenous self-healing process of concrete and to optimize the mix design and exposure conditions to maximize its efficiency.

This licentiate thesis summarizes the main findings of the first 2.5 years of the PhD project. Several factors affecting autogenous self-healing were studied, including the amount of unhydrated cement, mix composition, age of material, self-healing duration and exposure conditions. The process was investigated both externally, at the surface, and deeper inside of the crack, by evaluating the crack closure and chemical composition of formed self-healing products. In addition, the flexural strength recovery was also studied. It was observed that a large amount of cement in the concrete mix does not ensure an efficient autogenous self-healing of cracks. A very dense and impermeable binder microstructure limited the transport of calcium and silicone ions to the crack and diminished the precipitation of the healing products. Addition fly ash increased the crack closure ratio close to the crack mouth, but its presence did not support the recovery of the flexural strength, presumably due to a very limited formation of load bearing phases inside the crack. Calcium carbonate was detected mainly at the crack mouth, whereas calcium silicate hydrate (C-S-H) and ettringite were found deeper inside the crack. The formation of C-S-H and ettringite presumably resulted in a regain of the flexural strength. On the other hand, calcite crystals formed close to the surface of the specimen controlled conditions inside the crack through its external closure. Healing exposure based on pure water appeared to be inefficient even despite the application of different temperature cycles and water volumes. The application of a phosphate-based retarding admixture in the curing water resulted in the highest self-healing efficiency. The admixture presumably inhibited the formation of a dense hydration shell on the surface of the unhydrated cement grains and promoted the precipitation of calcium phosphate compounds inside the crack. In addition, water mixed with microsilica particles caused a regain of the flexural strength through formation of C-S-H in the crack.

Keywords: cementitious materials, self-healing, exposure, fly ash, calcite, C-S-H, cracking

STRESZCZENIE

Beton jest kruchym materiałem, podatnym na powstawanie rys z powodu niskiej wytrzymałości na rozciąganie. Naprawy konstrukcji betonowych są drogie oraz prowadzą do zwiększenia emisji dwutlenku węgla. Trwałość betonu mogłaby ulec poprawie gdyby posiadał on zdolność do samoleczenia rys. Samoleczenie to potencjał materiału do naprawy uszkodzeń wewnętrznych bez jakiegokolwiek interwencji z zewnątrz. W przypadku betonu, proces ten może być autogeniczny, dzięki zoptymalizowanemu składowi mieszanki betonowej, lub autonomiczny, gdy wprowadza się do matrycy cementowej dodatkowe substancje w formie kapsułek i/lub zarodniki bakterii. Samoleczenie autogeniczne wykorzystuje nieshydrytowane ziarna cementu, podczas gdy samoleczenie autonomiczne, materiał syntetyczny, np. w formie żywicy, lub produkujące kalcyt bakterie, uwalniane do rysy z pękniętej kapsułki lub aktywowane przez dostęp do wody i tlenu. Głównymi wadami metody autonomicznej są utrata urabialności betonu, pogorszenie właściwości mechanicznych materiału, niska wydajność, ograniczona trwałość kapsułek i bakterii podczas mieszania oraz bardzo wysoka cena. Z drugiej strony stwierdzono, że samoleczenie autogeniczne jest bardziej wydajne, opłacalne, bezpieczniejsze i łatwiejsze do wdrożenia na skalę przemysłową. Wiedza dotycząca mechanizmu autogenicznego samoleczenia oraz kluczowych czynników kontrolujących ten proces jest niestety ograniczona. W związku z tym, celem poniższych badań było lepsze zrozumienie procesu autogenicznego samoleczenia się betonu oraz optymalizacja składu mieszanki betonowej i warunków ekspozycji aby zwiększyć jego efektywność.

Niniejsza praca licencjacka podsumowuje 2,5-letnie badania wykonane w ramach pierwszej części doktoratu na temat „Samoleżącego się Betonu” na Luleå University of Technology w Szwecji. Przebadano wpływ głównych czynników, tj. ilość nieshydrytowanego cementu, skład mieszanki, wiek materiału, czas samoleczenia oraz warunki ekspozycji, na efektywność autogenicznego samoleczenia betonu. Proces ten został zbadany na zewnątrz rysy, jak i w jej wnętrzu, poddając ocenie stopień wypełnienia rysy, skład chemiczny wypełnienia oraz poziom regeneracji wytrzymałości na zginanie. Zaobserwowano, że duża ilość cementu w mieszance betonowej nie gwarantuje skutecznego autogenicznego samoleczenia rys. Bardzo gęsta, nieprzepuszczalna mikrostruktura spoiwa cementowego, najprawdopodobniej ogranicza transport jonów wapnia i krzemu do rysy oraz zmniejsza wytrącanie się produktów leczniczych. Dodatek popiołu lotnego przyczynił się do zwiększenia stopnia wypełnienia rysy na zewnątrz próbki, lecz jego obecność nie sprzyjała regeneracji wytrzymałości na zginanie, prawdopodobnie z powodu braku wypełnienia wewnątrz rysy. Węglan wapnia wykryto głównie na powierzchni, natomiast w głębszych partiach rysy – uwodniony krzemian wapnia (C-S-H) i ettringit, które prawdopodobnie miały wpływ na regenerację wytrzymałości na zginanie. Kalcyt powstały na powierzchni, poprzez zaklejenie rysy, jest prawdopodobnie odpowiedzialny za kontrolę warunków środowiskowych w jej wnętrzu. Zarysowane próbki betonowe przechowywane w wodzie, nie wykazały efektywnego samoleczenia, pomimo zastosowania zmiennych cykli temperatur oraz różnych objętości wody. Zastosowanie domieszki opóźniającej na bazie fosforanów skutkowało najwyższą skutecznością samoleczenia. Domieszka ta prawdopodobnie hamuje tworzenie się gęstej skorupy hydratacyjnej na powierzchni nieshydrytowanych ziaren cementu i sprzyja wytrącaniu się związków fosforanu wapnia wewnątrz rysy. Umieszczenie pękniętych próbek w mieszaninie wody i cząsteczek mikrokrzemionki doprowadziło do regeneracji wytrzymałości na zginanie dzięki tworzeniu się C-S-H wewnątrz rysy.

Słowa kluczowe: materiały na bazie cementu, samoleczenie, ekspozycja, popiół lotny, kalcyt, C-S-H, zarysowanie

SAMMANFATTNING

Betong är ett sprött material som är benäget att spricka på grund av dess låga draghållfasthet och reparationer är inte bara dyra utan ökar också koldioxidavtrycket. Att designa ett nytt betongmaterial med förmågan att självreparera sprickor skulle förbättra dess hållbarhet. Självläkande kan definieras som ett materials förmåga att reparera inre skador utan något externt ingripande. I fallet med betong kan processen vara autogen, baserad på en optimerad blandningskomposition, eller autonom, när ytterligare kapslar innehållande något läkande medel och / eller bakteriesporer införlivas i bindemedelsmatrisen. Den första processen använder icke-hydratiserade cementpartiklar som det läkande materialet medan den andra använder ett syntetiskt material eller bakterier som utfäller kalcit som frigörs i sprickan från en trasig kapsel eller aktiveras genom tillgång till vatten och syre. De huvudsakliga nackdelarna med den autonoma metoden är förlust av färsk betongbearbetbarhet, försämrade mekaniska egenskaper, låg effektivitet, låg överlevnad av kapslarna och bakterierna under blandning samt ett mycket högt pris. Å andra sidan befanns den autogena självläkningen vara mer effektiv, mer kostnadseffektiv, säkrare och lättare att implementera i fullskaliga applikationer. Kunskapen relaterad till mekanismer och nyckelfaktorer som styr det autogena självläkandet är ganska begränsad. Därför var syftet med detta forskningsarbete att bättre förstå den autogena självläkande processen för betong och att optimera blandningsdesign och exponeringsförhållanden för att maximera dess effektivitet.

Denna licentiatuppsats sammanfattar de viktigaste resultaten från de första 2,5 åren av doktorandprojektet. Flera faktorer som påverkade autogen självläkning studerades, inklusive mängden ohydratiserad cement, blandningskomposition, materialålder, självläkande varaktighet och exponeringsförhållanden. Den självläkande processen undersöktes både externt, vid ytan, och djupare i sprickan genom utvärdering av sprickförslutningen och den kemiska sammansättningen av uppkomna självläkande produkter. Dessutom studerades återhämtningen av böjhållfastheten. Det observerades att den stora mängden cement i betongblandningen inte säkerställer effektiv autogen självläkning av sprickor. En mycket tät, ogenomtränglig bindemedelsmikrostruktur begränsade transporten av kalcium- och silikonjoner till sprickan och minskade utfällningen av läkande produkter. Flygaska ökade det yttre sprickförslutningsförhållandet nära spricköppningen, men stödde inte återhämtningen av böjhållfastheten, förmodligen på grund av en mycket begränsad bildning av lastbärande faser inuti sprickan. Kalciumkarbonat detekterades huvudsakligen vid spricköppningen, medan kalciumsilikathydrat (C-S-H) och ettringit, återfanns djupare inuti sprickan. Uppkomsten av C-S-H och ettringit resulterade förmodligen i återfunnen böjhållfasthet. Å andra sidan, kalcitkristaller formerade nära provytan kontrollerade förhållandena inuti sprickan genom dess externa förslutning. Läkningsexponering baserad på rent vatten tycktes vara ineffektivt trots tillämpningen av olika temperaturcykler och vattenvolymer. Appliceringen av en fosfatbaserad retarderande blandning i hårdvattnet resulterade i den högsta självläkande effektiviteten. Blandningen inhiberade antagligen bildningen av ett kompakt hydratiseringsskal på ytan av de ohydratiserade cementkornen och främjade utfällning av kalciumfosfatföreningar inuti sprickan. Dessutom orsakade vatten blandat med mikrosilikapartiklar en återhämtning av böjhållfastheten genom bildning av C-S-H i sprickan.

Nyckelord: cementbaserade material, självläkande, exponering, flygaska, kalcit, C-S-H, sprickbildning

TABLE OF CONTENTS

ACKNOWLEDGEMENTS.....	V
SUMMARY	VII
STRESZCZENIE	IX
SAMMANFATTNING	XI
LIST OF FIGURES AND TABLES	XV
1. INTRODUCTION	3
1.1. BACKGROUND	3
1.2. AIM, OBJECTIVES AND RESEARCH QUESTIONS	4
1.3. SCIENTIFIC APPROACH	4
1.4. LIMITATIONS	5
1.5. STRUCTURE OF THE THESIS	5
1.6. LIST OF PAPERS AND CONTRIBUTIONS	6
2. SELF-HEALING CONCRETE – STATE-OF-THE-ART	11
2.1. AUTONOMOUS SELF-HEALING.....	13
2.2. AUTOGENOUS SELF-HEALING	19
2.3. EFFECT ON CONCRETE PROPERTIES	25
2.4. SUMMARY	29
3. EXPERIMENTAL SETUP	33
3.1. MATERIALS	33
3.2. CRACK GENERATION.....	36
3.3. ASSESMENT OF THE SELF-HEALING EFFICIENCY.....	36
4. RESULTS AND ANALYSIS.....	43
4.1. EFFECTS OF MIX COMPOSITION	43
4.2. EFFECT OF CRACKING AGE.....	44
4.3. EFFECT OF THE HEALING DURATION	47
4.4. EFFECT OF ENVIRONMENTAL EXPOSURE	48
5. DISCUSSION AND CONCLUSIONS	61
5.1. AUTOGENOUS SELF-HEALING MECHANISM – HYPOTHESIS	61
5.2. CONCLUSIONS.....	65
5.3. ADDRESSING RESEARCH QUESTIONS	66
6. FUTURE RESEARCH	71
7. REFERENCES	72
APPENDIX 1. PAPER I	
APPENDIX 2. PAPER II	
APPENDIX 3. PAPER III	

LIST OF FIGURES AND TABLES

Figures:

Figure 1.1. Self-healing of concrete by mimicking tissue healing; modified from (Tavangarian & Li, 2015).	3
Figure 2.1. Synthetic and biological route of self-healing, from (Blaiszik et al. 2010).	11
Figure 2.2. Approaches used for the self-healing of concrete: (a) autogenous self-healing, (b) bacteria based autonomous self-healing (left – metabolic conversion mechanism, right – enzymatic ureolysis), (c) capsule-based autonomous self-healing (Rajczakowska et al. 2019a, With permission from ASCE).	12
Figure 2.3. Changes in the number of publications related to autonomous and autogenous self-healing in the years 2003–2018 including only journals listed in the Web of Science (Rajczakowska et al. 2019a, With permission from ASCE).	12
Figure 2.4. The mechanism of crack healing (White et al., 2001).	15
Figure 2.5. Stress state in the vicinity of a planar crack as it approaches a spherical inclusion embedded in a linearly elastic matrix and subjected to a remote tensile loading perpendicular to the fracture plane. The left picture correspond to an inclusion three times stiffer than the matrix. The right image corresponds to an inclusion three times more compliant than the surrounding matrix (modified from White et al., 2001).	18
Figure 2.6. Simplified schematic representation of the fraction of the healing material available in cement paste: (a) microcapsules (2% of cement content), (b) unhydrated cement particles after 7 days of hydration (approx. 50% of cement content), (c) unhydrated cement particles after 28 days of hydration (approx. 30% of cement content).	20
Figure 2.7. Characteristic parts of chemical components of fibers (Nishiwaki, 2014).	25
Figure 2.8. Self-healing efficiency in relation to the mechanical properties of concrete for: (a) autonomous self-healing methods, (b) autogenous self-healing methods.	27
Figure 2.9. Price of different self-healing methods in comparison to the manual crack injection according to (Snoeck, 2015). Figure from (Rajczakowska et al. 2019a, With permission from ASCE).	28
Figure 3.1. Experimental setup in the context of all planned experiments.	33
Figure 3.2. (a) Grading curves of the UHPC mix and aggregates: (b) Grading curves of quartz, microsilica and cements applied in the study (Rajczakowska et al. 2019b).	35

Figure 3.3. Scheme of the tests performed to evaluate the self-healing efficiency.	36
Figure 3.4. (a) Scheme of a designed stand, (b) Optical microscope setup. (Rajczakowska et al. 2019c).	37
Figure 3.5. Parts of the crack studied in Experiment 1.	38
Figure 3.6. Scheme of the specimen preparation for SEM evaluation in Experiment 2 (Rajczakowska et al. 2019c).	39
Figure 4.1. (a) Flexural strength of cracked samples measured before healing (bH) and after healing (H), (b) flexural strength recovery ratio S for each type of mix. (Rajczakowska et al. 2019b).	43
Figure 4.2. Example of light microscope images of the crack before healing. Four images were taken for each sample: (a) A1, (b) B1, (c) U1; and after 21 days of storage in water: (d) A1, (e) B1, (f) U1. (Rajczakowska et al. 2019b).	43
Figure 4.3. Crack closure ratio for each mortar mix calculated according to formula 3.2. (Rajczakowska et al. 2019b).	44
Figure 4.4. SEM BE images (300x) of the crack at the surface for: (a) A1, (b) B1, (c) U1. (Rajczakowska et al. 2019b).	44
Figure 4.5. (a) The mean flexural strength measured before healing but after cracking (bH) and after healing of the initially cracked samples (h) (b) flexural strength recovery ratio S calculated according to the equation X for mixes U1 and U12. (Rajczakowska et al. 2019b).	45
Figure 4.6. (a) Light microscope image of the crack before healing for sample U12; (b) Light microscope images of the crack after 21 days of healing for sample U12; (c) crack closure ratio for samples U1 and U12; (d) SEM BSE image (300x) of the crack at the surface for the sample U12; (e) SEM BSE image (300x) of the self-healing products deposited on the PVA fiber in the specimen U12 (Rajczakowska et al. 2019b).	45
Figure 4.7. SEM SE images (1000x and ~300x) of the crack plane for U1 and U12. (Rajczakowska et al. 2019b).	48
Figure 4.8. Spatial distribution of the self-healing products inside the specimens after 21 days (BSE images, 1500x) (Rajczakowska et al. 2019b).	48
Figure 4.9. (a) Transmission time evolution for samples A1, B1, U1 and U12, (b) transmission time recovery ratio evolution for samples A1, B1, U1 and U12 (Rajczakowska et al. 2019b).	49
Figure 4.10. (a) pH changes vs time for Exposures 5-9; Crack closure ratio for Exposures 5-9: (b) Surface 1, (c) Surface 2(Rajczakowska et al. 2019c).	50
Figure 4.11. Example images of the Surface 1 observed with the optical microscope before (0 days) and after healing (28 days) and the SEM (BSE, 200x)	51

and cross-sections (SEM BSE, 200x) of the specimens healed for 28 days in Exposures 5-9 (water immersion, water evaporation, dry/wet cycles, water/1 mm, water/ 5 mm) (Rajczakowska et al. 2019c).

Figure 4.12. (a) Surface 1 Exposure 6 (SEM BSE 600x); (b) Surface 1 Exposure 7 (SEM BSE 600x); (c) Cross-section 1 Exposure 6 (SEM BSE 600x); (d) Cross-section 1 Exposure 7 (SEM BSE 100x) (Rajczakowska et al. 2019c). 52

Figure 4.13. (a) Surface 1 Exposure 5 (SEM BE 600x), (b) Surface 1 Exposure 8 (SEM BSE 600x), (c) Surface 1 Exposure 9 (SEM BSE 600x), (d) Cross-section 1 Exposure 5 (SEM BSE 600x), (e) Cross-section 1 Exposure 8 (SEM BSE 600x), (f) Cross-section 1 Exposure 9 (SEM BSE 600x) (Rajczakowska et al. 2019c). 52

Figure 4.14. Representative images of surfaces and cross-sections of specimens healed at various temperature variation cycles (Exposure 10 and 11) (Rajczakowska et al. 2019c). 53

Figure 4.15. (a) pH changes in time for Exposures 5, 10, and 11; Crack closure ratio for different temperature exposures: (b) on Surface 1, (c) on Surface 2 (Rajczakowska et al. 2019c). 53

Figure 4.16. (a) Calcite on the surface of the crack healed in 40°C (EXP 10, SEM SE image 150x) , (b) Calcite inside the crack (Cross-section 1) healed in 40°C (EXP 10, SEM BSE image 800x), (c) Ettringite on the surface of the crack healed in 5°C (EXP 11, SEM SE image 200x), (d) Ettringite on the surface of the crack healed in 5°C (EXP 11, SEM SE image 200x) (Rajczakowska et al. 2019c). 54

Figure 4.17. Representative images of the surface and cross-sections of the specimens healed in Exposures 2 (retarder) and 1 (accelerator) (Rajczakowska et al. 2019c). 54

Figure 4.18. (a) pH changes in time for Exposures 5, 1, and 2; Crack closure ratio for Exposures 5, 1, and 2: (b) on Surface 1, (c) on Surface 2 (Rajczakowska et al. 2019c). 55

Figure 4.19. Different forms of calcite on the Surface 1 of EXP 1 specimen: (a) SEM BE 2500x, (b) SEM BE 200x, (c) EXP 1 Cross-section 1 – visible calcite layer (SEM BE 200x), (d) EXP 1 Cross-section 2 healing products (SEM BE 100x) (Rajczakowska et al. 2019c). 55

Figure 4.20. (a) Self-healing products at Cross-section 1 at the top of the crack – close to the crack opening (EXP 2, SEM BSE image 600x) , (b) Self-healing products at Cross-section 1 at the bottom of the crack (EXP 2, SEM BSE image 100x), (c) Self-healing products at Cross-section 2 at the top of the crack (EXP 2, SEM BSE image 600x), (d) Self-healing products at Cross-section 2 at the bottom of the crack (EXP 2, SEM BSE image 600x) (Rajczakowska et al. 2019c). 56

Figure 4.21. (a) Si/Ca atomic ratio of the self-healing products vs the crack length measured at Cross-sections 1 and 2 for the Exposure 2 (Retarder), (b) Ca/P atomic 56

ratio of self-healing products vs crack the length at measured at Cross-sections 1 and 2 for the Exposure 2 (Retarder) (Rajczakowska et al. 2019c).

Figure 4.22. Representative images of surfaces and cross-sections of specimens healed in Exposures 3 (lime water), 4 (Coca-Cola) and 12 (water and 1.25%w microsilica particles) (Rajczakowska et al. 2019c). 57

Figure 4.23. (a) pH changes in time for Exposures 5, 3, 3, 4 and 12; Crack closure ratio for Exposures 5, 3, 3, 4 and 12: (b) on Surface 1, (c) on Surface 2 (Rajczakowska et al. 2019c). 58

Figure 4.24. Si/Ca atomic ratios: (a) Exposure 4 (Coca-Cola); (b) Exposure 3 (Lime water), (c) Exposure 12 (microsilica) (Rajczakowska et al. 2019c). 58

Figure 4.25. Exposure 4, Self-healing products in the Cross-section 1 (a) at the bottom of the crack (SEM BSE image 400x) , (b) in the middle of the crack (SEM BSE image 600x); Self-healing products at Cross-section 2 (c) in the middle of the crack (SEM BSE image 600x), (d) at the top of the crack (SEM BSE image 100x) (Rajczakowska et al. 2019c). 59

Figure 4.26. (a) Self-healing products in the Cross-section 1 in the middle of the crack (EXP 12, SEM BSE image 400x) , (b) Self-healing products at Cross-section 2 at the bottom of the crack (EXP 12, SEM BSE image 400x), (c) Self-healing products at the Cross-section 1 in the middle of the crack (EXP 3, SEM BSE image 500x), (d) Self-healing products at the Cross-section 2 in the middle of the crack (EXP 3, SEM BSE image 1000x) (Rajczakowska et al. 2019c). 59

Figure 4.27. Crack closure of selected exposures: (a) Surface 1, (b) Surface 2 (Rajczakowska et al. 2019c). 60

Figure 4.28. Strength recovery for selected exposures (Rajczakowska et al. 2019c). 60

Figure 5.1. The proposed self-healing mechanism scheme (Rajczakowska et al. 2019b). 61

Figure 5.2. Possible self-healing mechanism for samples exposed to phosphate based retarder exposure conditions (Rajczakowska et al. 2019c). 64

Tables:

Table 2.1. The most common healing agents for self-healing concrete. 16

Table 2.2. Capsule shell materials. 18

Table 2.3. Supplementary Cementitious Materials and mineral additives used for autogenous self-healing (Rajczakowska et al. 2019a, With permission from ASCE). 21

Table 2.4. Previous studies addressing effects of exposure on the efficiency of the autogenous self-healing of Portland cement based materials. 23

Table 2.5. Types of fiber material for self-healing concrete.	24
Table 2.6. Environmental impact of ultra-high performance concrete (UHPC) in comparison to ordinary concrete presented in the form of CO ₂ emissions (Rajczakowska et al. 2019b).	28
Table 2.7. Summary of limitations of autonomous and autogeneous self-healing strategies (With permission from ASCE, Rajczakowska et al. 2019a).	29
Table 3.1. Mortar mix compositions.	34
Table 3.2. Chemical composition of the applied cements.	34
Table 3.3. Exposure conditions applied in this study with justification (Rajczakowska et al. 2019c).	35
Table 4.1. Results of the SEM-EDS analysis (Rajczakowska et al. 2019b).	47
Table 5.1. Summary of the results of the Experiment 2 (Rajczakowska et al. 2019c)	62

1

Introduction

It is most important in creative science not to give up. If you are an optimist you will be willing to "try" more than if you are a pessimist.

Stanislaw Ulam

1. INTRODUCTION

1.1. Background

Concrete is, next to steel, one of the most popular structural materials. Over the years, various modifications of concrete compositions have been proposed in order to improve its properties. Lately, the decrease of the environmental impact of concrete has been extensively studied. Lowering the carbon footprint of concrete can be done in two different ways, i.e. by the modification of the mix compositions such as replacing cement by so-called Supplementary Cementitious Materials (SCM) or by lowering maintenance and repair costs. The former can be done by developing concrete with waste materials, e.g. fly ash or blast furnace slag which are industrial by-products, whereas the latter can be achieved by designing a material with self-healing properties. Possibly, it is also a combination of the two ways, by adding SCMs and improve the design.

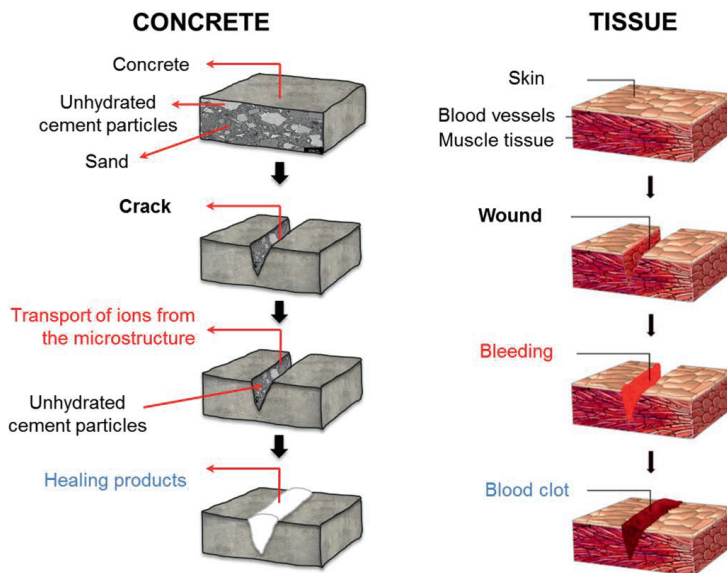


Figure 1.1. Self-healing of concrete by mimicking tissue healing; modified from (Tavangarian & Li, 2015).

The self-repair of tissue and bones in biological materials has always been an interesting concept. Mimicking natural phenomena and mechanisms gives often the possibility to develop new materials with smart behavior. The self-healing characteristic, i.e. the ability of material to sense and repair inner damage without human intervention, is one of the most desirable properties in material science. Recently, attention has been paid to the self-healing phenomena in cementitious materials. Concrete is a brittle material with low tensile strength. In order to increase the tensile strength of concrete additional reinforcement has to be implemented, usually made of steel. Concrete provides an alkaline environment, which protects the steel reinforcement from corrosion. Unfortunately, due to its brittleness, concrete is prone to cracking not only due to the external mechanical loading but also as a result of drying or autogenous shrinkage. The cracks create a passage for acidic ions to

reach the reinforcement leading to its corrosion and consequently to the deterioration of concrete. Consequently, the material's strength decreases, which is a serious issue.

Concrete composites have the natural ability to heal cracks (Figure 1) and to regain mechanical properties and limit the ingress of aggressive media. Many scientists aim to enhance and to control that ability. Succeeding in healing concrete cracks could lead to more sustainable construction and lowering of the maintenance costs. The potential of autogenous self-healing of concrete was already noticed over 100 years ago. Nowadays, various techniques are being investigated in order to accelerate it and to increase the potential benefits of this process.

1.2. Aim, objectives and research questions

This research focused on the autogenous self-healing of cementitious materials. Due to a lack of confirmed, indisputable, fully understood governing mechanism, the efficiency of the autogenous self-healing process still brings concerns and does not ensure successful full-scale applications. Therefore, the objectives of this study were as follows:

- to understand the mechanisms behind the autogenous self-healing of concrete,
- to use that knowledge to fully control it,
- to develop/design a cementitious material (or a set of materials) having specific chemical composition that under certain environmental conditions will be capable to self-repair, both internally and externally.

The research questions guiding this investigation were formulated as follows:

RQ1: What is the most reliable self-healing approach for concrete considering the efficiency, impact on fresh and hardened properties, cost, safety, and full-scale applications?

RQ2: How does the mix composition affect the efficiency of the self-healing process?

RQ3: How does the concrete age affect the efficiency of the self-healing?

RQ4: What is the effect of the environmental exposure on the self-healing efficiency, morphology and composition of the healing products, both inside and at the surface of the cracks?

RQ5: How and to what extent does the addition of Supplementary Cementitious Materials contribute to the self-healing process?

1.3. Scientific approach

The initial part of the study consisted of extensive literature studies. The aim was to compare the autogenous and autonomous self-healing approaches in terms of, e.g. their influence on the original properties of fresh and hardened concrete and functionality. In addition, the current knowledge related to the mechanisms and factors affecting each self-healing method was investigated. Based on the performed analysis, the knowledge gaps were identified and used to build the research program for this study.

Consequently, the focus of this study was on the autogenous self-healing of concrete, as it was found to be a more feasible self-healing approach with respect to both; the material properties and full-scale applications. The research program consisted of the experimental verification of the effects of various parameters on the efficiency of the self-healing process; related to both the mix composition of concrete as well as the self-healing exposure conditions. Both internal and external crack closure was investigated, with focus on the spatial distribution and chemical composition of the healing products formed inside the crack. In addition, the recovery of the mechanical properties was measured as an important parameter with respect to the possible future real-life applications. Based on the acquired results, a mechanism of autogenous self-healing for selected conditions was proposed. An initial half-scale laboratory investigation was also performed.

1.4. Limitations

The following limitations of the current study can be listed:

- The effect of crack parameters, such as thickness, tortuosity and length, was not explicitly studied. Their significant influence, particularly the crack width, on the efficiency of the self-healing is well-known, therefore in this study the crack opening was aimed to be kept similar for all specimens. For this purpose, the polyvinyl alcohol fibers were added to all the mixes so it is easier to control the crack width during the crack induction. However, it is certainly a simplified approach.
- The study was intended as a preliminary investigation of multiple factors affecting the self-healing in order to obtain an efficient self-healing performance. Therefore, the number of specimens representing specific mixes in each experiment is limited. The results of the analysis are aimed to be interpreted, at this stage, as qualitative, not quantitative.
- In order to fully confirm the chemical composition of the precipitated self-healing phases, the performed elemental analysis should be complemented by an evaluation of the mineralogical composition using for example X-ray powder diffraction (XRD). Larger specimens should be tested, thus increasing the amount of the analyzed phases.

1.5. Structure of the thesis

This licentiate thesis summarizes the outcomes of the 2.5 years of a PhD project at Luleå University of Technology concerning self-healing concrete. The thesis consists of six chapters which are briefly described below:

Chapter 1 describes in general the aim and scope of the research together with its limitations.

Chapter 2 is the state-of-the-art review on self-healing concrete.

Chapter 3 presents the materials and methods applied in the study.

Chapter 4 contains the main results acquired during the investigation.

Chapter 5 focuses on the discussion of the results and formulating conclusions.

Chapter 6 is summarizing the thesis and indicates future research (until the PhD).

1.6. List of papers and contributions

I. Autogenous Self-Healing: A Better Solution for Concrete.

State-of-the-art journal paper

Magdalena Rajczakowska, Karin Habermehl-Cwirzen, Hans Hedlund, Andrzej Cwirzen,

Journal of Materials in Civil Engineering, 2019, 31(9), 03119001.

[https://doi.org/10.1061/\(ASCE\)MT.1943-5533.0002764](https://doi.org/10.1061/(ASCE)MT.1943-5533.0002764)

Main findings:

In this paper, two concrete self-healing methods were compared, i.e. autogenous and autonomous self-healing based on capsules and bacteria. The critical review indicated that the autogenous is a more compatible approach with less negative impact on the original concrete properties. It was also found to be cheaper, safer and more feasible in terms of full-scale applications. However, a systematic study on the healing mechanism was missing. On the other hand, the autonomous method causes the loss of the workability of concrete and deteriorates the mechanical properties of the hardened material. In addition, a number of problems were indicated, such as the low survivability of the capsules and bacteria in harsh concrete environment, the high price and the lack of full-scale evaluation.

Contributions:

Andrzej Cwirzen proposed the concept of the paper. Magdalena Rajczakowska developed the methodology, performed the literature studies and their analysis, and wrote the original draft of the paper. Karin Habermehl-Cwirzen and Andrzej Cwirzen helped in writing, reviewing and editing of the paper. Hans Hedlund was responsible for the supervision and project administration.

II. Does a High Amount of Unhydrated Portland Cement Ensure an Effective Autogenous Self-Healing of Mortar?

Magdalena Rajczakowska, Lennart Nilsson, Karin Habermehl-Cwirzen, Hans Hedlund, Andrzej Cwirzen,

Materials, 2019, 12(20), 3298.

<https://doi.org/10.3390/ma12203298>

Main findings:

The main aim of this paper was to examine whether the commonly accepted hypothesis that a high amount of unhydrated cement promotes self-healing was correct. For this reason, ultra-high performance concrete and mortars with a low water-to-cement ratio and high cement content were studied. Additionally, cement mixed with fly ash was applied as well as aging effects were verified on 12-month-old UHPC samples. The analysis was conducted on the crack surfaces and inside of the cracks. The results strongly indicated that the formation of a dense microstructure and rapidly hydrating, freshly exposed anhydrous cement particles could significantly limit or even hinder the self-healing process. The availability of anhydrous cement appeared not to guarantee development of a highly

effective healing process. The fly ash was found to promote external crack closure but a strength recovery was observed only in OPC mortars.

Contributions:

Andrzej Cwirzen proposed the concept of the paper. Magdalena Rajczakowska developed the methodology. Lennart Nilsson and Magdalena Rajczakowska prepared the specimens and performed the testing. Magdalena Rajczakowska carried out the results analysis and wrote the original draft of the paper. Karin Habermehl-Cwirzen and Andrzej Cwirzen helped in writing, reviewing and editing of the paper. Hans Hedlund was responsible for the supervision and project administration.

III. The Effect of Exposure on the Autogenous Self-Healing of Ordinary Portland Cement Mortars

Magdalena Rajczakowska, Karin Habermehl-Cwirzen, Hans Hedlund, Andrzej Cwirzen,

Submitted to *Materials*, 2019

Main findings:

The aim of this paper was to investigate and understand effects of various potentially applicable curing solutions on the efficiency of the crack closure occurring both superficially and internally. Four groups of exposures were tested, including the exposure with different water immersion regimes, variable temperatures, application of chemical admixtures and usage of solutions containing micro-particles. The self-healing process was evaluated externally and internally at different depths with the use of optical and scanning electron microscopes (SEM). The results showed a very limited self-healing in all pure water-based exposures even despite the application of different cycles, temperatures or water volumes. The addition of a phosphate-based retarding admixture demonstrated the highest crack closure both internally and externally. The highest strength recovery and a very good crack closure ratio was achieved in water exposure containing micro-silica particles. Changes in the chemical composition of the self-healing material were observed with increasing distance from the surface of the specimen.

Contributions:

Magdalena Rajczakowska and Andrzej Cwirzen suggested the concept of the paper. Magdalena Rajczakowska developed the methodology, prepared the specimens, performed the testing, carried out the results analysis and wrote the original draft of the paper. Karin Habermehl-Cwirzen and Andrzej Cwirzen helped in writing, reviewing and editing of the paper. Hans Hedlund was responsible for the supervision and project administration.

2

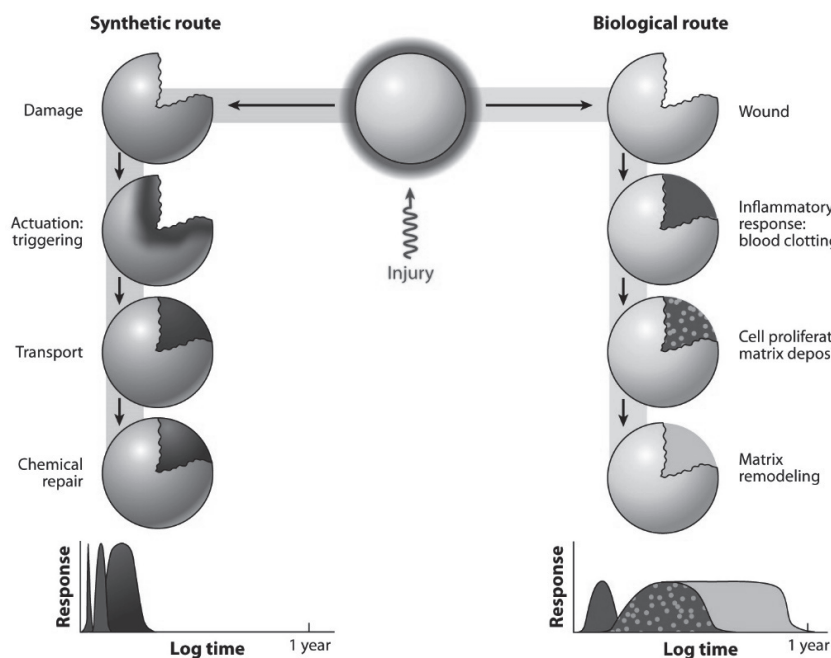
Self-healing concrete State-of-the-art

The first 90% of the job takes 90% of the time. The remaining 10% of the job requires another 90% of the time. The first condition of immortality is death.

Stanislaw Lem

2. SELF-HEALING CONCRETE – STATE-OF-THE-ART

Following nature has always been an inspiration for development of new materials. In particular, the self-repair of tissue and bones is considered as an extremely fascinating concept. Self-healing can be described as an ability of material to sense and repair inner damage without external intervention. Biological systems can serve as an example for man-made materials (Figure 2.1). In both cases, the initiation of the mechanism is the occurrence of the “injury”. The biological system initiates an inflammatory response, followed by the cell proliferation and, finally, matrix remodeling. It is a time consuming process. The synthetic response follows similar steps (triggering, transport, chemical repair), however, the rate of healing can be adjusted by a proper design of the material (Blaiszik et al. 2015).




 Blaiszik BJ, et al. 2010.
Annu. Rev. Mater. Res. 40:179–211

Figure 2.1. Synthetic and biological route of self-healing, from (Blaiszik et al. 2010).

This concept of materials with self-healing properties has been widely studied in polymer science (e.g. White et al., 2001; Thakur & Kessler, 2015; Zheng & McCarthy, 2012). Various autonomic self-healing strategies have been implemented including, e.g. the application of microcapsules.

Concrete is the most frequently applied structural material. The binder used for concrete production is primarily ordinary Portland cement (OPC). Over the recent years, the annual world cement production has reached around 1.7 billion tons (Yang et al 2015, Gartner, 2004). At the same time, it was estimated that the worldwide production of OPC contributes to emission of as much as 7% of the total global CO₂. Therefore, design of a more environmentally friendly material is urgently required.

In addition, concrete exhibits brittle behaviour and very limited tensile strength. This makes it prone to cracking which provides a way for acidic ions to reach the reinforcement leading to its corrosion and deterioration of concrete microstructure. Cracking severely contributes to shorter life-time of concrete structures and high maintenance costs. Concrete composite having the ability to heal cracks and to regain mechanical properties is a scientific goal for many researchers. It could not only lead to a reduction of the cost of structural repairs but also, possibly by proper alternative mix design, help to reduce the CO₂ emissions.

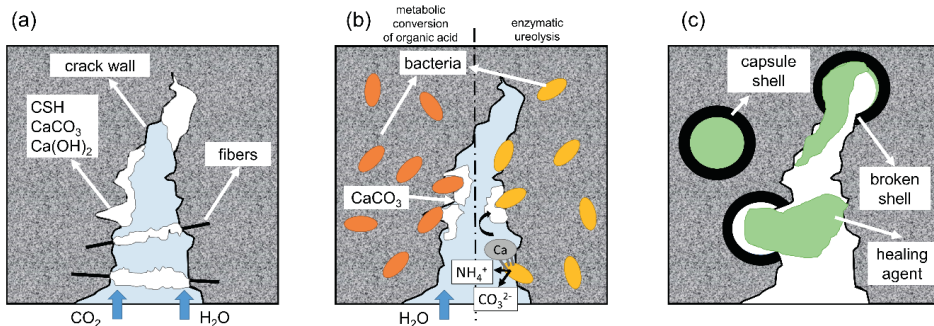


Figure 2.2. Approaches used for the self-healing of concrete: (a) autogenous self-healing, (b) bacteria-based autonomous self-healing (left – metabolic conversion mechanism, right – enzymatic ureolysis), (c) capsule-based autonomous self-healing (Rajczakowska et al. 2019a, With permission from ASCE).

There are two types of self-healing processes in cement-based composites, i.e. autogenous (Figure 2.2a) and autonomous (Figure 2.2bc). The autogenous self-healing involves only the original concrete ingredients, which promote the crack repair due to their specific chemical composition and under favorable environmental conditions (De Rooij et al. 2013). On the other hand, the autonomous self-healing uses external components, such as microcapsules or bacteria to facilitate the damage restoration (Cailleux and Pollet 2009; Da Silva et al. 2015; Jonkers 2007).

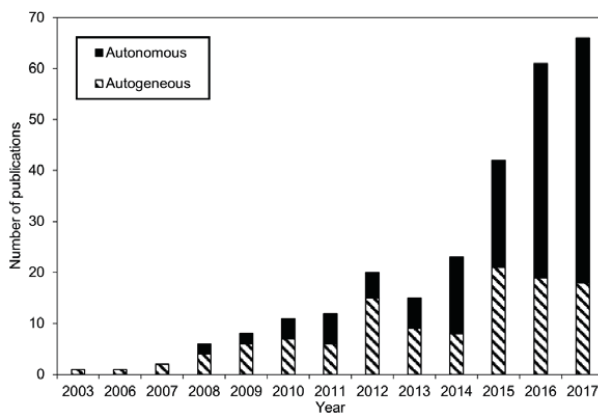


Figure 2.3. Changes in the number of publications related to autonomous and autogenous self-healing in the years 2003–2018 including only journals listed in the Web of Science (Rajczakowska et al. 2019a, With permission from ASCE).

The autonomous self-healing attracted significant attention in the recent years due to very promising results obtained from small-scale laboratory studies (Figure 2.3). Nevertheless, the focus of that research, being primly the so-called “proof-of-concept”, was mainly on the advantages of such systems. It neglected effects of original properties of concrete, upscaling, complexity and price.

In the following sections, the mechanisms of autonomous (bacteria and capsule-based) and autogenous self-healing approaches are presented together with factors influencing the efficiency of the process as well as their effects on the concrete properties. The advantages and disadvantages of both methods are compared and knowledge deficiencies indicated.

2.1. Autonomous self-healing

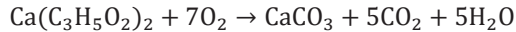
2.1.1. Bacteria-based approach

One of the first applications of bacteria to seal cracks in concrete was mentioned by Gollapudi et al. (1995). The use of bacteria-modified mortars, which could be applied externally for concrete repair was the topic of many research projects (Oriol et al., 2002; De Muynck et al., 2008; Van Tittelboom et al., 2010; Ramakrishnan et al., 2013). Recently, the use of bacteria for self-healing concrete was also studied.

Mechanism of the bacterial self-healing

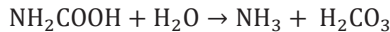
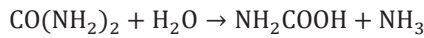
There are two main mechanisms governing bacterial self-healing of concrete, i.e. bacterial metabolic conversion of organic acid (Figure 2.2b left) and enzymatic ureolysis (Figure 2.2b right). The self-healing product that fills the crack is calcium carbonate.

In the first process, bacteria act as a catalyst and transform a precursor compound to a suitable filler material. As a result, calcium carbonate-based minerals are produced which act as a type of bio-cement that seals the cracks (Jonkers, 2011). One of the calcium precursors, often used in research due to its positive effect on concrete strength, is calcium lactate. In this case, the reaction occurring in the crack can be formulated as follows:



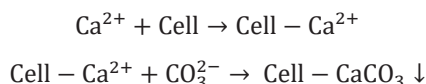
In addition to this reaction, the produced CO_2 reacts locally with $\text{Ca}(\text{OH})_2$ inside of the crack leading to the production of five more CaCO_3 molecules thus making the process six times more effective than the autogenous self-healing (Jonkers, 2007).

The second mechanism called ureolysis is based on the bacterial production of urease which catalyzes the hydrolysis of urea ($\text{CO}(\text{NH}_2)_2$) into ammonium (NH_4^+) and carbonate (CO_3^{2-}) ions (e.g. Tittleboom et al. 2010). The reactions can be presented as follows:



The bacteria surface can serve as a nucleation site due to the cell wall being negatively charged and, therefore, can attract ions from the environment, e.g. Ca^{2+} . Those ions

deposited on the surface of the bacteria cell react with CO_3^{2-} and lead to the precipitation of CaCO_3 :



Factors affecting bacterial self-healing

The ability of bacteria to survive in a concrete-based environment is one of the most important factors affecting the efficiency of bacterial self-healing. Unfortunately, during the cement hydration the compressive stresses tend to crush the bacteria. Therefore, spores might be considered a better solution. However, changes in the concrete porosity during maturing may lead to the decreased viability of spores and survival time reaching only several months (Paine, 2016). For this reason, the so-called protection solutions have been used, including e.g. silica gel (Tittleboom et al., 2010), polyurethane (PU) prepolymer (Wang et al., 2011), diatomaceous earth (Wang et al., 2012), porous expanded clay particles (Jonkers, 2011), microcapsules (Wang et al., 2014), Graphite Nanoplatelets (GNP) (Khaliq & Ehsan, 2016) and calcium alginate (Palin et al., 2016). An optimum pH is also required for bacterial-activated self-healing. The bacteria should be able to survive in the highly-alkaline environment present in the early-age concrete as well as the lower pH of the carbonation phase in the matured concrete (Zhang et al. 2016; Seifan et al. 2017). The extreme temperature (55°C for 4 h) and pH (13.6 for 4 h), developing in the first couple of hours after mixing, were observed to decrease the bacteria viability (Williams et al. 2016).

The exposure conditions appeared to be an important factor for the bacterial self-healing process. The presence of water is a compulsory condition for the process to develop (Jonkers & Schlangen, 2007; Luo et al. 2015). Various healing conditions and their influence on the efficiency of the bacterial self-healing were also tested (Wang et al. 2014). The cracked specimens were subjected to five incubation conditions: 20 deg. and RH>95%, immersion in water, immersion in a deposition medium (0.2 M urea and 0.2 M $\text{Ca}(\text{NO}_3)_2$), wet-dry cycles with water, and wet-dry cycles with a deposition medium (16h water/medium; 8h air, 60%RH). The samples exposed to wet-dry cycles with water had the highest healing efficiency in terms of healed crack area, water permeability and maximum the healable crack width. Due to the fact, that water is not always present in real-life conditions, an application of a hydrogel as a carrier (protection) for bacterial spores during the process of mixing and hydration and as a water reservoir was proposed (Wang et al. 2014). Samples with hydrogel and bacteria showed a distinct superiority in the crack healing efficiency. Cracks narrower than 0.3 mm were completely healed. In the case of cracks between 0.3 and 0.4 mm healing ratios reached 40-90%. The maximum healed crack-width was around 0.5 mm (Wang et al., 2014).

Different types of calcium salts can be used in bacterial self-healing systems, such as calcium chloride (Paine, 2016), calcium nitrate (Paine, 2016) or calcium lactate (Jonkers, 2011). The type of calcium salt affected the efficiency of the self-healing process. The usage of calcium chloride (CaCl_2) was found to be not optimal due to chloride (Paine, 2016). Calcium nitrate ($\text{Ca}(\text{NO}_3)_2$) was more compatible as it is often used as a setting accelerator or anti-freeze agent. It reacts with calcium hydroxide ($\text{Ca}(\text{OH})_2$) forming calcium hydroxynitrate – a mineral with needle-shaped crystals that functions as micro-reinforcement for the cement matrix. However, it is not certain if it can provide a sufficient amount of Ca^{2+} ions (Paine, 2016). Calcium lactate ($\text{C}_4\text{H}_6\text{CaO}_4$) was shown to increase the concrete strength (Jonkers, 2011).

The nutrients, which aid the germination of the spores and provide a source of growth for bacterial cells, also effected the efficiency of self-healing as well as concrete properties, especially when added directly into the concrete mix. The two most popular nutrients are yeast extract and urea. The latter was said to be questionable because of the formation of ammonium ions which resulted in the environmental nitrogen loading (Paine, 2016).

It was observed that the precipitation of calcium carbonate was the highest within the crack rim next to the surface. The reason for this might be the shortage of oxygen. Zhang et al. (2016, 2017) introduced a new solution, i.e. a controlled-oxygen-releasing tablet (ORT) containing CaO_2 and lactic acid with a suitable ratio of 9:1. As a result, a new binary concrete crack self-healing system was able to supply molecular oxygen for the precipitation of the microbial calcium.

2.1.2. Capsule-based approach

The encapsulation of the healing agent is one of the most studied approaches. In contrast to autogenous healing, the healing component is contained in microcapsules, which are added to the concrete mix. After hardening, the repair occurs when the forming crack propagates through the capsule, breaking it and releasing the healing agent, (Figure 2.2c). As a result, not only the crack propagation is blocked but also the material is repaired by filling the crack with the healing agent. The permeability is usually decreased and some regain of strength can occur (Wang et al., 2017). This method was initially applied for structural polymers (White et al., 2001). The proposed system consisted of a microcapsule with the healing agent and a catalytic chemical trigger (Figure 2.4).

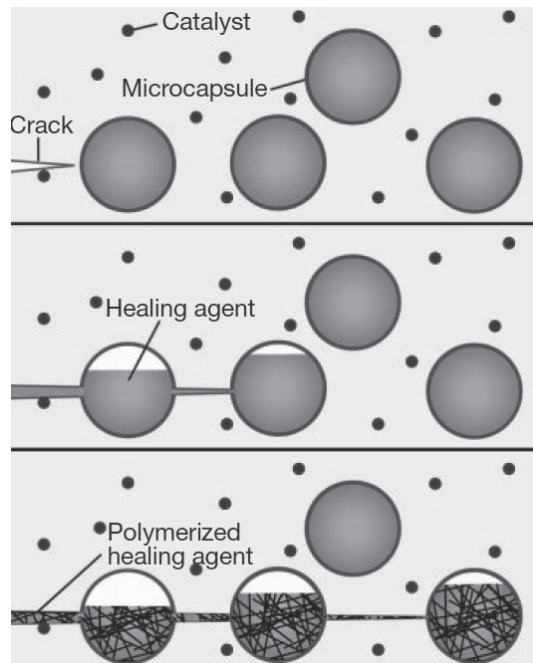


Figure 2.4. The mechanism of crack healing (White et al., 2001).

Mechanism of the capsule-based systems

The mechanism of the capsule-based self-healing systems consists of three components. The first is the trigger, which depicts the process of activating the capsule by damaging its walls. The next component is the healing agent, i.e. the substance, being the core of capsule, which is released into the crack upon activation. Finally, the capsule shell material (different protection coatings) which is used to prevent the contact of the healing agent with the healed matrix. The effectiveness of the self-healing system depends on the compatibility of those components with the repaired matrix and their successful interaction.

The most popular mechanism is based on a mechanical trigger. The stresses associated with the crack formation lead to the breakage of the brittle capsule material and to the release of the healing agent. Another solution is to use chemical triggers such as chloride ions (Xiang et al. 2015), pH (Sisomphon et al. 2011). In that case, chloride ions penetrate the concrete matrix through nano-cracks before the actual formation of micro-cracks. These chloride ions are then used to initiate the healing mechanism. The sensitivity of the chloride trigger appeared to be higher (Xiang et al. 2015). The encapsulated healing agent might also be released after the cement matrix is attacked by carbon dioxide. The carbonation results in a decrease of the strength of the matrix surrounding the capsules and additionally changes the microstructure thus leading to the breakage of the capsules (Sisomphon et al. 2011). Expanded clay lightweight aggregate was used impregnated with a sodium monofluorophosphate (Na_2FPO_3) solution and encapsulated by a cement paste layer to produce a self-healing system in blast-furnace slag cement mortars.

Various types of healing agents for the self-healing concrete are applied (Table 2.1). They can be divided in three groups: one-, two- and multi-component healing agents. The one-component self-healing agents have the ability to act alone without the need for additional chemical compounds or catalysts, e.g. sodium silica (Na_2SiO_3). On the other hand, two- and multi-component systems require another substance for instance, dicyclopentadiene (DCPD), to achieve the maximum efficiency. The polymerization (ROMP) process uses a Grubbs catalyst (transition metal catalyst), which incorporates a high metathesis method (Gillford et al., 2014). Unfortunately, the two-component systems are more complex and have the risk of an inappropriate mixing of the two compounds resulting in the insufficient cracks sealing. The healing agent should have a low viscosity to enable its penetration into the concrete binder matrix. An optimum fluidity is yet another important factor controlling the transportation through the cracks. Finally, the healing material has to solidify in the desired place.

Table 2.1. The most common healing agents for self-healing concrete.

Healing agent	Reference
Epoxy resin	(Han & Xing, 2016)
	(Dong et al., 2016)
	(Perez et al., 2015)
	(Wang et al., 2017)
Two component PU foam	(Tittleboom et al., 2011)
	(Hilloulin et al., 2015)
Methyl methacrylate MMA	(Dry & McMillan, 1996)
	(Yang et al., 2011)
	(Gillford et al., 2014)
Sodium silicate (Na_2SiO_3)	(Alghamri et al., 2016)
	(Tan et al., 2016)
	(Kanellopoulos et al., 2016)
	(Kanellopoulos et al., 2015)

	(Mostavi et al., 2015)
Sodium monofluorophosphate (Na ₂ FPO ₃)	(Sisomphon et al., 2011) (Dong et al., 2015)
Cyanoacrylates (CA)	(Dry, 2000) (Joseph et al., 2007)
Silica sol	(Tan et al., 2016)
Tung oil	(Cailleux & Pollet, 2009)
Minerals and expansive powders	(Qureshi et al., 2016)
Dicyclopentadiene (DCPD)	(Gillford et al., 2014)

Epoxy resins are one- or two-component healing agents, which belong to the group of reactive polymers or prepolymers. The epoxy resin E-51 was successfully applied reacting with a curing agent (BGE and MC120D) leading to the formation of healing products inside cracks (Dong et al. 2016). The solution proved to be successful in sealing of the cracks, reducing the chloride penetration and recovery of the strength. The microstructure of the material became denser leading to an increased compressive strength.

The PU foam system is another alternative. In this case, the involved polymerization does not depend on the mix ratio of the two compounds and they both have a low viscosity promoting penetration. In addition, the expansion takes place, which pushes the healing agent out of the capsule and later fills the crack with an additional volume (Tittleboom et al., 2011).

Sodium silica was originally applied in concrete technology to reduce the porosity (Gillford et al., 2014). It reacts with Ca(OH)₂ creating silicates which bind the concrete. It is a one-component self-healing system. Firstly, it reacts with the Ca(OH)₂ present in the cement matrix after the hydration process. Afterwards, the sodium hydroxide reacts with the silica. Water is an essential condition for the processes to occur. The reaction products seal the cracks and enable a strength gain (Gillford et al., 2014).

The reaction of sodium monofluorophosphate (Na₂FPO₃) capsule-based self-healing solution applied in the blast furnace slag cementitious material is comparable to the protection against tooth enamel decay where fluorapatite is formed on enamel (Sisomphon et al. 2011). In the slag concrete, the healing agent hydrolyzed in the pore solution. The formed phosphate and fluoride ions reacted with portlandite and calcium carbonate phases resulting in the formation of fluorapatite and carbonate fluorapatite. Apatite has a higher hardness than calcium carbonate, therefore it improved the strength of the concrete. It also lead to a better bonding between unreacted particles and hydration products (Sisomphon et al., 2011).

The capsule shell plays an important role in the efficiency of the encapsulation techniques. It provides protection for the healing agent during the mixing process and hydration of Portland cement. It prevents a premature reaction of the healing agent with the hardener/catalyst. The shell has to be strong enough to withstand the mixing process and the hydration stresses but at the same time, it should easily rupture due to a forming crack. The most important factors governing capsules self-healing systems include, the capsule diameter, the shell thickness, the surface texture and the shape of the capsule, (Tittelboom et al., 2011; Hilloulin et al., 2015; Qureshi et al., 2016; Kanellopoulos et al., 2015; Xiang et al., 2015; Mostavi et al., 2015; Gillford et al., 2013; Sisomphon et al., 2011; Yang et al., 2011; Han & Xing, 2016; Kanellopoulos et al., 2016; Lv et al., 2016; Tan et al., 2016; Wang et al., 2017; Perez et al., 2015; Dong et al., 2015). The dimensions of the microcapsules range from several microns (Perez et al., 2015; Yang et al., 2011; Kanellopoulos et al., 2016; Han & Xing, 2016) to several millimeters (Tittelboom et al.,

2011; Hilloulin et al., 2015). In addition, various materials may be used for the capsule shells (Table 2.2).

Table 2.2. Capsule shell materials.

Capsule material	Reference
Glass	(Tittleboom et al., 2011) (Qureshi et al., 2016)
Ceramic	(Tittleboom et al., 2011)
Polymeric	(Kanellopoulos et al., 2016) (Lv et al., 2016) (Hilloulin et al., 2015)
LWA	(Sisomphon et al., 2011) (Alghamri et al., 2016)
Silica	(Yang et al., 2011) (Perez et al., 2015)
Urea formaldehyde	(Gillford et al., 2014) (Mostavi et al., 2015) (Han & Xing, 2016) (Wang et al., 2017)
Polystyrene resin	(Dong et al., 2015)

The healing systems based on capsules and using the mechanical trigger concept require a good understanding of the micromechanical behavior of a single microcapsule. The nanoindentation technique enables to study the mechanical properties of the capsule on the microscale (Lv et al. 2016). The diameter of the capsule as well as the shell thickness are crucial in terms of the force needed to break it. Their increase lead to higher required forces (Lv et al., 2016).

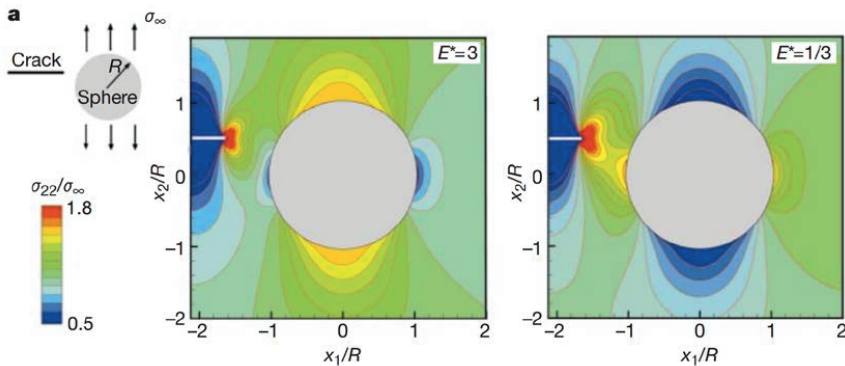


Figure 2.5. Stress state in the vicinity of a planar crack as it approaches a spherical inclusion embedded in a linearly elastic matrix and subjected to a remote tensile loading perpendicular to the fracture plane. The left picture correspond to an inclusion three times stiffer than the matrix. The right image corresponds to an inclusion three times more compliant than the surrounding matrix (modified from White et al., 2001).

Micromechanical modelling using the Eshelby-Mura equivalent inclusion method was also performed to investigate the crack/microcapsule interaction (White et al. 2001, Figure 2.4.). Three components were included in this model: the crack, the linearly elastic matrix and the spherical inclusion. The matrix-inclusion system was subjected to the far-field

tensile loading, perpendicular to the crack plane. It was observed that the relation between the stiffness of the matrix and the inclusion had a significant effect on the stress distribution around the sphere and next to the crack tip. When the inclusion was stiffer than the matrix, the stresses (Figure 2.5. left) next to the crack tip were asymmetric which may lead to the deflection of the crack and passing around the capsule. On the other hand, in the case of a stiffer matrix, the crack is attracted towards the inclusion thus enabling the trigger to activate the healing agent (White et al., 2001). This simulation showed that too stiff inclusions may lead to a failure of the trigger mechanism, whereas shell material which is not stiff enough may not survive the mixing process thus leading to a premature release of the healing agent. The bonding between capsule and matrix is strongly related to the interfacial transition zone (ITZ) (Huang et al., 2016). The behaviour of capsules is similar to the aggregate in concrete, i.e. the interface between binder matrix and capsule shell is weakened. This may cause capsule debonding upon cracking instead of breakage and subsequent healing agent release. For this reason, it is important that the ITZ has mechanical properties corresponding to the surrounding cement matrix (Mauludin and Oucif 2018a,b).

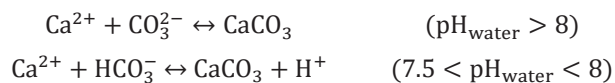
2.2. Autogenous self-healing

According to RILEM's definition, the autogenous self-healing is a process, which occurs when the recovery of a material from damage involves only its original components (De Rooij et al., 2011). In other words, the self-healing ability of concrete and other cementitious materials is possible only due to their specific chemical composition and, in addition, under favorable environmental conditions. This phenomenon has been studied since the beginning of the nineteenth century. The healing of cracks in water retaining structures, culverts and pipes was noticed by the French Academy of Science in 1836 (Wu et al., 2012). Afterwards, many researchers not only observed the presence of autogenous healing products in the cracks of concrete but also tried to verify its physicochemical background.

2.2.1. Mechanism of the autogenous self-healing

The causes of self-sealing of cracks in concrete were identified as related to dissolution, continuous hydration, deposition and crystallization, etc. (Hearn and Morley, 1997). The autogenous healing was noticed to reduce the water permeability of concrete by more than an order of magnitude (Hearn, 1998). The most significant changes in the permeability were observed in the first 100 hours of testing. The autogenous healing of concrete was found to be a flow-dependent process, i.e. the water has to flow through the cracks exposed to the atmosphere.

The CaCO_3 formation in the cracks was found to be the main reason of the autogenous healing mechanism in concrete. The calcite formation in the area of water bearing cracks can be formulated in the following way (Edvardsen, 1999):



The location of the CaCO_3 crystals depends on the temperature, the pH value, the CO_2 partial pressure, the saturation index of calcite and the concentration of Ca^{2+} and CO_3^{2-} ions in the solution (Edvardsen, 1999).

Two major types of self-healing products were distinguished, one crystal-like consisting of portlandite/calcite and the other gel-like primarily made of calcium silicate hydrate (C-S-H) (Huang et al., 2013). The amount of formed portlandite was higher (~ 80%) than C-S-H (< 15%) in comparison with the surrounding binder matrix. It was observed that the self-healing process tends to slow down after approximately 300 hours (Huang et al., 2013).

The physico-chemical principles behind the autogenous self-healing are still not completely understood. Often, only the surface cracks are evaluated, therefore the results regarding products of self-healing can be misleading. In general, the causes of autogenous self-healing can be divided into three main groups: physical, chemical and mechanical (De Rooij et al., 2011). The physical causes consist of swelling of the cement matrix. Chemical causes, most often mentioned in the literature, are the continued hydration of cement particles and formation of calcium carbonate. The mechanical causes include filling of the cracks with fine particles originating from the broken surface of concrete or transported with water inside the crack.

2.2.2. Factors affecting the autogenous self-healing

In general, several factors affecting the efficiency of autogenous healing can be distinguished. The autogenous self-healing is a time dependent phenomenon (Huang et al., 2013). The time has an influence on the type of the involved mechanism, including an ongoing hydration at an early age and precipitation of calcium carbonate, later. Environmental conditions and temperature are critical when it comes to the self-healing efficiency.

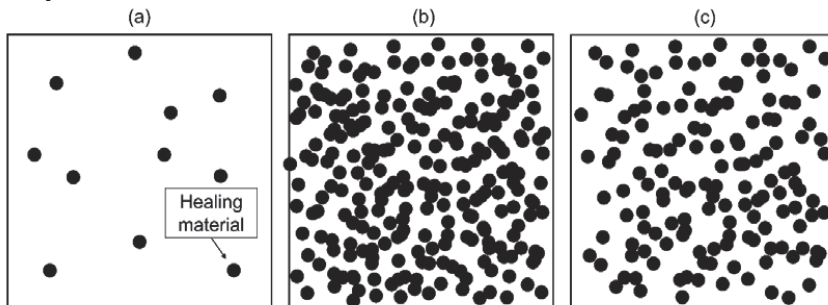


Figure 2.6. Simplified schematic representation of the fraction of the healing material available in cement paste: (a) microcapsules (2% of cement content), (b) unhydrated cement particles after 7 days of hydration (approx. 50% of cement content), (c) unhydrated cement particles after 28 days of hydration (approx. 30% of cement content).

Standing water appeared to be generally better than flowing water as it does not “wash out” the ions necessary for the chemical reactions to occur (Jiang et al., 2015). Various water regimes lead to different healing efficiencies (Roig-Flores et al. 2015). Higher temperatures were found to increase the crack closure ratio (Roig-Flores et al., 2016). The mechanism and kinetics of the self-healing process, with respect to the formation of different phases depending on the distance from the surface, is not yet fully understood (Gagné & Argouges, 2012). It was found to be related to the differences in the concentrations of calcium and carbonate ions (Sisomphon et al. 2012). The crack geometry affects the crack closure ratio that can be reached because of the self-healing products formation. The wider the crack ($\geq 200 \mu\text{m}$), the faster was the initial process due to more space available for the formation of the healing products and easier supply of carbon dioxide and water (Gagné & Argouges, 2012). However, the overall closure factor of cracks

was observed to be higher for smaller cracks (around 50 μm) which were easier to fill. Cracks wider than 300 μm lead only to 20% efficiency (Gagné & Argouges, 2012). The mix proportions also contribute to the self-healing performance. A lower water-to-binder ratio and the presence of higher amounts of unhydrated cement particles lead to a higher self-healing efficiency (Gagné & Argouges, 2012).

The availability of the healing material is a significant limitation in the case of capsule based systems. Usually, the maximum amount of capsules is limited to 2wt% due to problems with the workability and strength of the hardened matrix. Consequently, the number of capsules is relatively low which results in a low probability that the forming crack will actually rupture the capsule (Figure 2.6a). On the contrary, in the autogenous self-healing mechanism, which relies on unhydrated cement particles (Huang et al., 2013), the probability will be significantly higher (Figure 2.6bc). This fact may also affect the efficiency of the autogenous healing in elements subjected to cycling loading.

In the following sections, the influence of the main factors on the autogenous self-healing is discussed.

Effect of admixtures and alternative binders

In the last decade, the effects of the concrete mix composition and the presence of mineral additives on the autogenous self-healing of concrete were studied (Table 2.3). It was observed that the use of expansive additive (CSA: calcium sulfoaluminate) and crystalline additive (CA: reactive silica and some crystalline catalysts) enhanced the surface crack closing (Sisomphon et al., 2012). With these additives the maximum healed crack width increased from width from 150 μm to 400 μm . The water permeability of the healed specimens decreased significantly. Calcium carbonate precipitation was noticed especially on the mouth of the crack. The additives increased the pH of the samples which improved the environmental conditions for the calcium carbonate precipitation. The concrete mixtures with CA showed a more stable behavior and the highest healing rates. Other studies showed that, in general, the self-healing of concrete did not improve significantly by the addition of CA (Roig-Flores et al., 2016). On the other hand, the CA tended to speed up the self-healing process and remained efficient even in the exposure to air, in contrast to the specimens without CA, which always required water immersion (Ferrara et al. 2014). Other studies showed the healing of cracks having a maximum crack width of 0.2 mm. It was also indicated that a crack healing (closure) of about 80% was needed to achieve a 20% recovery in strength. In the case of one component mortars, a very good self-healing was observed when chemical expansive additives were applied (Jiang et al. 2015). On the other hand, in the case of multi-component mortars, addition of silica, swelling and crystalline admixture gave the best results (Jiang et al. 2015).

Table 2.3. Supplementary Cementitious Materials and mineral additives used for autogenous self-healing (Rajczakowska et al. 2019a, With permission from ASCE).

SCM/additions	References
Slag	(Alyousif et al. 2015; Darquennes et al. 2016; Gruyaert et al. 2014; Huang et al. 2014; Hung et al. 2018; Jiang et al. 2015; Mehdipour et al. 2018; Olivier et al. 2016; Qian et al. 2009; Qiu et al. 2016; Ryou et al. 2015; Sahmaran et al. 2013; Sahmaran et al. 2015; Schlangen et al. 2006; Van Tittelboom et al. 2012)
Fly ash	(Alyousif et al. 2015; Gruyaert et al. 2014; Herbert and Li 2013; Herbert and Li 2012; Hung and Su 2016; Hung et al. 2018; Kan and Shi 2012; Liu et al. 2017; Liu et al. 2017b; Ma et al. 2014b; Mehdipour et al. 2018; Na et al. 2012; Özbay et al. 2013b; Qian et al. 2009; Ryou

	et al. 2015; Sahmaran et al. 2013; Sahmaran et al. 2015; Şahmaran et al. 2008; Sherir et al. 2016; Sherir et al. 2017a; Sherir et al. 2017b; Siad et al. 2015; Siad et al. 2017; Suryanto et al. 2016; Termkhajornkit et al. 2009; Van Tittelboom et al. 2012; Yildirim et al. 2014; Zhang and Zhang 2017; Zhu et al. 2012)
Lime	(Jo et al. 2015; Siad et al. 2015; Yildirim et al. 2014)
Silica	(Jiang et al. 2015; Nishiwaki et al. 2015; Ryou et al. 2015)
Metakaolin	(Ryou et al. 2015)(69)
Crystalline admixtures	(Ahn and Kishi 2010; Ferrara et al. 2014a; Ferrara et al. 2016a; Jiang et al. 2014; Jiang et al. 2015; Jo et al. 2015; Qureshi and Al-Tabbaa 2016; Roig-Flores, M. et al. 2015; Roig-Flores, M. et al. 2016; Sherir et al. 2016; Sherir et al. 2017a; Sherir et al. 2017b; Siad et al. 2017; Sisomphon et al. 2012; Sisomphon et al. 2013)
Fibers	(Alyousif et al. 2015; Ferrara et al. 2016; Ferrara et al. 2017; Herbert and Li 2013; Herbert and Li 2012; Homma et al. 2009; Hung and Su 2016; Kan et al. 2010; Kan and Shi 2012; Kim, D. J. et al. 2014; Liu et al. 2017; Liu et al. 2017; Ma et al. 2014; Mehdipour et al. 2018; Nishiwaki et al. 2012; Nishiwaki et al. 2014; Nishiwaki et al. 2015; Özbay et al. 2013; Roig-Flores et al. 2015; Sherir et al. 2017; Sherir et al. 2017; Siad et al. 2015; Sisomphon et al. 2013; Snoeck and De Belie 2012; Suryanto et al. 2016; Yang et al. 2011; Yildirim et al. 2014; Yu et al. 2010; Zhang and Zhang 2017; Zhu et al. 2012; Zhu et al. 2016)

Self-healing of a crack having width of up to 200 µm within 42 days was observed for self-healing concrete containing alternative binders (blast furnace slag and fly ash) (Tittelboom et al. 2012).

Two mechanisms of autogenic self-healing were investigated, including the precipitation of CaCO₃ crystals and the ongoing cement hydration. The formation of calcium carbonate appeared to be the dominant process. However, only the surface of the crack was assessed. The increased water-to-binder (W/B) ratio resulted in a decreased amount of the unhydrated binder, which led to a decreased autogenous healing efficiency (Tittelboom et al., 2012). Findings from different experimental setups gave different conclusions, which might be related to various time spans of the used testing procedures. On the other hand, others showed a higher self-healing efficiency of a cement paste containing 66wt% of slag (Huang et al. 2014). The unreacted blast furnace slag present in the bulk matrix was found to heal the microcracks having a width of around 10 µm. However, the required condition was a proper activation with a saturated Ca(OH)₂ solution (Huang et al. 2014). The influence of blast furnace slag (BFS) on the self-healing of concrete was also studied by others (Darquennes et al., 2016; Olivier et al., 2016). The obtained results confirmed that BFS mortars had a slower hydration rate and consequently, more unhydrated particles were available. As for the early-age concrete, the main healing mechanism is the ongoing hydration, the slag mortar showed a higher self-healing capacity than the Portland cement-based mortar. In addition, X-ray microtomography showed that the self-healing at early age is characterized by a “double kinetics”, which tends to be faster during the first two weeks and is slowing down later (Olivier et al., 2016). The main observed healing product was C-S-H. Cracked slag-mortar specimens subjected to the chloride penetration test revealed that the material characteristics was a secondary parameter affecting the chloride migration. The most significant was the crack width (Darquennes et al., 2016).

Effect of exposure

Only a limited number of studies focused on the effects of exposure on the autogenous self-healing of concrete (Table 2.4). Majority of the studies presented the results only for the surface crack closure, revealing that a very small crack width could be healed with a constant water immersion regime (Qian et al. 2009; Qian et al. 2010; Yang et al. 2011; Şahmaran et al. 2013; Jiang et al. 2014, 2015). Internal self-healing evaluation with the use of X-ray microtomography suggested that there was no self-healing present inside of specimens submerged in water, (Suleiman and Nehdi, 2018). Temperature and relative humidity cycles also did not yield satisfactory results (Suleiman and Nehdi, 2018). Wet/dry cycles lead to the self-healing of crack widths below 50 µm for Engineered Cementitious Composites (ECC) (Yang et al. 2009). The self-healing process was observed to be faster in the beginning and slowing down after approximately 5 curing cycles (Yang et al. 2009; Yang et al. 2011; Kan and Shi, 2012; Qian et al. 2010; Huang et al. 2014). Freeze/thaw cycles with both water and deicing salt as well as the air curing were found inefficient to induce self-healing (Şahmaran et al. 2013, Zhu et al. 2012; Qian et al. 2009, Qian et al. 2010). Sea water demonstrated a good effect on the self-healing performance of the ordinary Portland cement concrete, resulting in a crack closure for widths up to 0.5 mm, although significantly diminishing the compressive strength of the material (Palin et al. 2015).

Table 2.4. Previous studies addressing the effects of the exposure on the efficiency of the autogenous self-healing of Portland cement based materials.

Exposure type	Reference
Constant water immersion	(Qian et al. 2009; Qian et al. 2010; Yang et al. 2011; Şahmaran et al. 2013; Jiang et al. 2014, 2015; Suleiman and Nehdi, 2018)
Wet/dry cycles	(Qian et al. 2010; Yang et al. 2009; Yang et al. 2011; Kan and Shi, 2012; Qiu et al. 2016)
Temperature	(Reinhardt & Jooss, 2003; Suleiman and Nehdi, 2018).
Relative humidity	(Suleiman and Nehdi, 2018).
Freeze-thaw cycles	(Zhu et al. 2012; Şahmaran et al. 2013)
Sea water	(Palin et al. 2015; Danner et al. 2019)
Air/CO ₂	(Qian et al. 2009; Qian et al. 2010; Şahmaran et al. 2013)
NaOH/dry cycles	(Qiu et al. 2016)
Saturated Ca(OH) ₂ solution	(Huang et al. 2014; Huang & Ye, 2015)

Independently of the exposure, the self-healing products consisted mainly of calcite and calcium hydroxide (Qian et al. 2009; Jiang et al. 2015; Kan and Shi, 2012; Şahmaran et al. 2013; Zhu et al. 2012) as well as C-S-H (Kan and Shi, 2012; Şahmaran et al. 2013; Zhu et al. 2012). Mixes containing slag showed a slightly different behavior. The water-based exposure lead to the precipitation of calcite due to the carbonation mechanism. On the other hand, NaOH-based exposure resulted in the formation of calcite and C-S-H which was related to the alkali activation processes (Qiu et al. 2016). The exposure to a solution of calcium hydroxide resulted in the formation of C-S-H, ettringite, hydrogarnet and OH-hydrocalcite inside the crack (Huang et al. 2014).

Effect of fibers

Lately, it has been noticed that Fiber Reinforced Cementitious Composites (FRCC) and Engineered Cementitious Composites (ECC) have strong self-healing behavior. The FRCC can be divided into several groups based on the volume fraction of fibers. The first group

consists of low or moderate volume fractions of fibers, i.e. between 0.2% and 1% (Cuenca & Ferrara, 2017). The fibers in this case usually are added to control the plastic shrinkage cracking rather than for structural reasons. Higher amount of fibers (1-2%) can serve as a secondary reinforcement improving, e.g. the fracture toughness and the fatigue resistance. The ECC are designed and optimized to be used to enhance micromechanical properties or repaired/modified structures. They are characterized by a strain-hardening behavior, i.e. they are able to withstand the increasing load and deformation after the first cracking (Li, 1998). For this effect to occur, the so-called steady cracking is required which is achieved through fibers bridging. When the crack propagates the bridging stress increases because of the fiber/matrix debonding and stretching segments of fibers. The crack flanks start to flatten when the bridging stresses reach the value of the applied load. On the contrary to the Griffith residual strength concept, relating a decreasing tensile load to a bigger crack size, here, the tensile load is independent of the crack length (Li, 1998).

Table 2.5. Types of fiber material for self-healing concrete.

Healing agent	Reference
Polyvinyl alcohol (PVA)	(Keskin et al., 2016)
	(Yang et al., 2009)
	(Sahmaran et al., 2013)
	(Yang et al., 2011)
	(Liu et al., 2017)
	(Siad et al., 2017)
	(Nishiwaki et al., 2012)
	(Nishiwaki et al., 2014)
	(Nishiwaki et al., 2015)
	(Snoeck et al., 2014)
(Kan & Shi, 2012)	
Ethylene vinyl alcohol (EVOH)	(Nishiwaki et al., 2012)
	(Nishiwaki et al., 2014)
Polyacetal (POM)	(Nishiwaki et al., 2012)
Polypropylene (PP)	(Sanjuan et al., 1997)
	(Nishiwaki et al., 2012)
Polyethylene (PE)	(Nishiwaki et al., 2014)
	(Homma et al., 2009)
Natural fibers	(Snoeck & de Belie, 2012)
	(Snoeck et al., 2015)
	(Kim et al., 2014)
Steel	(Nishiwaki et al., 2014)
	(Ferrara et al., 2016)
	(Homma et al., 2009)

Gray (1984) observed the autogenous healing at the interface of steel fibers and cement matrix already in the 1984. It was highlighted that the presence of water was a necessary condition for the process to take place. In the recent years, many studies aimed to understand the principle behind the effects of fibers on the self-healing. Although, it is still not clear, whether fibers can be classified as a novel method for self-healing, it is agreed that they facilitate the process. Healed mixes containing fibers showed a formation of calcium carbonate as well as C-S-H, (Keskin et al., 2016; Yang et al., 2009; Sahmaran et al., 2013; Yang et al., 2011; Liu et al., 2017; Kan & Shi, 2017).

There are two types of phenomena related to the presence of fibers and autogenous self-healing of concrete; the limitation in crack width and polarity of the used fiber material. As mentioned earlier, the FRCC and, to even greater extent, the ECC are able to control the

extent of plastic cracking. In addition, the ECC induce a strain hardening behavior, which leads to the formation of many small cracks having a width below 100 μm .

It was also observed that for cracks narrower than 100 μm the water tightness was recovered completely for all types of synthetic fibers (Nishiwaki et al., 2014). In addition, a high ratio of mechanical recovery was achieved. Cementitious composites with reduced crack widths (between 50 and 80 μm) were produced by adding polyvinyl alcohol (PVA) fibers (Yang et al., 2009; Liu et al., 2017; Siad et al., 2017) and (Kan & Shi, 2017).

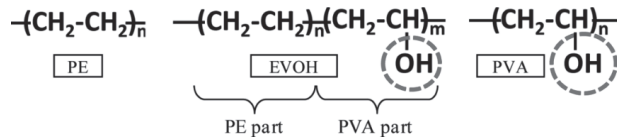


Figure 2.7. Characteristic parts of chemical components of fibers (Nishiwaki, 2014).

The second phenomenon related to the positive effect of fibers on the efficiency of self-healing in concrete is associated with the polarity of the fiber material. It was observed that some types of fibers have polarity groups (Figure 2.7). For instance, PVA has a high polarity strength due to the presence of OH-radical whereas polypropylene (PP) fibers do not have any polarity strength (Nishiwaki et al., 2014). The polarity enables the fibers to act as nucleation sites and attract Ca^{2+} ions. The samples with PVA fibers achieved a better self-healing efficiency than the ones with fibers that did not exhibit polarity (Nishiwaki et al., 2014; Choi et al., 2016). A similar behavior was observed for the natural fibers (Snoeck, 2015). Thanks to their hydrophilic nature, e.g. flax fibers acted as nucleation sites for calcium crystals.

2.3. Effect on concrete properties

2.3.1. Fresh and young concrete

In the case of autonomous systems there are several problems related to their effect on the original fresh concrete properties as well as the incompatibility with the concrete environment leading to a decreased self-healing efficiency.

The survivability of bacteria during concrete mixing process is a problem (Jonkers 2007; Jonkers et al. 2010; Paine 2016) unless an encapsulation protection is applied, e.g. into silica gel (Van Tittelboom et al. 2010). As studies focused mostly on pastes and mortars with bacteria, the aggregate effect on the bacteria endurance was not addressed (De Koster et al. 2015; Zhang et al. 2016). On the other hand, some of the capsule protection systems with high specific surface area led to a decreased workability when more than 5%wt was added (Wang et al. 2012b). Even though the bacteria did not affect the hydration of cement binder (Luo and Qian 2016a), the nutrients had significant influence on the setting time and hydration heat (Luo and Qian 2016b; Luo and Qian 2016a, Wang et al. 2014c). Some nutrients were observed to lower the early strength of concrete due to possible delayed hydration (Luo and Qian 2016a; Mors and Jonkers 2017).

The durability of the capsule during mixing is crucial from the point of view of the self-healing process. The premature breaking leads to the initiation of the process too early by leakage of the healing agent into the cement matrix, and subsequent shortage of this substance when the actual cracking occurs. From this perspective, the material used as well as the geometrical properties of the capsule (shell thickness, shape, and diameter) are of the most importance. Some other helpful solutions included, e.g. covering the capsule with a

mortar layer or attaching the capsules to the reinforcement (Van Tittelboom et al., 2015). The effects of the capsules on the fresh concrete properties were determined after the application of the capsules into several systems. Capsules with variable brittleness, i.e. exhibiting elastic behaviour during mixing and brittle after drying, improved the survival rate of the capsules but affected the strength of the paste negatively (Dong et al., 2017; Gruyaert et al., 2016b; Kanellopoulos et al., 2017).

A reduced workability and an increase of hydration heat was observed for the Gelatin-gum Arabic and polyuria shell capsules with sodium silicate (Giannaros et al. 2016). An increased porosity and worse workability were the outcome of applying silica microcapsules containing an epoxy sealing compound (CAP) and amine-functionalized nanosilica particles (NS) (Perez et al., 2015b).

The autogenous self-healing approach, from definition, should not interfere with the fresh concrete properties as the ingredients consist only of typical concrete components (De Rooij et al. 2013). However, in some cases, the mix compositions which are particularly successful in self-healing, demonstrate certain disadvantages with respect to, e.g. a decreased workability or higher porosity. The ECC owe their good healing capability to the usage of fibers, which reduce the crack width (Li, 2012; Yu et al., 2018). The higher the volume fraction of the fibers, the lower the workability (Swamy & Mangat 1974; Bui et al., 2003; Kuder et al., 2007; Li & Li, 2013). A uniform dispersion of fibers is critical when it comes to their effectiveness therefore they require a special mixing procedure (Li & Li, 2013). Tighter crack widths were obtained for ECC with an addition of fly ash (FA) (Yang et al., 2007). The workability (Juenger & Siddique, 2015) and drying shrinkage of concrete with fly ash improved (Yang et al. 2007), however, it resulted in a higher porosity of binder matrix (Zhang et al., 2014; Termkhajornkit et al., 2009). Cementitious materials with high amounts of unhydrated cement, e.g. ultra-high-performance concrete, which is believed to promote self-healing by continued hydration mechanism, also exhibit several negative properties. Firstly, the low water-to-cement ratio decreases the workability and requires the addition of plasticizer (Wang et al., 2012a). This in turn leads to an altered setting time (Şahmaran et al., 2006). In addition, the large amounts of ultrafine particles in the case of UHPC causes a higher viscosity of the mix and a fast decrease in workability (Wang et al., 2015). In addition, the high amount of cement is responsible for an extensive hydration heat and shrinkage (Wang et al., 2015).

2.3.2. *Hardened concrete*

The hardened concrete properties of autonomous self-healing systems are often severely altered due to the addition of microcapsules and bacteria. The higher the volume fraction of the capsules, the more successful the self-healing behavior of the material. However, as the microcapsules usually needed to be applied in a volume fraction of above 2% to achieve the required self-healing efficiency, a decrease in mechanical properties was observed, as the porosity of concrete was higher and the capsule material's strength was significantly lower (Li et al., 2013; Kanellopoulos et al., 2016; Lv et al., 2016a, b; Perez et al., 2015b; Wang et al., 2014c; Dong et al., 2017; Giannaros et al., 2016; Wang et al., 2013, 2014c; Arce et al., 2017). A negative effect on the strength of the concrete was also found in the case of Super Absorbent Polymer (SAP) addition (Lee et al., 2016; Mignon et al., 2015b, 2017b; Snoeck et al., 2014). The increased size of the microcapsule resulted in worse mechanical properties of concrete (Dong et al., 2017; Kanellopoulos et al., 2016; Wang et al., 2013). Moreover, the Young modulus of the material was observed to decrease, as the microcapsules, having a lower Young modulus than concrete, served as weak inclusions inside the binder matrix (Wang et al., 2017b). The bond between the cement matrix and the

capsule is a critical parameter. Capsule debonding was noticed because of a lower fracture toughness of the cement matrix around the capsule. This caused the propagation of the cracks around the capsule (Kanellopoulos et al., 2016).

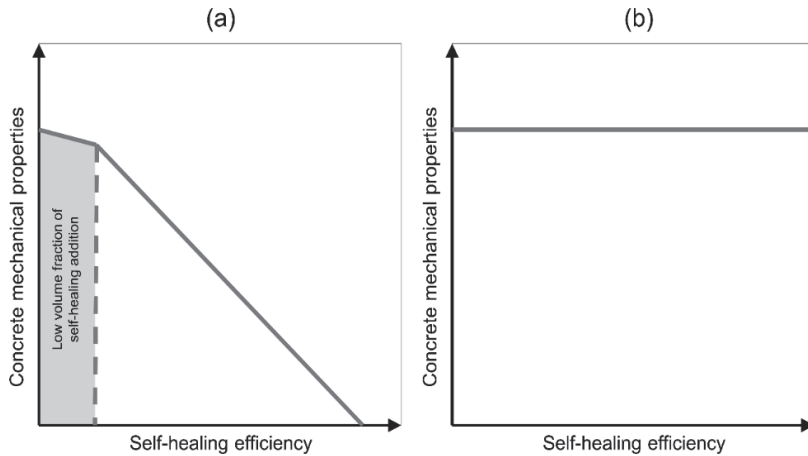


Figure 2.8. Self-healing efficiency in relation to the mechanical properties of concrete for: (a) autonomous self-healing methods, (b) autogenous self-healing methods.

Bacterial concrete also demonstrated a loss of strength as a consequence of the increase in the porosity of the cement matrix (Bundur et al., 2017a, b, c; Da Silva et al., 2015; Jonkers et al., 2010; Luo & Qian, 2016a; Palin et al., 2017; Wang et al., 2014c; Xu & Yao, 2014). Nutrients such as yeast extract, calcium acetate, or peptone also worsened the mechanical properties of the material (Jonkers et al., 2010; Xu & Yao, 2014).

Based on the performed analysis it could be concluded that, in general, the efficiency of the autonomous method increases with an increasing volume fraction of capsules but at the same time the mechanical properties tend to worsen (Figure 2.8a). On the other hand, the autogenous self-healing methods are primarily neutral with respect to the hardened concrete properties (Figure 2.8b). The ECC as well as UHPC are characterized by a very good compressive strength and high durability (Zhang et al., 2014; Li et al., 2001). Nevertheless, the addition of fly ash lead to worse mechanical properties (Zhang et al., 2014; Yang et al., 2007; Termkhajornkit et al., 2009) and increased sorptivity (Zhang et al., 2014). PVA fibers appeared to worsen the ECC behaviour in comparison to PE fibers (Yu et al., 2018).

2.3.3. Full-scale applications and price

There are only several studies addressing the feasibility of self-healing methods in real life applications (e.g. Keskin et al., 2016; Gruyaert et al., 2017; Pina-Zapardiel et al., 2016; Van Tittelboom et al., 2016). Unfortunately, majority of research is still done at the small scale, in the laboratory, serving primarily as a “proof of concept”. In addition, the price of the autonomous self-healing methods is relatively high (Figure 2.9) (da Silva et al., 2015; Lee et al., 2016; Mors & Jonkers, 2017; Snoeck, 2015; Wang et al., 2012b). Some of the approaches were cost-effective, i.e. they were cheaper than a manual injection of the cracks, e.g. SAP based and several bacteria methods (Figure 2.9, Snoeck 2015). At the same time,

the microcapsule-based self-healing methods were significantly more expensive, e.g. PU capsules.

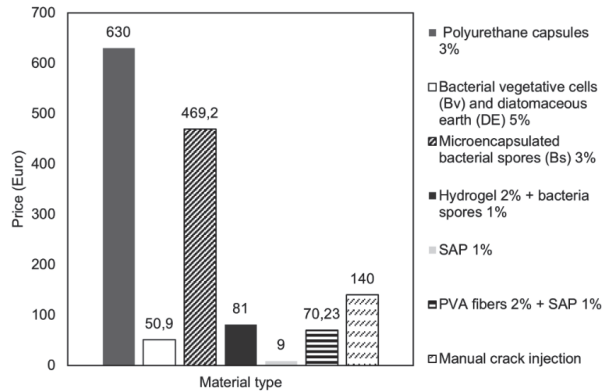


Figure 2.9. Price of different self-healing methods in comparison to the manual crack injection according to (Snoeck, 2015). Figure from (Rajczakowska et al. 2019a, With permission from ASCE).

The autogenous methods do not contribute to a higher price as they consist only of original concrete components. Nevertheless, it is important to remember that the higher amount of binder promoting the continued hydration mechanism has an influence on the production costs (Wang et al., 2015). For instance, the price of ECC was found to be 11.5 higher than ordinary concrete (Pan et al., 2015). However, the assessment of the self-healing costs cannot be done without taking into consideration potential reduction in the maintenance and repair expenses.

Another downside related to a higher amount of binder is its environmental impact. The effect on the CO₂ emissions of the mix composition of UHPC in comparison to ordinary concrete might be estimated as twice as high (Rajczakowska et al. 2019b). Therefore, in order to balance the high carbon footprint, the self-healing process should be efficient enough.

Table 2.6. Environmental impact of ultra-high performance concrete (UHPC) in comparison to ordinary concrete presented in the form of CO₂ emissions (Rajczakowska et al. 2019b).

Ingredient	CO ₂ emissions kg/kg	UHPC kg/m ³	Ordinary concrete kg/m ³	CO ₂ emissions	
				UHPC kg/m ³	Ordinary concrete kg/m ³
Cement	0.931 (Kwon & Wang, 2019)	1000	400	931	372.4
Water	0.000196 (Kwon & Wang, 2019)	220	160	0.04312	0.03136
Quartz	0.0234 (Lin et al. 2017)	300	0	7.02	0
Fine aggregate	0.0026 (Kwon & Wang, 2019)	700	1100	1.82	2.86
Coarse aggregate	0.0075 (Kwon & Wang, 2019)	0	730	0	5.475
Silica	1.05 (Kwon & Wang, 2019)	200	0	210	0

Superplasticizer	0.25 (Kwon & Wang, 2019)	22.5	0	5.625	0
Element thickness reduction (Randl et al. 2014)				33%	0
Total CO ₂ emissions (kg/m ³)				763	381

2.4. Summary

The main focus of this section was to review the mechanisms and main factors promoting the autogenous and autonomous self-healing processes. In addition, the influence of each method on the properties of concrete was investigated. Autogenous self-healing process is connected to the following disadvantages: the loss of workability due to addition of fibers, a higher demand for cement resulting in an increased hydration heat, a higher shrinkage, an increased crack risk, and a higher CO₂ footprint (Rajczakowska et al. 2019a). Additionally, factors such as inappropriate exposure conditions, e.g. a lack of water, concrete age, and a high water-to-binder ratio or too short healing time, affect negatively the efficiency of this process. On the other hand, autonomous methods appeared to cause significantly more problems. Advantages and disadvantages of each method have been listed in Table 2.7 (Rajczakowska et al. 2019a).

Table 2.7. Summary of the limitations of autonomous and autogeneous self-healing strategies (Rajczakowska et al. 2019a, With permission from ASCE).

Area	Autonomous self-healing methods	Autogenous self-healing methods
Fresh and young concrete	<ul style="list-style-type: none"> • Low survival rate of capsules and bacteria during the mixing process, • Loss of workability with increased number of capsules • Bacteria nutrients slow down or even completely hinder hydration of Portland cement leading to lower strength values 	<ul style="list-style-type: none"> • Loss of workability due to fibers • Higher amount of cement resulting in an increased hydration heat, higher shrinkage, an increased crack risk • Problems with proper fiber dispersion and sensitivity to mixing process • Insufficient fiber-matrix bond
Hardened concrete	<ul style="list-style-type: none"> • Glass capsules increase the risk of alkali silica reaction • Material incompatibility between the capsule shell and the binder matrix results in a negative alteration of microstructure and chemical composition of the surrounding binder matrix • The increase of the volume fraction of capsules, decreases the compressive strength and the fracture toughness of the matrix • Reduction of the Young's Modulus of elasticity of the binder matrix due to a lower Young's Modulus of the capsule material as well as the presence of voids left by ruptured capsules • Higher volume fraction of bacteria leads to a strength loss • SAP application greatly decreases the strength of concrete 	<ul style="list-style-type: none"> • The hydrophilic nature of PVA fibers causes their premature rupture under tension, • The use of fly ash decreases the compressive strength

Efficiency	<ul style="list-style-type: none"> • Too low stresses created by the forming crack are not able to break the capsule shell • Capsules with switchable properties of the shell are often not brittle enough to be broken by the forming crack • Premature polymerization of the healing agent inside the capsule due to contact with moisture lowers the probability and effectiveness of the healing process • Lack of water and oxygen hinders the healing process in the case of bacteria-based systems • Capsules might be debonded from the surrounding matrix causing crack formation around it instead of breaking the capsule • The high viscosity of the healing agent can cause problems with efficient penetration of the crack • The total maximum volume fraction of capsules is limited due to workability issues and loss of strength which leads to a lower healing efficiency • Chemical interaction between epoxy and hardener or bacteria with nutrient can hinder the healing process 	<ul style="list-style-type: none"> • Age of the specimen at cracking has a great influence on the healing efficiency • The healing process might take several days/weeks • Exposure conditions might be a limitation for the healing to occur • Only limited crack widths can be fully healed
Price and full scale	<ul style="list-style-type: none"> • Very high price in comparison to the methods used for autogenous healing • Difficult to apply on the full scale 	<ul style="list-style-type: none"> • Higher CO₂ foot print due to higher amount of binder

Summarizing, autogenous self-healing methods based on traditional concrete technology appear to be cheaper, easier and safer than autonomous methods. Therefore, the autogenous method appears to be a significantly more feasible solution for real life applications. However, there are several issues which have not been fully addressed by now:

- The mechanism behind the autogenous self-healing concrete is not fully understood, by now. A detailed analysis of the physico-chemical processes allowing concrete to repair its cracks should be performed. In addition, due to current trends aiming to replace the ordinary Portland cement with different binders, the mechanism of the autogenous self-healing should be studied with respect to various mix compositions. In addition, the effect of exposures on the process should be investigated in systematic way;
- The efficiency of the autogenous self-healing should be improved. There is still not a lot of information about the successful internal crack closure. In addition, the recovery of both: the transport and the mechanical properties should be addressed;
- The methodology of the self-healing process evaluation is not objective. A standardized approach should be proposed, e.g. independent from crack geometry, in order to obtain trustworthy results and to be able to compare the efficiency of different methods;
- “Bulletproof” full-scale applicability of neither of the self-healing methods has so far been demonstrated which makes it unreliable for investors. The approach that is not only a research obsession but has also a chance to become a real-life solution is yet to be developed.

3

Experimental setup

A scientist in his laboratory is not a mere technician:
he is also a child confronting natural phenomena that impress him
as though they were fairy tales.

Maria Skłodowska-Curie

3. EXPERIMENTAL SETUP

The work conducted within the scope of this thesis consisted of two main experiments. Experiment 1 (E1) aimed to verify the basic commonly-accepted hypothesis regarding the relation between the self-healing efficiency and the amount of the unhydrated cement available. This was achieved by testing Ultra High Performance Concrete (UHPC), being an example of a mix composition with an extremely high cement content. In addition, the effect of the following factors were analyzed; type of cement (with and without fly ash), mix compositions (UHPC and High Performance mortars) and, sample age (1-day vs 12 months). The output of this part enabled the formulation of initial hypothesis describing the self-healing mechanism (Figure 3.1). The Experiment 2 (E2) focused on one group of key factors determined in E1. In this part of the research, one type of cement-based mortar was healed in twelve different environmental conditions. The other two factors including the effects of fly ash/slag and a less dense microstructure will be evaluated within the follow-up study.

The following subsections contain a description of the used materials and applied experimental setup.

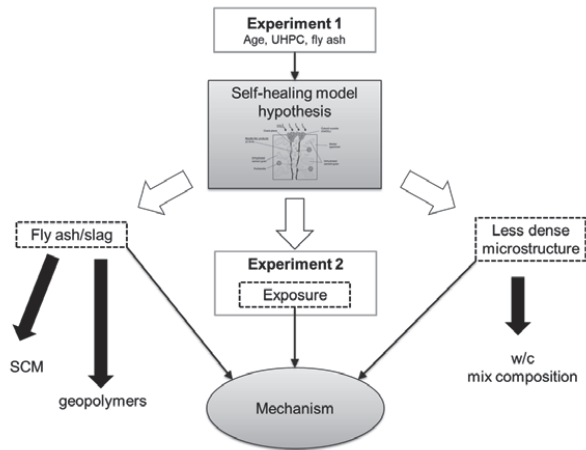


Figure 3.1. Experimental setup in the context of all planned experiments.

3.1. Materials

3.1.1. Mortar mixes

The composition of the mortar mixes is listed in Table 3.1. In total, four types of mortar mixes were tested: Ultra High Performance (U), and normal strength mortars based on CEM I 42.5 N (mortar A), CEM II/A-V 52.5 N Portland-fly ash commercial blend with approximately 20% of fly ash content (mortar B) and mortar based on CEM I 42.5 N with a water to cement ratio of 0.35 and a cement-to-sand ratio of 1. Mortars U, A and B were tested within the Experiment 1 whereas Mortar C was put to the test in the Experiment 2. The chemical composition of the applied cements is shown in Table 3.2.

Table 3.1. Mortar mix composition.

Ingredient	Experiment 1			Experiment 2
	U kg/m ³	A kg/m ³	B kg/m ³	C kg/m ³
Cement type	CEM I 42.5 N	CEM I 42.5 N	CEM II/A-V 52.5 N Portland-fly ash 20%	CEM I 42.5 N
w/c	0.22	0.45	0.45	0.35
Cement	1000	675	675	960
Water	220	303.7	303.7	336
Quartz	300	0	0	0
B15	350	1196	1196	960
B35	350	0	0	0
Condensed Micro silica (Elkem 920)	200	0	0	0
Superplasticizer	22.5	0	0	7.7
PVA fibres	1.5%vol	1.5%vol	1.5%vol	1.0%wt
28 day compressive strength [MPa]	143 ± 11	39.5 ± 2.5	36.5 ± 2.0	-

Table 3.2. Chemical composition of the applied cements.

Chemical analysis	Mean value (%)	
	CEM I 42.5 N	CEM II/A-V 52.5 N
CaO	63.30	57.1
SiO ₂	21.20	22.2
Al ₂ O ₃	3.40	6.20
Fe ₂ O ₃	4.10	3.40
MgO	2.20	2.90
Na ₂ O	0.18	0.31
K ₂ O	0.56	1.20
SO ₃	2.70	3.50
Cl	<0.01	0.06
Loss of ignition	2.50	-
Water soluble Cr ⁶⁺	< 2mg/kg	< 2mg/kg
Na ₂ O-eq.	0.55	1.10

The grading curves of all the materials are shown in Figure 3.2. Baskarpsand AB provided sands B15, B35 and the quartz filler type Norquartz 45. The micro silica, type 920, was delivered by Elkem. The grading curves were calculated based on the Scanning Electron images of the particles according to the procedure presented in (Tole et al. 2018).

BASF MasterGlenium SKY 600 superplasticizer was applied in the UHPC mix whereas Sika ACE30 superplasticizer was used in Mortar C. Polyvinyl alcohol (PVA) fibers having a length of 5 mm and an average thickness of 0.025 mm, were added to each studied mix. PVA fibers were proven to increase the self-healing efficiency due to their high polarity, serving as nucleation sites for the self-healing products (Nishiwaki et al., 2015, Choi et al., 2016). They were also found to limit the crack width and to facilitate the control of the crack opening during the crack generation with the use of the three-point bending test (Yang et al., 2009).

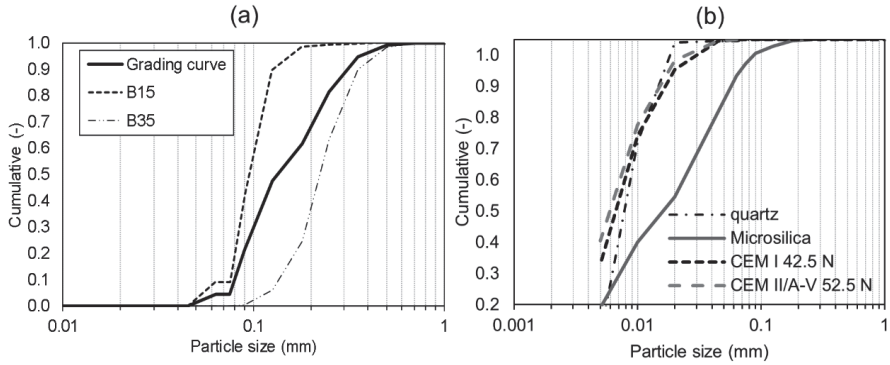


Figure 3.2. (a) Grading curves of the UHPC mix and aggregates: (b) Grading curves of quartz, microsilica and cements applied in the study (Rajczakowska et al. 2019b).

Two sizes of mortar specimens were tested. The $4 \times 4 \times 16 \text{ cm}^3$ and $1.2 \times 1.2 \times 6 \text{ cm}^3$ beams were studied in the Experiment 1 whereas only beams having the dimensions of $1.2 \times 1.2 \times 6 \text{ cm}^3$ in the Experiment 2. Standard steel beams were used for $4 \times 4 \times 16 \text{ cm}^3$ specimens. In the case of the small beams, Teflon molds were used thus avoiding the application of demolding oil. The mixes were produced with a Hobart mixer and a small vacuum mixer type Bredent.

3.1.2. Exposures

The self-healing exposure conditions applied in the Experiment 2 are listed in Table 3.3. Experiment 1 included only full water immersion (Exposure 5, Table 3.3). The used Sika Accelerator contained, according to the producer, 40-60% of Nitrate salts and 40-60% of water. The producer specification stated that SIKa retarder consisted of modified phosphates with sodium metaphosphate (20-30%), sodium gluconate $\text{C}_6\text{H}_{11}\text{NaO}_7$ (2-5%), and water (70-80%). The commercially available drink Coca-Cola was also used. The composition of this substance is not fully known however, in general, it should contain water, high fructose corn syrup, white sugar, carbonic-acid gas, phosphoric acid (approximately 530 mg/L (Bello et al., 1996) and caffeine (Choi et al., 2019). The micro silica used was Microsilica Grade 920D produced by Elkem. The pH value of each medium was checked with pH-indicator strips 30 minutes after the start of the experiment, 15 h, 24 h and every seven days after that.

Table 3.3. Exposure conditions applied in this study with justification (Rajczakowska et al., 2019c).

Exposure	Abbreviation	Justification
Air	EXP 0	Non-healed samples
Deionized water mixed with Accelerator in proportions 3:1 (immersion)	EXP 1	Increasing the rate of hydration process inside the crack; possibly faster healing; different composition of hydrates (Elkhadiri et al. 2009; Escalante-Garcia & Sharp, 1998; Matschei & Glasser, 2010)
Deionized water mixed with Retarder in proportions 3:1 (immersion)	EXP 2	Slowing down the hydration – more hydrates can precipitate on the surface of unhydrated cement grains (Escalante-Garcia & Sharp, 1998; Kjellsen et al. 1991)
Saturated lime water immersion	EXP 3	More Ca^{2+} ions in the solution, higher pH

Coca-Cola immersion	EXP 4	Introducing phosphate anions into the self-healing solution; possibly beneficial retarding effect of sugar on the hydration of self-healing products
Deionized water immersion	EXP 5	Reference exposure
Deionized water immersion with cyclic evaporation (72 h cycle)	EXP 6	Changing of the water regime by introducing the cycles of evaporation as well as different volume of water in order to modify the concentration of ions inside the crack
Dry/wet (deionized water) cycles 24 h/24 h	EXP 7	
Deionized water immersion up to 1 mm height of the sample	EXP 8	
Deionized water immersion up to 5 mm height of the sample	EXP 9	Increasing/decreasing the rate of the hydration process as well changing the hydration products composition. Possible ettringite formation leading to a higher strength regain in case of lower temperature (Liu et al., 2017; Xu et al. 2012)
Water immersion temperature cycle 24 h/ 20°C and 24 h/ 40°C	EXP 10	
Water immersion temperature cycle 24 h/ 20°C and 24 h/ 5°C	EXP 11	
Deionized immersion with microsilica particles 1.25%w	EXP 12	Providing the nucleation sites inside the crack for the self-healing products

3.2. Crack generation

The beams were cracked with the use of a standard three-point bending test with 0.5 mm/s displacement rate, at 1 day (Experiment 1; mortars A, B and U), 12 months (Experiment 1; mortar U) and 7 days (Experiment 2) after casting. The procedure was stopped when a crack opening of around 200 μm was reached which was assessed visually during the test.

3.3. Assessment of the self-healing efficiency

The evaluation of the self-healing process was performed with respect to both crack closure and mechanical properties during both Experiment 1 and Experiment 2 (Figure 3.3).

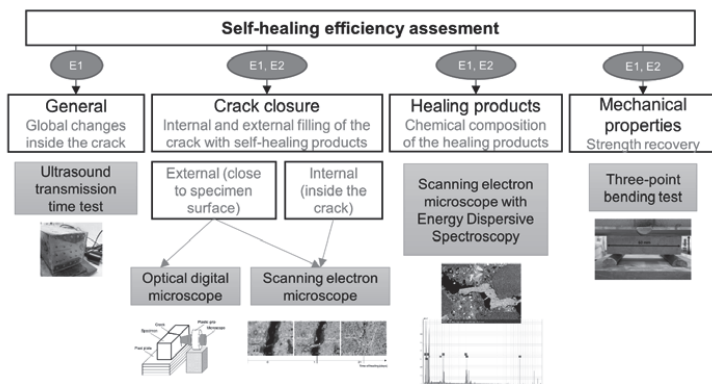


Figure 3.3. Scheme of the tests performed to evaluate the self-healing efficiency.

In addition, during the Experiment 1, the global structural changes in the specimens were monitored with the use of an ultrasound transmission time test. The chemical composition of the healing products was assessed with the use of a Scanning Electron Microscope (SEM)

with Energy Dispersive Spectroscopy (EDS). In the following subsection a detailed description of the applied measuring techniques is described.

3.3.1. Ultrasound transmission

A Pundit Lab instrument with exponential transducers of 54 kHz frequency was applied. The measuring procedure followed the BS EN 12504-4:2004 (2004). The 4 x 4 x 16 cm mortar beams were tested. The transmission time for each specimen was measured before cracking ($t_{t,0}$), after cracking ($t_{t,i}$) as well as, after 14 ($t_{t,14}$) and 21 ($t_{t,21}$) days of healing. The transmission time recovery ratio R_t was determined as a measure of the self-healing efficiency defined as:

$$R_{t,i} = \frac{t_{t,0} - t_{t,i}}{t_{t,0}} \quad (3.1)$$

where i is the moment in time of healing, $t_{t,0}$ is the transmission time before cracking and $t_{t,i}$ is the transmission time at the moment i of healing. A positive sign of the transmission time recovery ratio R_t indicates a beneficial influence of the healing process with a possible closure of the crack whereas a negative sign indicates no healing.

3.3.2. Crack closure

The surface crack closure due to the self-healing was evaluated using a digital light microscope, type Dino-Lite Pro AM-413T with a 1.3 MP camera and field of view of 1280 x 1024 pixels. The image spatial resolution was 7 μm per pixel. A special stand was developed in order to control the position of the microscope with respect to the specific part of the crack. A stand for the specimens was also made from rectangular plastic sheet plates. The goal of this setup was to obtain the images of the same fragment of the crack both before and after healing (Figure 3.4). The image processing methodology was applied in order to gather quantitative information regarding the crack closure of the specimens. The acquired images were converted to 8-bit grayscale and filtered with the use of a median filter with 2-pixel kernel. The histogram thresholding method was used to segment the crack area from the rest of the image, both before and after healing. The ImageJ software was used for the image processing, (Schneider et al. 2012).

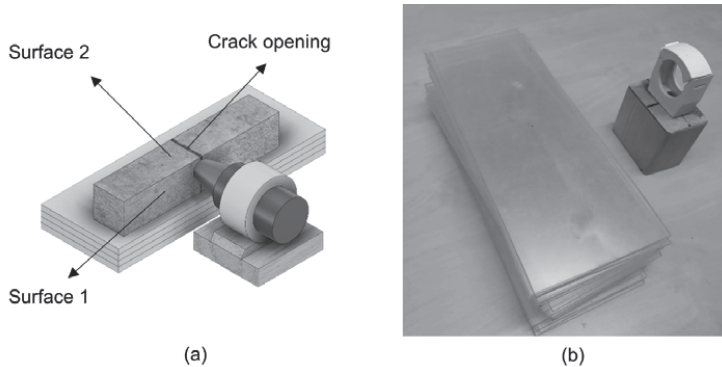


Figure 3.4. (a) Scheme of a design stand, (b) Optical microscope setup. (Rajczakowska et al., 2019c).

The binarised images of cracks, i.e. where white pixels (of value 1) depict the crack area and black pixels (value 0) – the rest of the sample (Rajczakowska et al. 2019a) were applied for the calculation. For each specimen the total analyzed crack length reached approximately 1 cm per image. The global crack closure ratio C was calculated, defined as follows:

$$C = \frac{A_b - A_h}{A_b} \quad (3.2)$$

where A_b and A_h are the area (sum of white pixels) of the crack before and after healing, respectively.

3.3.3. Healing products

The healing products formed inside the crack were analyzed both close to the surface as well as inside the specimen with the use of SEM. A Jeol JSM-IT100 Scanning Electron Microscope with both secondary electron (SE) and backscatter electron (BSE) imaging modes was used.

In the case of the Experiment 1, the crack surface and crack plane were analyzed after 21 days of healing (Figure 3.5). In the Experiment 2, a special procedure for preparation of the specimens was developed (Figure 3.6).

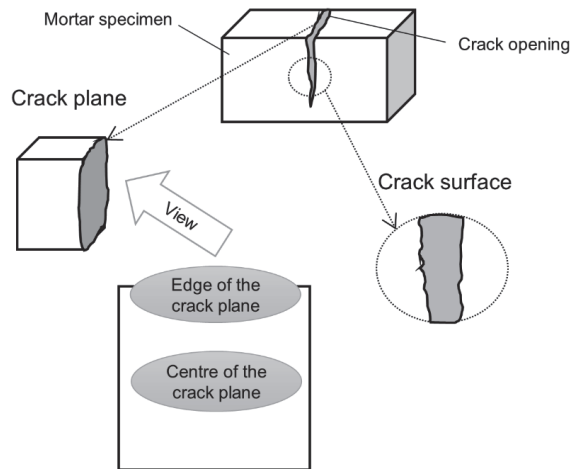


Figure 3.5. Parts of the crack studied in Experiment 1.

Firstly, after 28 days of healing, the surface of the crack was investigated to verify the formation of healing products (Surface 1). Afterwards, specimens were cut and impregnated with a low viscosity epoxy resin under vacuum, grinded and polished using Struers CitoVac and Lab system. A set of grinding plates sprayed with diamond particles having sizes of 9, 3 and 1 μm was used as the grinding media. Two cross-sections were prepared, i.e. Cross-section 1 located around 1 mm below Surface 1 and Cross-section 2 approximately 5 mm below Surface 1 in the middle of the specimen.

The chemical composition of the healing products was examined by the EDS analysis. A Bruker Energy-dispersive X-ray spectroscopy (EDS) was used.

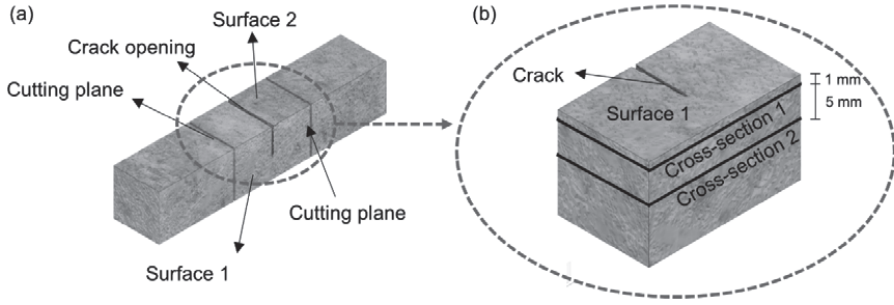


Figure 3.6. Scheme of the specimen preparation for SEM evaluation in Experiment 2 (Rajczakowska et al. 2019c).

3.3.4. Mechanical properties

The recovery of the flexural strength was tested on the 1.2 x 1.2 x 6 cm specimens in both experiments. In the case of the Experiment 1, three samples per set were investigated and average values were calculated. The mechanical strength recovery of the precracked samples, index S_p was defined as:

$$S_p = \frac{S_{av,h} - S_{av,0}}{S_{av,0}} \quad (3.3)$$

where $S_{av,0}$ is the mean value of the flexural strength of the precracked samples. $S_{av,h}$ depicts the strength of the specimens healed in water for 21 days. A positive sign of the strength recovery index S indicates an increase in strength whereas the negative sign may suggest a lack of effect of the healing process on the mechanical parameters. The first group of specimens was precracked on the same day as the healed samples and stored in the room temperature in the air. Both precracked and healed specimens were tested on the same day.

In the case of the Experiment 2, the procedure was altered. Five specimens per set ($N=5$) were tested in order to decrease the standard deviation. The flexural strength recovery S was calculated as follows:

$$S = \frac{1}{N} \sum_{i=1}^N \frac{S_{h,i} - S_{0,i}}{S_{0,i}} \quad (3.4)$$

where $S_{h,i}$ and $S_{0,i}$ are the values of flexural strength of specimen i after and before healing, respectively.

3.3.5. Amount of unhydrated cement

Fragments of specimens A1, U1 and U12 were impregnated in epoxy resin, grinded and polished using Struers CitoVac and Labosystem. A set of grinding plates sprayed with diamond particles having sizes of 9, 3 and 1 μm was applied. The amount of the unhydrated cement was calculated based on the BSE image grey histogram by thresholding the white particles.

4

Results and analysis

The sentence 'the snow is white' is true if, and only if, the snow is white.

Alfred Tarski

4. RESULTS AND ANALYSIS

4.1. Effects of mix composition

The effects of the mix composition on the self-healing efficiency were determined taking into account the crack closure ratio, the morphology of the self-healing products and the flexural strength recovery. Three mixes, cracked after 1 day, were compared, i.e. Ultra-High Performance Concrete mix (mix U1) and two high performance mortars, with (mix B1) and without fly ash (mix A1).

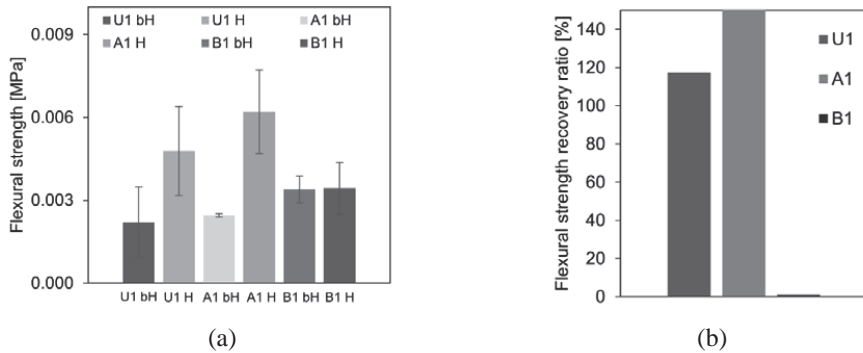


Figure 4.1. (a) Flexural strength of cracked samples measured before healing (bH) and after healing (H), (b) flexural strength recovery ratio S for each type of mix. (Rajczakowska et al. 2019b)

The flexural strength recovery ratio was calculated based on the Equation 3.3 (Figure 4.1b). Only the sample with fly ash (mix B1) did not exhibit any strength regain after 21 days of healing (Figure 4.1). The other stored in water mixes demonstrated an increased flexural strength in comparison with the flexural strength of the pre-cracked samples kept in air. An evidently high standard deviation of the measurements might be related to differences in the geometrical characteristics of the cracks including their length and tortuosity.

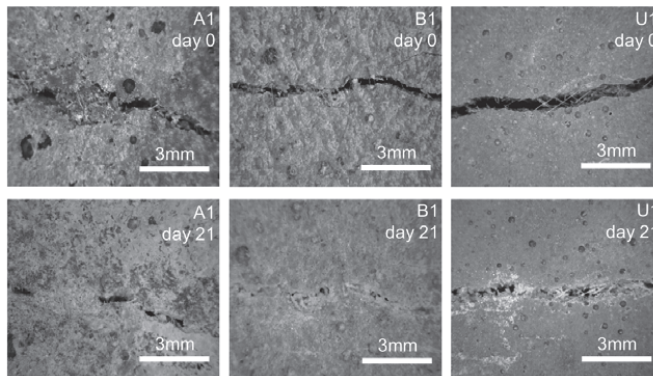


Figure 4.2. Example of light microscope images of the crack before healing. Four images were taken for each sample: (a) A1, (b) B1, (c) U1; and after 21 days of storage in water: (d) A1, (e) B1, (f) U1. (Rajczakowska et al. 2019b)

In contrast to the strength recovery results, the best visible self-healing (Figure 4.2be) as well as the highest crack closure ratio (Figure 4.3) were observed in the case of the mix B1, which contained fly ash. The inconsistency could be related to the fact that the calculated crack closure ratio is a measure of the external surface self-healing which does not include internal healing. The PVA fibers supported formation of healing phases by creating nucleation sites due to their hydrophilic nature (Kan et al., 2010).

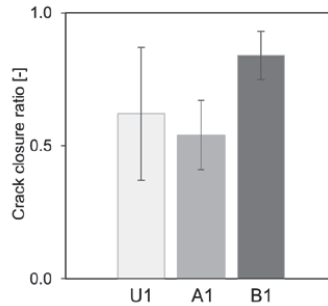


Figure 4.3. Crack closure ratio for each mortar mix calculated according to formula 3.2. (Rajczakowska et al. 2019b)

Only self-healing products with cuboid-like morphology were detected indicating the formation of calcite at the surface of the crack (Figure 4.4). The calcite crystals were visible in all the specimens, in the vicinity of the crack edge as well as on the surface of the PVA fibers.

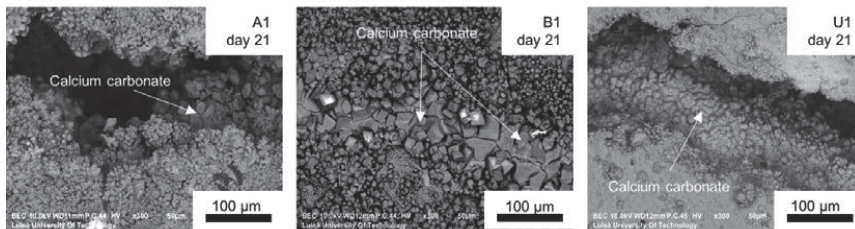


Figure 4.4. SEM BE images (300x) of the crack at the surface for: (a) A1, (b) B1, (c) U1. (Rajczakowska et al. 2019b)

The main phase formed in the crack of the specimen B1 was calcium carbonate. No strength recovery was observed which further indicated that despite a very good crack closure ratio only a very limited amount of the C-S-H precipitated inside the crack.

4.2. Effect of cracking age

The UHPC concrete samples containing very high amounts of unhydrated cement were cracked 1 day (mix U1) and 12 months (mix U12) after casting. It was expected that both samples would demonstrate very good self-healing properties even after one year. The results did not indicate a definite effect of the age on the efficiency of the self-healing process. The differences between mix U1 and U12, in both visual filling of the crack (Figure 4.2cf; Figure 4.6ab) as well as the calculated crack closure ratio (Figure 4.6c) are

hardly noticeable. The flexural strength recovery was higher in the case of the U1 samples suggesting precipitation of different healing products inside the crack (Figure 4.5). At the surface of the crack, calcite was the main phase forming (Figure 4.6d). The majority of the cuboid-crystals were precipitated on the PVA fibers bridging the crack (Figure 4.6e).

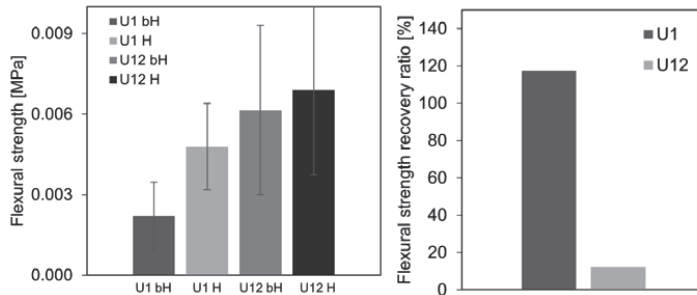


Figure 4.5. (a) The mean flexural strength measured before healing but after cracking (bH) and after healing of the initially cracked samples (h) (b) flexural strength recovery ratio S calculated according to the equation X for mixes U1 and U12. (Rajczakowska et al. 2019b).

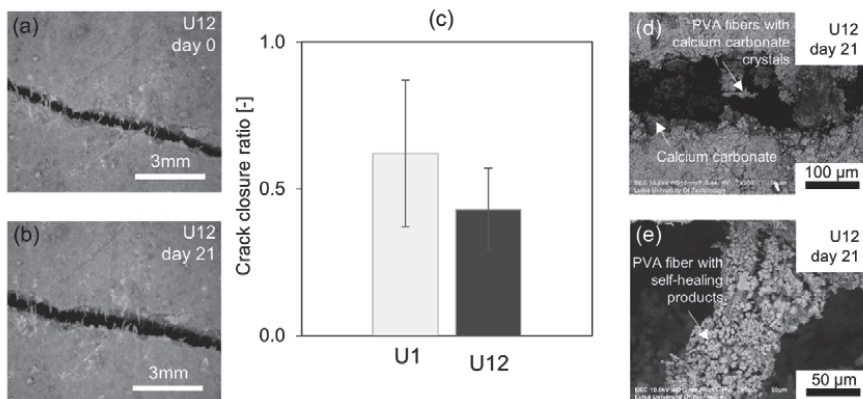


Figure 4.6. (a) Light microscope image of the crack before healing for sample U12; (b) Light microscope images of the crack after 21 days of healing for sample U12; (c) crack closure ratio for samples U1 and U12; (d) SEM BSE image (300x) of the crack at the surface for the sample U12; (e) SEM BSE image (300x) of the self-healing products deposited on the PVA fiber in the specimen U12 (Rajczakowska et al. 2019b).

Different flexural strength recovery ratios were presumably related to the amount of the C-S-H formed inside cracks and, thus, to the presence of unhydrated cement particles. However, the performed SEM analysis of the polished sections of the specimens showed nearly the same of number of anhydrous cement particles; 17.02 % for the mix U1 and 17.34 % the for mix U12. Additional, a SEM analysis of the internal crack planes showed that in fact the amount of the formed C-S-H was higher in the non-aged samples, (Figure 4.7). Calcium carbonate was found in both specimens. The self-healing products observed in the specimen U1 included also ettringite which could be related to its later transformation to the monosulphate (Xu et al., 2012). The presence of ettringite possibly also enhanced the strength regain of the non-aged samples (Gonzalez et al., 1997).

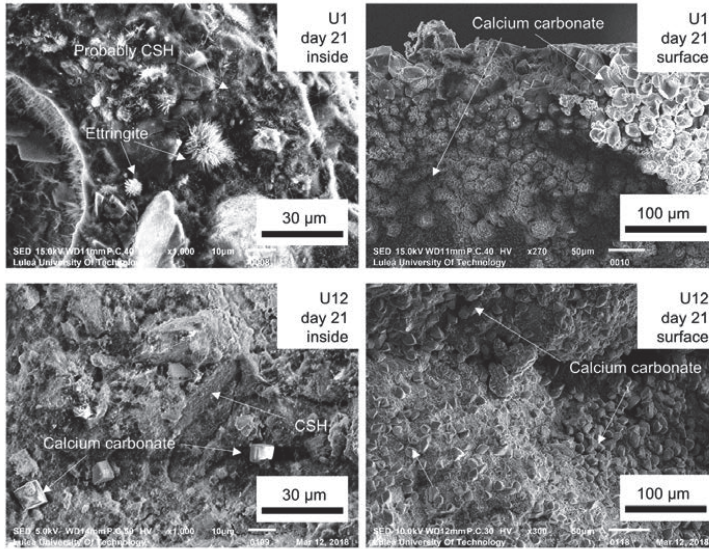


Figure 4.7. SEM SE images (1000x and ~300x) of the crack plane for U1 and U12. (Rajczakowska et al. 2019b).

The chemical composition of the healing products was investigated in the two distinct areas of the crack plane, i.e. close to the crack mouth (Area A, Figure 4.8) as well as inside of the crack plane (Area B, Figure 4.8). The elemental analysis indicated the presence of two main phases (Table 4.1). The cubic-like morphology with no silicon was classified as calcite (Product type 1), whereas the needle-like morphology with the Ca/Si ratio of approximately 1 was classified as C-S-H. Area B was the major location for the C-S-H products while the Area A, close to the surface was dominated by calcite.

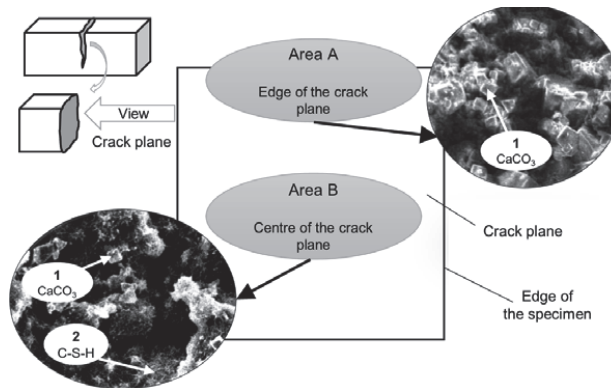


Figure 4.8. Spatial distribution of the self-healing products inside the specimens after 21 days (BSE images, 1500x) (Rajczakowska et al. 2019b).

Table 4.1. Results of the SEM-EDS analysis (Rajczakowska et al. 2019b).

Elements	Atomic Norm. %	
	Product type 1	Product type 2
C	18.48	18.45
Ca	19.08	8.39
Si	0.00	7.36
Al	0.00	0.95
O	62.44	63.85
K	0.00	1.00
Ca/Si	0.00	1.14

4.3. Effect of the healing duration

The healing evolution in time was investigated with the use of the ultrasound transmission time test for mixes A1, B1, U1, and U12. All specimens showed a comparable behavior (Figure 4.8). After precracking the measured transmission time increased significantly. However, later a continuous decrease was observed which was related to the formation of the healing products. The transmission time recovery, calculated according to the Equation 3.1, presented a corresponding, but inverse trend (Figure 4.9) for all the specimens. Recovery of the transmission time was achieved at around 14 days of healing in water for all the mixes (Figure 4.9). Others observed a similar tendency (Kan & Shi, 2012; Ma et al., 2014).

The observed trends are presumably related to the hydration process of the unhydrated cement particles exposed at the crack plane. Due to a small amount of unhydrated cement inside the crack and due to a relatively high amount of water, the resulting water-to-cement ratio inside the crack is very high. This presumably led to the accelerated hydration, and thus to a faster formation of the healing products at the beginning of the process (Huang et al., 2013). A thick layer of the healing products could form on cement grains and limit their dissolution and release of Ca and Si ions. Consequently, the healing processes would be slowed down and eventually stopped (Huang et al., 2013).

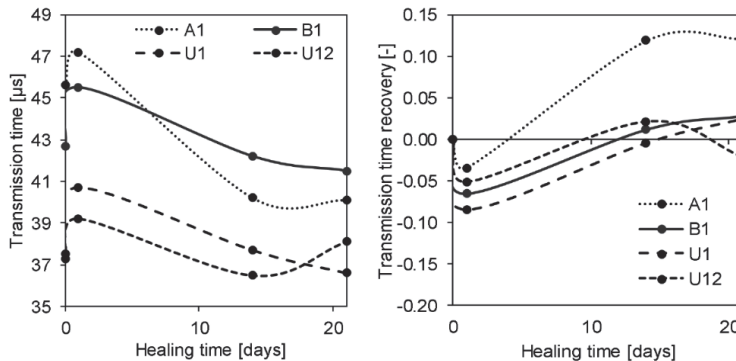


Figure 4.9. (a) Transmission time evolution for samples A1, B1, U1 and U12, (b) transmission time recovery ratio evolution for samples A1, B1, U1 and U12 (Rajczakowska et al. 2019b).

4.4. Effect of environmental exposure

Twelve different exposures were tested. All samples were mortars based on Portland cement having the w/c ratio of 0.35 and the cement to sand ratio of 1. The following exposure groups were analyzed: different water immersion regimes, temperature cycles, water containing accelerating/retarding chemical admixtures, water containing additional ions or particles.

4.4.1. Water immersion

In general, the immersion in water did not result in effective self-healing after 28 days, neither at the surface of the crack, nor internally (Figure 4.11). The images by the optical microscope before and after 28 days of healing as well as SEM images of the Surface 1, Cross section 1 and Cross-section 2 after 28 days of healing are shown in Figure 4.11 for Exposures 5, 6, 7, 8 and 9 (water immersion, water evaporation, dry/wet cycles, water/1 mm and water/5 mm).

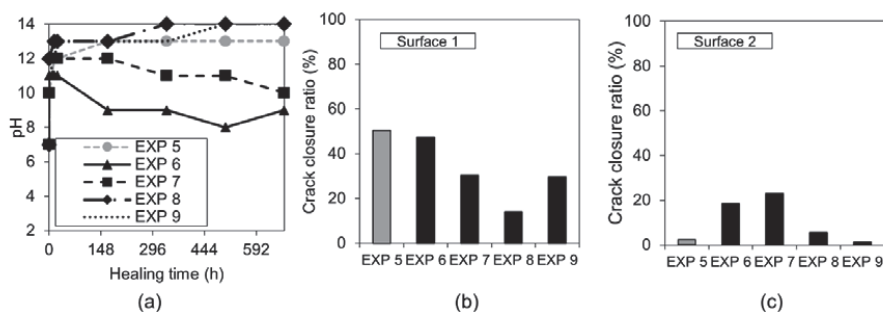


Figure 4.10. (a) pH changes vs time for Exposures 5-9; Crack closure ratio for Exposures 5-9: (b) Surface 1, (c) Surface 2. (Rajczakowska et al. 2019c).

Exposures 5, 8 and 9 had high pH-values throughout the experiment, after the initial increase during the first 12 hours of testing. On the other hand, in the case of Exposures 6 and 7, the pH value reached around 13 after the first 12 h but was followed by its continuous decrease down to 9-10 after 28 days (Figure 4.10a).

The crack closure ratio, calculated according to Formula 3.2 was the highest for Exposures 5 and 6 (water immersion and water evaporation, respectively) on both observed surfaces, Figure 4.10bc. The internal self-healing was observed only for the Exposure 6, with calcite-like products having the Si/Ca ratio of 0.18 (Figure 4.12c). Externally, Exposure 6 led to the closing of the cracks having a width of approximately 50 μm with calcite crystals (Figure 4.12a). Wet-dry cycles (Exposure 7) exhibited a very limited external healing with calcite crystals (Figure 4.12b) and showed no internal crack closure (Figure 4.12d).

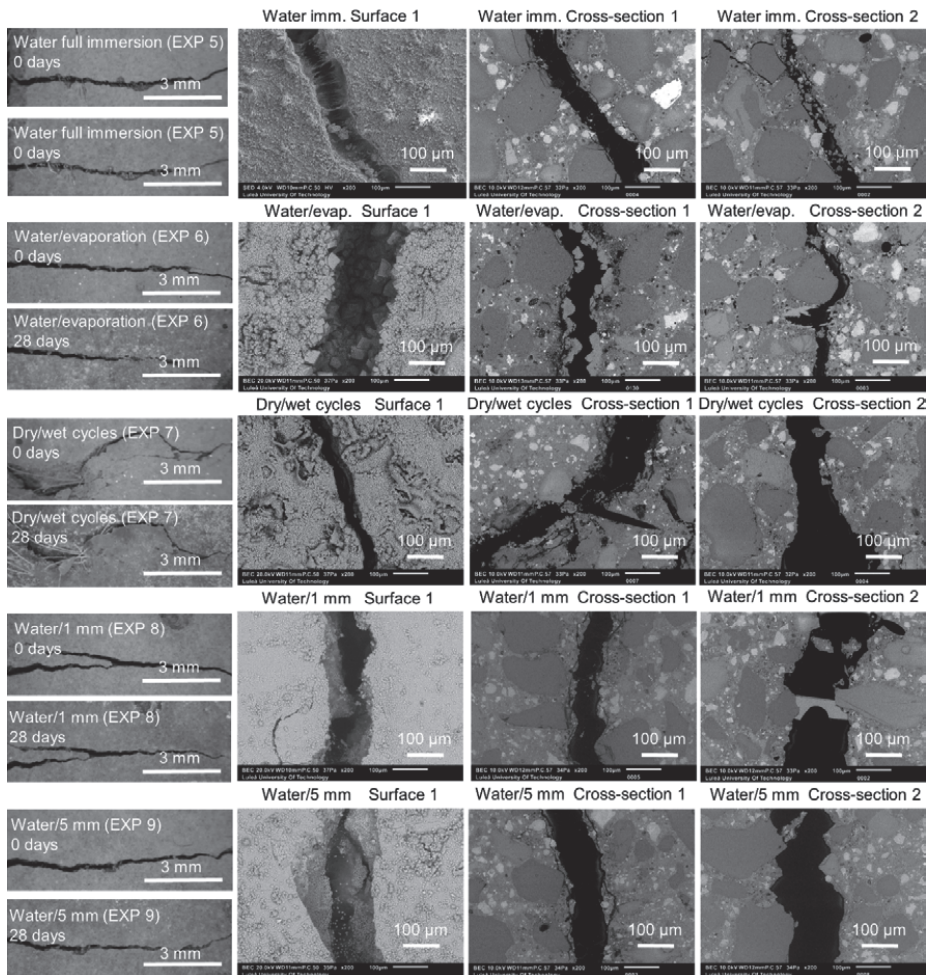


Figure 4.11. Example images of the Surface 1 observed with the optical microscope before (0 days) and after healing (28 days) and the SEM (BSE, 200x) and cross-sections (SEM BSE, 200x) of the specimens healed for 28 days in Exposures 5-9 (water immersion, water evaporation, dry/wet cycles, water/1 mm, water/ 5 mm) (Rajczakowska et al., 2019c).

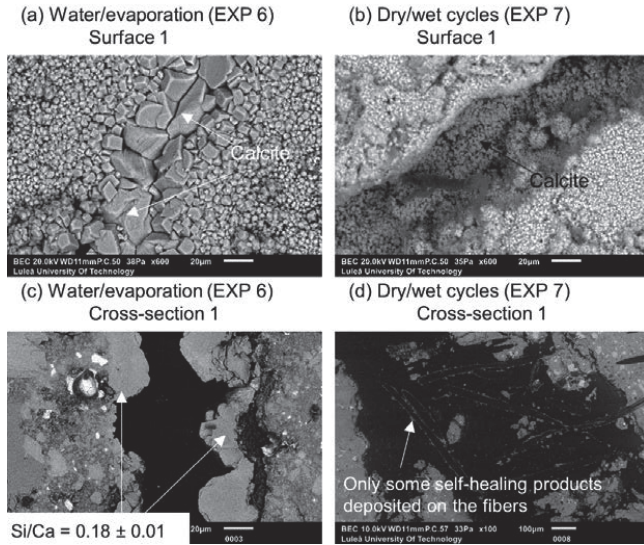


Figure 4.12. (a) Surface 1 Exposure 6 (SEM BSE 600x); (b) Surface 1 Exposure 7 (SEM BSE 600x); (c) Cross-section 1 Exposure 6 (SEM BSE 600x); (d) Cross-section 1 Exposure 7 (SEM BSE 100x) (Rajczakowska et al., 2019c).

Formation of ettringite was observed on the Surface 1 of specimens cured in Exposures 5, 8 and 9 (Figure 4.13). The formation was presumably supported by the water exposure and release of sulfates from anhydrous cement grains (Collepari, 2003).

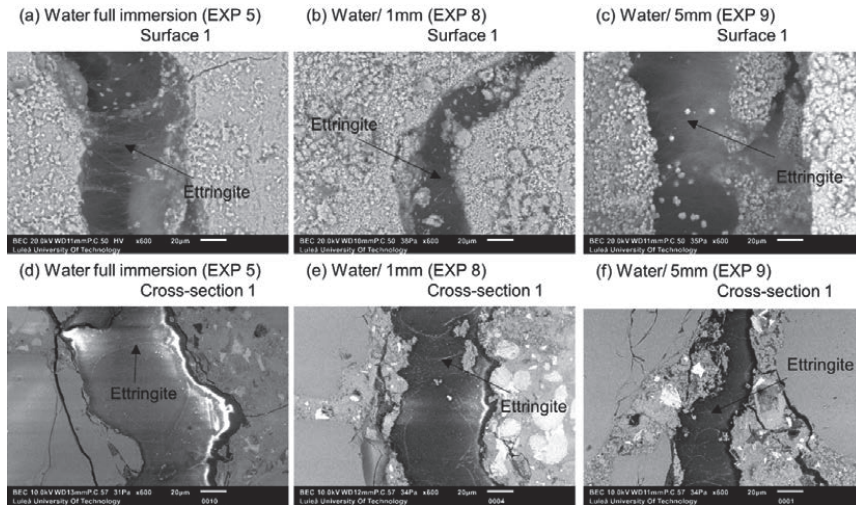


Figure 4.13. (a) Surface 1 Exposure 5 (SEM BE 600x), (b) Surface 1 Exposure 8 (SEM BSE 600x), (c) Surface 1 Exposure 9 (SEM BSE 600x), (d) Cross-section 1 Exposure 5 (SEM BSE 600x), (e) Cross-section 1 Exposure 8 (SEM BSE 600x), (f) Cross-section 1 Exposure 9 (SEM BSE 600x) (Rajczakowska et al., 2019c).

4.4.2. Temperature cycles

Both applied temperature cycles (Exposure 10 and 11) resulted in similar crack closure ratio of approximately 60% (Figure 4.14) both on Surface 1 and Surface 2 (Figure 4.15bc). First cycle consisted of a full water immersion for 24h at 20°C and 24h at 40°C (Exposure 10). The second cycle included a water storage at 20°C for 24 h followed by a storage at 5°C (Exposure 11). The reference sample (Exposure 5) was cured in water having a temperature of 20°C (Exposure 5). The representative images taken after 28 days of healing are shown in Figure 4.14.

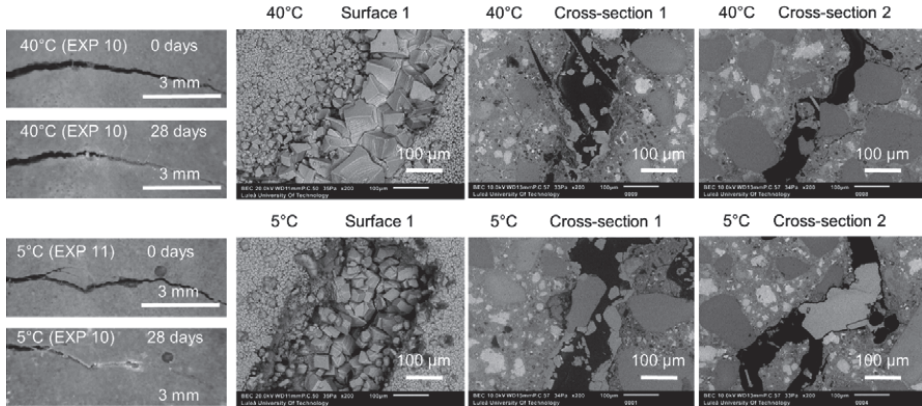


Figure 4.14. Representative images of surfaces and cross-sections of specimens healed at various temperature variation cycles (Exposure 10 and 11) (Rajczakowska et al., 2019c).

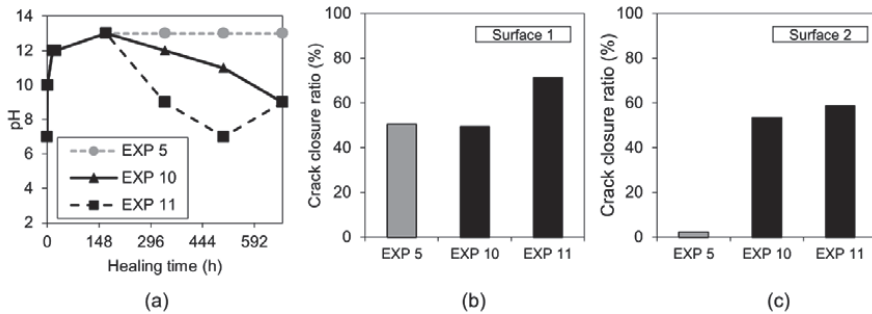


Figure 4.15. (a) pH changes in time for Exposures 5, 10, and 11; Crack closure ratio for different temperature exposures: (b) on Surface 1, (c) on Surface 2 (Rajczakowska et al., 2019c).

In contrast to the reference Exposure 5, both Exposures 10 and 11 demonstrated a decrease of the pH value over time, Figure 4.15a. The tendency was stronger for the Exposure 11 (5°C). In the case of the Exposure 10, calcite formed at the Surface 1, (Figure 4.16ab) while ettringite formed inside the crack with calcite on the crack edge for the Exposure 11 (Figure 4.16cd). The formation of ettringite at low temperatures was observed by others, (Liu et al. 2017). In general, no internal self-healing was visible on Cross-sections 1 and 2 for either of the exposures.

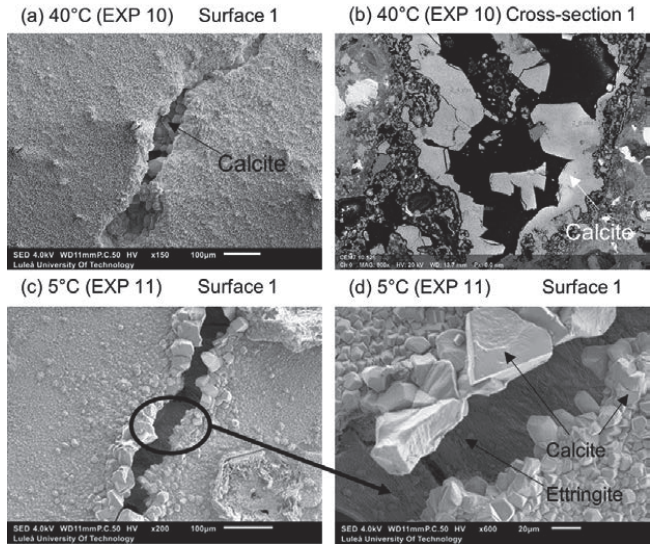


Figure 4.16. (a) Calcite on the surface of the crack healed in 40°C (EXP 10, SEM SE image 150x), (b) Calcite inside the crack (Cross-section 1) healed in 40°C (EXP 10, SEM BSE image 800x), (c) Ettringite on the surface of the crack healed in 5°C (EXP 11, SEM SE image 200x), (d) Ettringite on the surface of the crack healed in 5°C (EXP 11, SEM SE image 200x) (Rajczakowska et al., 2019c).

4.4.3. Accelerating and retarding admixtures

The effect of admixtures modifying the hydration rate was verified with the use of a phosphate-based retarder and nitrate-based accelerator. The images of the Surface 1 before and after 28 days of healing as well as Cross-sections 1 and 2 after 28 days of healing are shown in Figure 4.17.

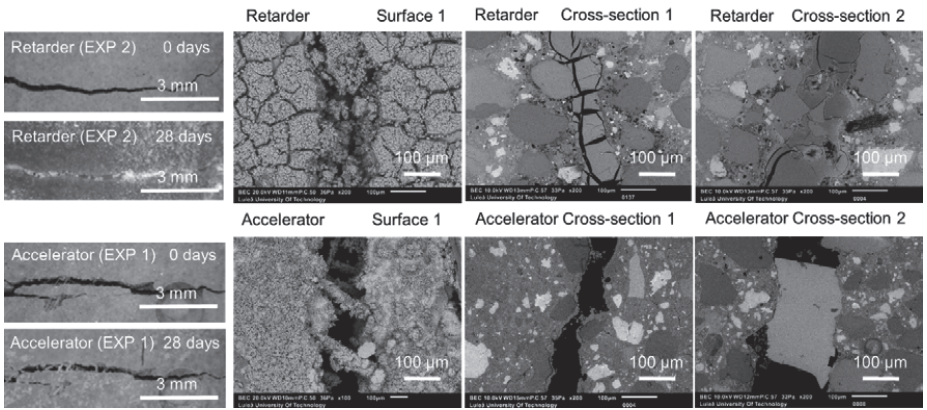


Figure 4.17. Representative images of the surface and cross-sections of the specimens healed in Exposures 2 (retarder) and 1 (accelerator) (Rajczakowska et al., 2019c).

The exposure to the retarder showed a considerably higher external crack closure ratio than exposure to the accelerator or the reference water exposure. The trend was the same at both Surfaces 1 and 2 (Figure 4.18bc). Surprisingly, cracks healed in the Exposure 2 appeared to be fully filled with healing products, not only externally but, as verified with SEM, also internally (Figure 4.17).

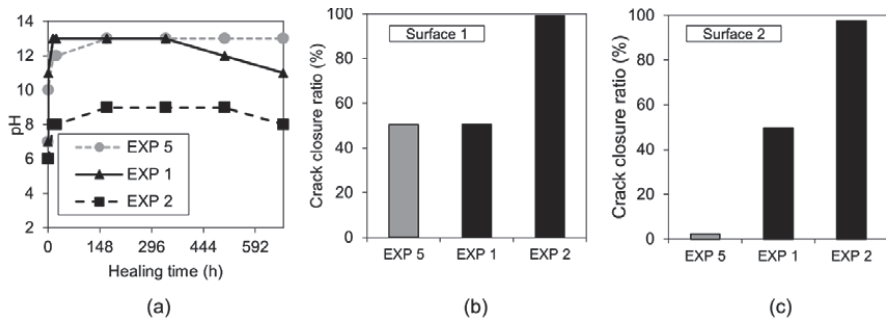


Figure 4.18. (a) pH changes in time for Exposures 5, 1, and 2; Crack closure ratio for Exposures 5, 1, and 2: (b) on Surface 1, (c) on Surface 2 (Rajczakowska et al., 2019c).

The pH values of Exposure 1 (accelerator) essentially followed the behavior of the reference solution (exposure 5, water immersion) (Figure 4.18a). Exposure 2 (retarder) showed a relatively low pH value of approximately 9, which was maintained nearly constant throughout the entire experiment duration (Figure 4.18a).

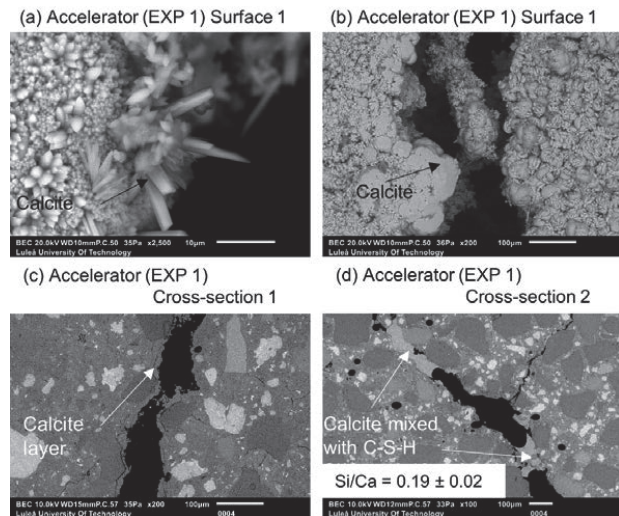


Figure 4.19. Different forms of calcite on the Surface 1 of EXP 1 specimen: (a) SEM BE 2500x, (b) SEM BE 200x, (c) EXP 1 Cross-section 1 – visible calcite layer (SEM BE 200x), (d) EXP 1 Cross-section 2 healing products (SEM BE 100x) (Rajczakowska et al., 2019c).

The SEM analysis revealed the formation of calcium carbonate crystals having various morphologies on the Surface 1 of the specimen exposed to the Exposure 1

(accelerator) (Figure 4.19ab). This phenomenon was not observed in case of the reference Exposure 5 (Figure 4.11). The local pH variations were presumably related to different amounts of CO_3^{2-} and Ca^{2+} ions present in the used healing solutions, (Kirov et al., 1972; Choi et al., 2017). Hardly any healing material was found in Cross-sections 1 and 2 in the Exposure 1 (accelerator) (Figure 4.19cd). Only small deposits of calcite-like products having the Si/Ca ratio of approximately 0.19 were visible inside the crack.

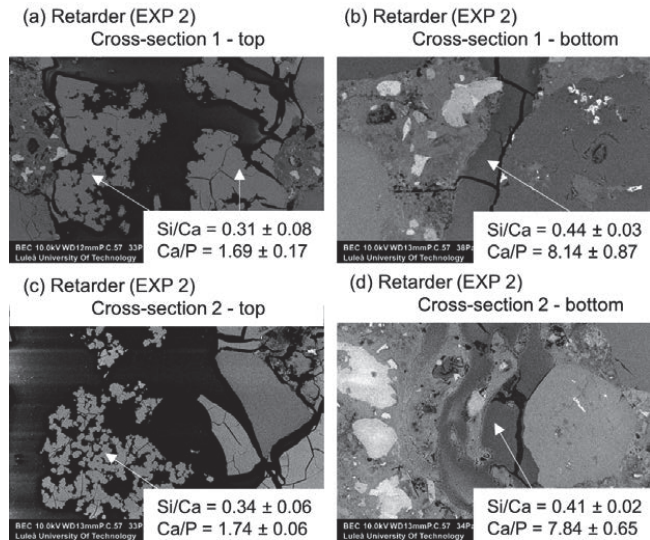


Figure 4.20. (a) Self-healing products at Cross-section 1 at the top of the crack – close to the crack opening (EXP 2, SEM BSE image 600x), (b) Self-healing products at Cross-section 1 at the bottom of the crack (EXP 2, SEM BSE image 100x), (c) Self-healing products at Cross-section 2 at the top of the crack (EXP 2, SEM BSE image 600x), (d) Self-healing products at Cross-section 2 at the bottom of the crack (EXP 2, SEM BSE image 600x) (Rajczakowska et al., 2019c).

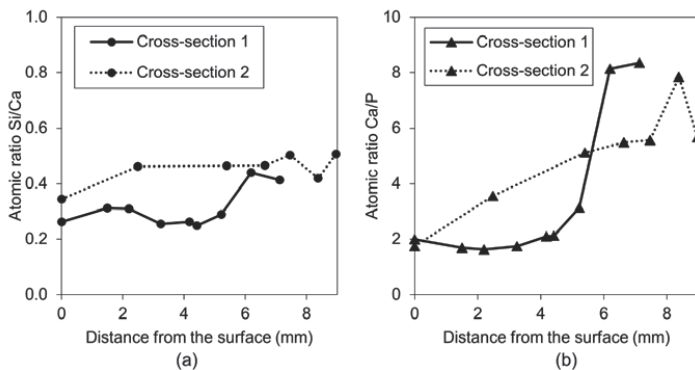


Figure 4.21. (a) Si/Ca atomic ratio of the self-healing products vs the crack length measured at Cross-sections 1 and 2 for the Exposure 2 (Retarder), (b) Ca/P atomic ratio of self-healing products vs crack the length at measured at Cross-sections 1 and 2 for the Exposure 2 (Retarder) (Rajczakowska et al., 2019c).

Large amounts of Calcium and Phosphorus with traces of Silicon and Aluminum were found inside of the cracks subjected to the Exposure 2 (retarder). The calculated Si/Ca as well as Ca/P ratios increased with the crack depth for Cross-sections 1 and 2 (Figure 4.20 and Figure 4.21). This could indicate higher concentrations of ions transported from unhydrated cement particles and from the binder matrix deeper inside the cracks.

The retarding effect of the used substance is related to the presence of phosphorus. In the process, phosphate anions bond with calcium ions and form unstable calcium hydrogen phosphate preventing the formation of the C-S-H, (Kalina et al. 2016). Later, the phosphate compounds dissolve and less soluble phases are formed, including secondary C-S-H and calcium hydroxyapatite (HAP) (Kalina et al. 2016). A sufficiently high concentration of phosphates might also lead to the additional precipitation of HAP (Bénard et al. 2005). The healing observed in the Exposure 2 (retarder) could be related to those reactions. The observed cracking of the phases formed inside the cracks during the healing process could be related to ongoing chemical reactions. For instance, the conversion of HAP precursor, amorphous calcium phosphate (ACP), into the HAP resulted in shrinkage, (Bénard et al., 2008). The HAP was found to be preceded by the precursors' growth, which additional supports the formulated hypothesis, (Van Kemenade & De Bruyn, 1987; Meyer & Weatherall, 1982). The low pH of the retarder solution could be also related to the formation of the calcium phosphate (Mekmene et al., 2009).

4.4.4. Additional ions/particles in the self-healing solution

Self-healing solutions with additional phosphate ions (Exposure 4, Coca-Cola), calcium ions (Exposure 3, lime water) and microsilica particles (Exposure 12) demonstrated a noticeable external self-healing after 28 days (Figure 4.22). Internal self-healing was only visible for Coca-Cola and microsilica exposure (Figure 4.22).

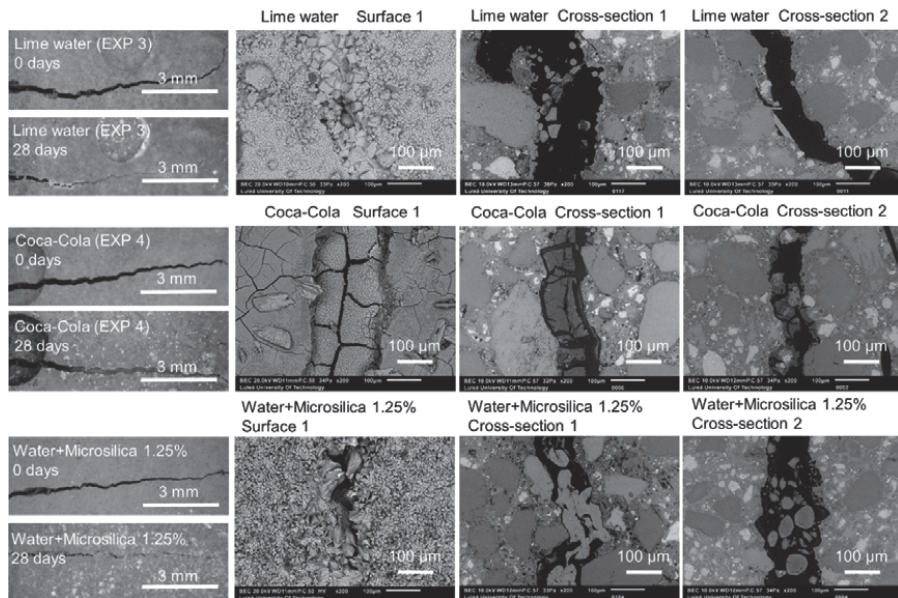


Figure 4.22. Representative images of surfaces and cross-sections of specimens healed in Exposures 3 (lime water), 4 (Coca-Cola) and 12 (water and 1.25%w microsilica particles) (Rajczakowska et al., 2019c).

The crack closure ratio for Exposures 3, 4 and 12 was significantly higher than for the reference Exposure 5 (water immersion) on both Surfaces 1 and 2 (Figure 4.23bc) but lower than for the Exposure 2 (retarder). The pH values initially increased for all analyzed exposures. Later, a decrease was observed for Exposures 3 and 12. The pH of the Coca-Cola solution (Exposure 4) was similar as observed for the Exposure 2 (retarder). All exposures reached the pH value of 9 after 2 weeks of healing.

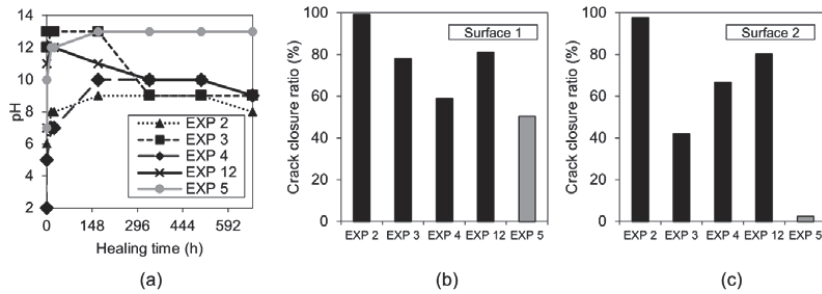


Figure 4.23. (a) pH changes in time for Exposures 5, 3, 3, 4 and 12; Crack closure ratio for Exposures 5, 3, 3, 4 and 12: (b) on Surface 1, (c) on Surface 2 (Rajczakowska et al., 2019c).

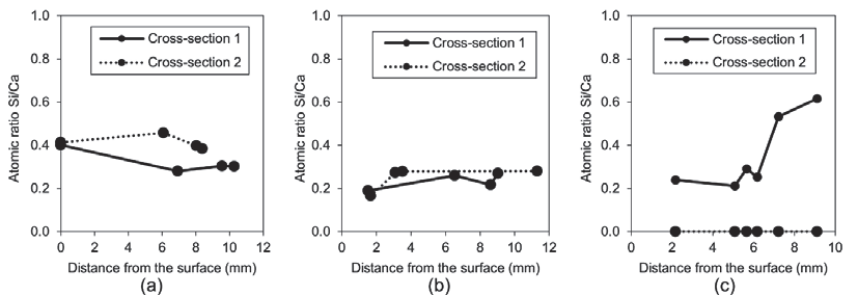


Figure 4.24. Si/Ca atomic ratios: (a) Exposure 4 (Coca-Cola); (b) Exposure 3 (Lime water), (c) Exposure 12 (microsilica) (Rajczakowska et al., 2019c).

Healing products formed inside of cracks in Exposures 3 and 4 compared to the Exposure 2, Figure 4.24ab. The Si/Ca ratios calculated for those specimens were relatively stable. The amount of silicon in the Exposure 4 was larger than in the Exposure 3 (Figure 4.24ab, Figure 4.25 and Figure 4.26). The mechanism of the self-healing observed in the Exposure 4 presumably followed a similar pattern as observed in the Exposure 2 (retarder) due to the presence of phosphate ions and sucrose (Zhang et al. 2010). The presence of the phosphate ions in the Coca-Cola solution resulted in the formation of calcium phosphate compounds inside the crack having a Ca/P ratio between 3 and 9 (Figure 4.25ab). Nevertheless, a more detailed mechanism could not be proposed due to the unknown chemical composition of the Coca-Cola drink. The efficiency of the self-healing was increased in the Exposure 3, due to the presence of additional calcium ions. The self-healing products which precipitated in the cracks were calcite, C-S-H and portlandite (Figure 4.26cd).

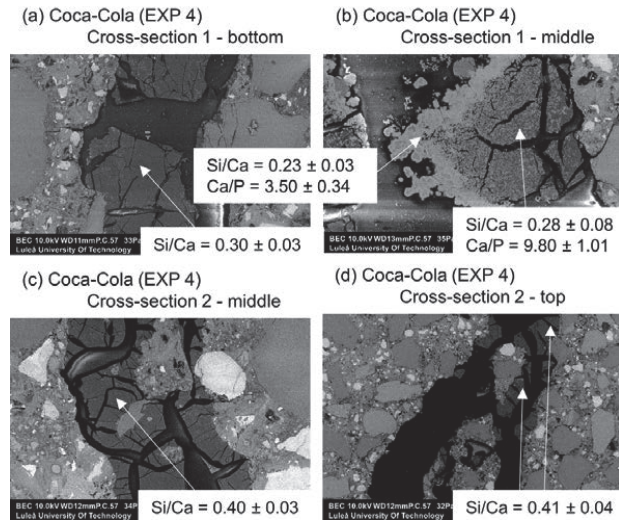


Figure 4.25. Exposure 4, Self-healing products in the Cross-section 1 (a) at the bottom of the crack (SEM BSE image 400x), (b) in the middle of the crack (SEM BSE image 600x); Self-healing products at Cross-section 2 (c) in the middle of the crack (SEM BSE image 600x), (d) at the top of the crack (SEM BSE image 100x).

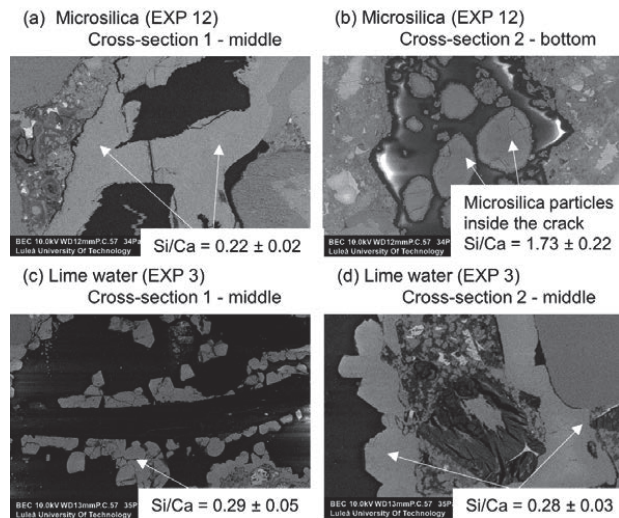


Figure 4.26. (a) Self-healing products in the Cross-section 1 in the middle of the crack (EXP 12, SEM BSE image 400x), (b) Self-healing products at Cross-section 2 at the bottom of the crack (EXP 12, SEM BSE image 400x), (c) Self-healing products at the Cross-section 1 in the middle of the crack (EXP 3, SEM BSE image 500x), (d) Self-healing products at the Cross-section 2 in the middle of the crack (EXP 3, SEM BSE image 1000x) (Rajczakowska et al., 2019c).

In case of the Exposure 12 (water with microsilica particles), a very dense calcite structure was observed inside of crack at the surface of the specimen and at the Cross-section 1 (Figure 4.22, Figure 4.26a). In contrast, inside the crack (at Cross-section 2) only

few agglomerates of microsilica particles were visible in several locations of the crack (Figure 4.26b). No additional self-healing products were detected.

4.4.5. Strength recovery

The flexural strength recovery was investigated only for selected exposures chosen based on the efficiency of the crack filling, i.e. Exposure 2 (Retarder), Exposure 3 Saturated limewater), Exposure 4 (Coca-Cola), Exposure 5 (reference, water immersion), Exposure 6 (water evaporation, and Exposure 12 (water with micro silica) and Exposure 0 (cured in the air). Additional, two exposures, Exposure 2a with 7 wt% of retarder and Exposure 12a with 2.5 wt% of microsilica in water were tested. The flexural strength recovery was calculated based on the Equation 3.4. Five specimens per Exposure were studied. Correspondingly, the crack closure ratio on Surfaces 1 and 2 were calculated for those specimens based on the images taken with the optical microscope.

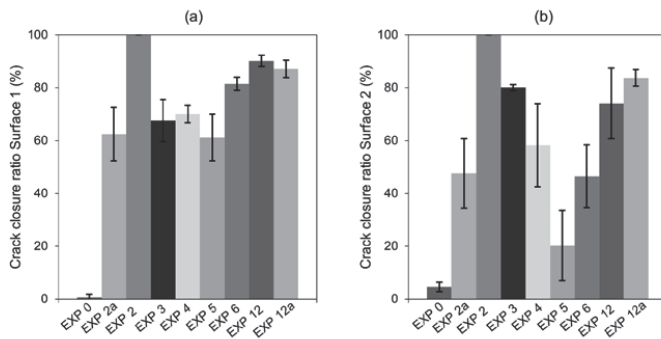


Figure 4.27. Crack closure of selected exposures: (a) Surface 1, (b) Surface 2 (Rajczakowska et al., 2019c).

The external self-healing for all selected exposures was very high on the Surface 1 (Figure 4.27a). However, relatively large variations were observed on the Surface 2 due to the large crack width (Figure 4.27b). Significant recovery of the flexural strength, reaching around 60% was only observed for specimens healed in the Exposure 12 (water with microsilica). Remaining exposures showed strength recovery values similar to samples cured in air. Unfortunately, the impressive internal self-healing observed in the Exposure 2 did not produce satisfactory strength regain results.

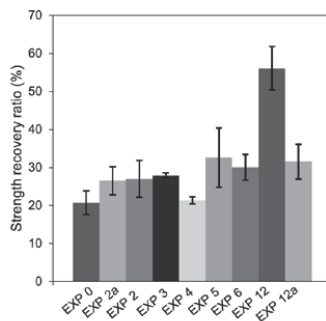


Figure 4.28. Strength recovery for selected exposures (Rajczakowska et al., 2019c).

5

Discussion and Conclusions

Any knowledge that doesn't lead to new questions quickly dies out:
it fails to maintain the temperature required for sustaining life.

Wisława Szymborska

5. DISCUSSION AND CONCLUSIONS

5.1. Autogenous self-healing mechanism – hypothesis

The Experiment 1 aimed to confirm a commonly accepted hypothesis regarding the dependence of the self-healing efficiency of concrete on the amount of available unhydrated material. For this reason, an “extreme” mix composition was chosen, i.e. the UHPC. Surprisingly, the results of the study did not confirm the expected self-healing potential of the UHPC. On the contrary, the mortar mixes with lower amount of cement and higher water-to-cement ratio showed a higher crack closure recovery. The results of the Experiment 1 suggested a specific pattern of self-healing shown in Figure 5.1.

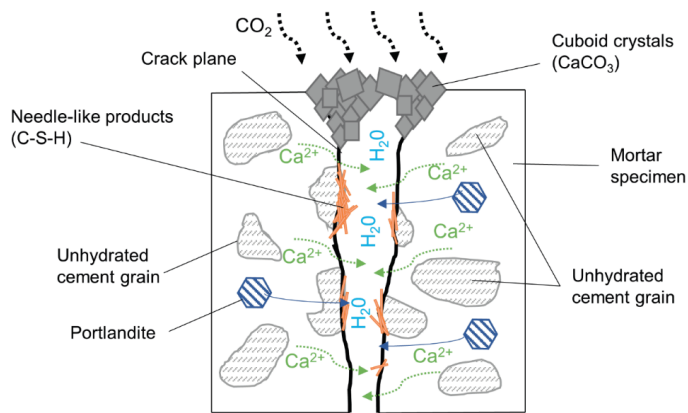


Figure 5.1. The proposed self-healing mechanism scheme (Rajczakowska et al., 2019b).

The self-healing mechanism consists of two processes, i.e. the formation of healing products at the crack mouth and inside the crack. Calcium carbonate forms at the crack mouth while a mix of calcium carbonate and other phases develop in the crack. The calcium carbonate forming at the crack mouth contributes to the enhanced durability of the healed material due to the closure of the crack and by preventing ingress of harmful substances inside the concrete microstructure. The formation of healing products in a crack may result in a strength recovery by formation of C-S-H or Ettringite (Granger et al., 2007ab). Those hydration products were observed inside the samples, which showed higher values of the flexural strength recovery ratio (A1 and U1) tested in the Experiment 1.

The calcite precipitation appears to be similar to the carbonation of Portland cement. The calcium ions, transported from the binder matrix, react with carbonate ions from the atmospheric carbon dioxide dissolved in water (Figure 5.1). The calcium originates from the unhydrated cement particles and portlandite. The formation of large amounts of calcite was primarily observed at the surface near the crack opening. This might indicate that conditions present in that area are optimal for the precipitation of calcium carbonate due to the sufficiently high amount of both, calcium and carbonate ions, (Sisomphon et al., 2012). The crack is closed by the cuboid crystals formed at the surface, which presumably leads to a higher ion concentration inside the crack. This in turn, enables the formation of other self-healing products inside the crack, including C-S-H, Ca(OH)₂ and ettringite (Huang et al., 2013).

The results of the Experiment 1 revealed that the crack closure was significantly smaller for the aged UHPC sample (U12) than for the 1-day-old sample (U1) which contained more interconnected pores. This indicates that the porosity of the binder matrix, and in particular, the amount of interconnected pores have a crucial role in the self-healing process. The growth rate of the hydration products inside the healed crack depends primarily on the concentration of calcium and silicone ions. Therefore, the permeability of the binder matrix affects the transport of those ions into the crack efficiently. A dense, less porous cement matrix, as for example in the case of the aged UHPC, will hinder the self-healing process.

The performed preliminary study revealed several fundamental unresolved problems related to the mechanism of the autogenous self-healing. As the self-healing efficiency of the UHPC was relatively low, it appears that the availability of unhydrated cement inside the crack plays secondary role in the self-healing mechanism and does not guarantee a satisfactory crack closure. Fly ash demonstrated an impressive external crack closure ratio with calcite crystals but at the same time possibly hindered the growth of C-S-H inside the crack. Those results indicated that the Secondary Cementitious Materials (SCMs) play a crucial role in the autogenous self-healing process.

An insufficient calcium and silicone ion concentration inside the crack is presumably governed by two major obstacles:

- Obstacle 1 – The impermeable binder matrix with low amount of interconnected pores related to the low water-to-binder ratio, high amounts of silica fume, etc.;
- Obstacle 2 – The impermeable shell of hydration products which is quickly formed on the surface of freshly exposed unhydrated cement.

The obtained results confirmed the dependency between the autogenous self-healing process and the two main groups of factors, i.e. the mix composition (related to the Obstacle 1) and the exposure conditions (related to the Obstacle 2). Only full water immersion exposure was investigated in the Experiment 1. The self-healing efficiency was possibly enhanced by increasing the ion concentration inside the crack and by introducing different chemical substances promoting the formation of self-healing products (Experiment 2). The Obstacle 2 was addressed by controlling the hydration rate inside the crack by adding to the healing liquid a retarding admixture. Four groups of exposures were tested: different water immersion regimes, the effects of the temperature, the presence of the hydration rate-modifying admixtures and of additional ions/particles in the self-healing solution. The summary of the observed effects of both internal and external self-healing for each applied exposure is presented in Table 5.1.

Table 5.1. Summary of the results of the Experiment 2 (Rajczakowska et al., 2019c).

Exposure	Abbreviation	External self-healing	Internal self-healing
Deionized water mixed with Accelerator in proportions 3:1 (immersion)	EXP 1	Very limited crack closure; Several calcite crystals of various shapes	Almost no healing; Several microns thick calcite layer under the surface, inside – few thicker deposits of calcite mixed with CSH (Si/Ca=0.19)
Deionized water mixed with Retarder in proportions 3:1 (immersion)	EXP 2	The crack almost completely healed; calcium phosphate compounds on the surface with some amount of sodium originating from the self-healing mixture	Very high internal crack closure; Calcium phosphate compounds as well as CSH; Si/Ca and Ca/P increasing with crack depth

Saturated lime water immersion	EXP 3	Very good external self-healing; dense layer of calcite crystals present at the surface	Almost no internal self-healing; few self-healing products with average Si/Ca of 0.3
Coca-Cola immersion	EXP 4	Efficient external crack closure; calcium phosphate compounds with Ca/P ranging from 1.5 to 2.5	Self-healing products visible inside with CSH-like precipitates with Si/Ca of around 0.3-0.4; some calcium phosphate products present
Deionized water immersion	EXP 5	Very limited external healing, ettringite and calcite crystals filling the crack	Ettringite visible close to the surface; no internal self-healing
Deionized water immersion with cyclic evaporation (72 h cycle)	EXP 6	Some crack closure; bigger calcite crystals covering the crack	Layer of calcite inside of the sample closure to the surface, few self-healing products in deeper parts of the crack
Dry/wet (deionized water) cycles 24 h/24 h	EXP 7	Almost no external self-healing with small calcite crystal layer at the surface	No internal self-healing except for few healing products deposited on the PVA fibers surface
Deionized water immersion up to 1 mm height of the sample	EXP 8	Minimal external healing, ettringite present; no noticeable differences between exposure 8 and 9	Ettringite visible close to the surface; no internal self-healing
Deionized water immersion up to 5 mm height of the sample	EXP 9		
Water immersion temperature cycle 24 h/ 20°C and 24 h/ 40°C	EXP 10	Very limited external healing, calcite crystals filling the crack	Hardly any internal healing with only single calcite crystals
Water immersion temperature cycle 24 h/ 20°C and 24 h/ 5°C	EXP 11	Efficient external crack closing; calcite crystals inside the crack as well as thick layer of ettringite	
Deionized immersion with microsilica particles 1.25%w	EXP 12	Very high external self-healing with densified calcite structure filling the crack	Agglomerates of microsilica particles inside the crack without self-healing products.

Exposure conditions modified by application of cyclic wetting, limiting used water volumes, did not result in satisfactory self-healing (exposures 5 to 9). Lower temperatures in the applied temperature cycles, promoted the formation of ettringite and resulted in crack closure. The further optimization of the concrete mix or increasing the time of the exposure to low temperatures could presumably lead to a higher self-healing efficiency.

The most efficient external and internal self-healing was observed in the case of the exposure based on phosphate retarder (Exposure 2). The mechanism possibly includes two distinct processes.

The first process is related to the retarding action of the admixture. In this case, the phosphate ions are adsorbed on the surface of unhydrated cement grains, leading to a slower formation of C-S-H, portlandite and ettringite (Figure 5.2). This inhibits the formation of a dense impermeable shell (Obstacle 2). The amount of C-S-H formed inside the crack increased with the distance from the surface of the specimen which indicates a higher concentration of calcium and silicate ions deeper inside the crack, thus supporting the proposed mechanism.

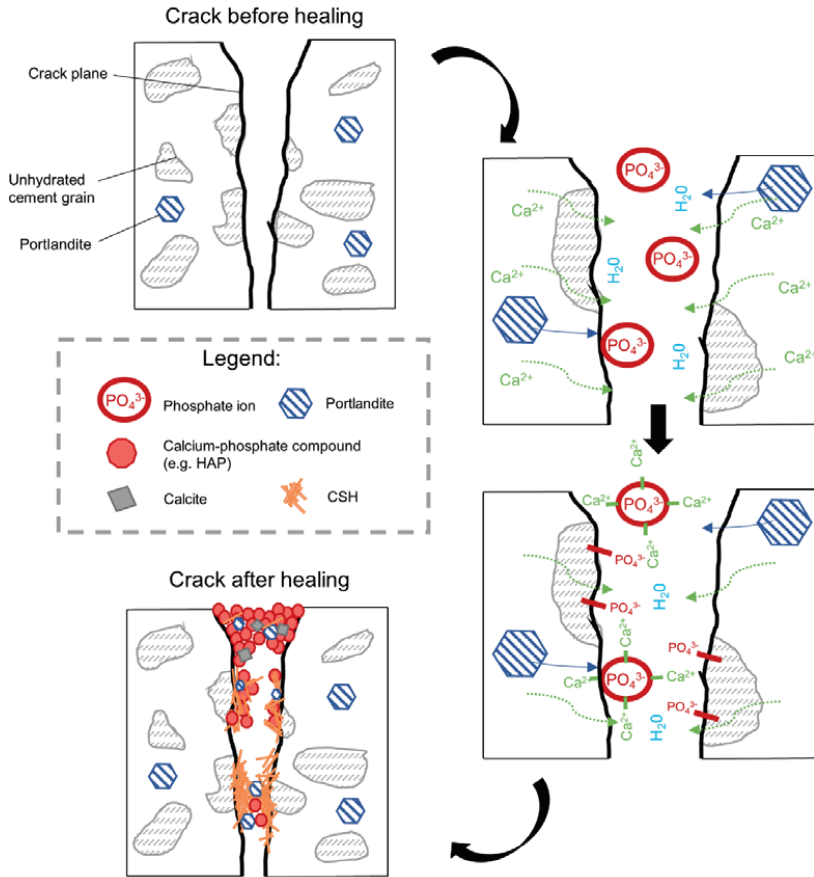


Figure 5.2. Possible self-healing mechanism for samples exposed to phosphate based retarder exposure conditions (Rajczakowska et al., 2019c).

The second process is based on a direct reaction between the phosphate ions from the retarder and the calcium ions from the unhydrated cement grains and from the cement matrix. This leads to the precipitation of calcium phosphate compounds inside the crack, contributing to the high closure ratio observed in the Exposure 2. A higher amount of phosphorus was observed closer to the crack mouth thus indicating that the precipitated phases in the location close to the surface of the sample consist mostly of calcium phosphate compounds such as the HAP (Figure 5.2). The reactivity of calcium released from C-S-H with phosphate anions contaminated water was earlier detected in the wastewater treatment studies (Maeda et al., 2018; Karageorgiou et al., 2007; Naus et al., 2007; Guan et al., 2013). Healing of crack by the HAP is beneficial as it forms more stable and less soluble compounds than calcium hydroxide, (Naus et al. 2007). However, its flexural strength is lower than for the C-S-H, which explains the lack of flexural strength recovery in the case of the Exposure 2. The improved strength of the HAP in biocomposites was achieved by addition of Carbon Nanotubes (CNTs) (Pei et al. 2019) which could serve as a possible future solution to this problem.

The Coca-Cola exposure, potentially containing sucrose and considerable amounts of phosphates, is expected to follow a similar mechanism as the described case using retarder. Nevertheless, a lack of reliable data on the precise chemical composition of this drink, makes a definite answer impossible.

The mixture of water and microsilica particles (Exposure 12) induced the highest flexural strength regain. The particles presumably served as nucleation sites for the hydration products inside the crack. The mechanism here appears to be similar as in the case of PVA fibers.

5.2. Conclusions

The following conclusions can be formulated:

- A large amount of cement in the concrete mix does not ensure the efficient autogenous self-healing of cracks;
- A dense and impermeable binder matrix microstructure having, e.g. a low water-to-cement ratio or a high amount of silica fume, limits the transport of calcium and silicone ions to the crack thus diminishing the precipitation of healing products;
- Fly ash supports the formation of a thick layer of calcite over the crack mouth. It does not support the flexural strength recovery due to the lack (or limited) formation of healing products inside the crack, in particular the load bearing phase C-S-H;
- Calcium carbonate (cuboid crystals) forms close to the surface of the sample, at the crack mouth, whereas C-S-H and ettringite (needle-like products) develop deeper inside the crack. The formation of C-S-H and ettringite is presumably connected to the flexural strength regain. On the other hand, calcite, which does not support the recovery of the mechanical properties, is possibly responsible for the control of conditions inside the crack, e.g. helping to obtain a higher calcium and silicone ion concentration inside the crack;
- Water alone is inefficient in promoting self-healing;
- A phosphate-based retarding admixture promotes the self-healing by crack closure at the crack mouth as well as internally; the self-healing mechanism is presumably based on two processes, i.e. inhibiting the formation of a dense hydration shell on the surface of unhydrated cement grains and the precipitation of calcium phosphate compounds inside the crack. Unfortunately, this exposure did not lead to the recovery of strength regain, suggesting that satisfactory internal crack closure does not necessarily contribute to the regain in mechanical parameters;
- Water mixed with microsilica particles supports an external crack closure as well as induces flexural strength regain. The silica particles possible act as nucleation sites for the formation of self-healing products.

5.3. Addressing research questions

RQ1: *What is a more reliable self-healing approach for concrete considering the efficiency, impact on fresh and hardened properties, cost, safety, and full-scale applications?*

Based on the performed critical literature review, it can be stated that the autogenous self-healing is more reliable than autonomous methods with respect to the impact on fresh and hardened concrete properties. It is also more cost effective, safer and feasible in terms of full-scale applications. Nevertheless, the efficiency of the process still has to be improved.

RQ2: *How does the mix composition affect the efficiency of the self-healing process?*

The mix composition is a governing factor when it comes to the efficiency of the autogenous self-healing process. A commonly accepted hypothesis states that the healing is more effective for mixes which have a high amount of unhydrated binder available. This would favor mixes with a low water-to-cement ratio and high amount of cement. However, this study demonstrated that a large amount of cement, such as in the case of Ultra High Performance Concrete (UHPC), does not ensure an efficient autogenous self-healing of cracks; Significantly higher crack closures were observed for the OPC mortar and mortar containing fly ash. A very dense, impermeable concrete matrix, i.e. for mixes with low water-to-cement ratio or high amount of silica fume, prevents the transport of calcium and silicone ions to the crack, diminishing the precipitation of healing products. To confirm thus hypothesis, further studies on mix compositions with varied water-to-cement ratios are needed.

RQ3: *How does the concrete age affect the efficiency of the self-healing?*

The self-healing efficiency diminishes with the age of the concrete for the mixes with a high amount of cement and a low water-to-cement ratio. It is presumably related to the densification of the cement matrix with age rather than to the decreasing amount of unhydrated cement.

RQ4: *What is the effect of the environmental exposure on the self-healing efficiency, morphology and composition of the healing products, both inside and at the surface of the crack?*

Exposure is a critical factor that has influence on the self-healing process. The commonly applied water exposure appeared to be an inefficient self-healing curing regime despite the application of different cycles and water volumes. A phosphate-based retarding admixture exhibited the highest self-healing efficiency; the crack closure was observed at the crack mouth as well as internally; the self-healing mechanism is presumably based on two processes, i.e. inhibiting of the formation of a dense hydration shell on the surface of unhydrated cement grains and the precipitation of calcium phosphate compounds inside the crack. Unfortunately, this exposure did not lead to the recovery of the strength, suggesting that satisfactory internal crack closure does not necessarily contribute to the regain in strength. Water mixed with microsilica particles demonstrated very well external crack closure as well as acceptable flexural strength regain. The silica particles possible act as

nucleation sites for the formation of self-healing products, having properties helping to regain the strength.

RQ5: *How and to what extent does the addition of Supplementary Cementitious Materials contribute to the self-healing process?*

Fly ash appeared to have contributed to the highest external crack closure ratio, with a visible thick layer of calcite covering the crack mouth; however, no flexural strength recovery was observed in this case, presumably due to a limited formation of load bearing healing products inside the crack. Further studies are needed to confirm this phenomenon.

6

Future research

One never notices what has been done; one can only see what remains to be done.

Maria Skłodowska-Curie

6. FUTURE RESEARCH

The preliminary experimental results presented in this licentiate thesis, combined with previous research, demonstrated that the logical pattern of self-healing behavior of cementitious materials exists. However, several mechanisms are to be determined in order to describe fully the phenomenon under different conditions. The verification of those mechanisms requires further experimental studies, in particular:

- Fly ash appeared to have a positive influence on the efficiency of the external crack closure, therefore different mix compositions should be tested in order to confirm the effect of fly ash and slag on the external self-healing. As the strength recovery was not successful in case of fly ash blended cement, the internal self-healing should be also investigated. A systematic experimental setup should be designed which takes into consideration the effect of the amount of SCMs as well as their chemical compositions. Self-healing products' elemental and possibly mineralogical compositions together with the spatial distribution of the precipitates inside the crack would give an insight into the self-healing mechanism;
- The density and the pore structure of the binder matrix, were hypothesized to have a significant influence on the availability of ions, e.g. calcium and silicate, inside the crack and, as a consequence, the precipitation of the self-healing products. Hence, mix compositions with varied water-to-cement ratios should be investigated. In addition, the effect of the porous network, both at micro and nano scale as well as particular types of porosity, e.g. capillary porosity, on the self-healing mechanism should be tested. Measurements of the ion concentrations inside the crack could give a deeper understanding of the process.
- Exposures containing a retarding admixture and microsilica particles significantly enhanced the self-healing efficiency, therefore more detailed studies on those exposures should be performed. Different kinds of chemical compositions and dosages of retarders could be compared. The effect of volume fractions in the exposure solution as well as microsilica grading on the self-healing efficiency should be studied. The mineralogical composition, solubility, durability and other physical properties of the calcium phosphate phase should be verified with respect to its full scale applicability. A combination of different exposures, could be tested, e.g. a retarding admixture together with microsilica particles.

7. REFERENCES

- Ahn, T., and Kishi, T. (2010). "Crack Self-Healing Behavior of Cementitious Composites Incorporating various Mineral Admixtures." *Journal of Advanced Concrete Technology*, 8(2), 171-186.
- Alghamri, R., Kanellopoulos, A., & Al-Tabbaa, A. (2016). Impregnation and encapsulation of lightweight aggregates for self-healing concrete. *Construction and Building Materials*, 124, 910-921.
- Alyousif, A., M. Lachemi, G. Yildirim, and M. Şahmaran. (2015). "Effect of self-healing on the different transport properties of cementitious composites." *J. Adv. Concr. Technol.* 13 (3): 112–123.
- Arce, G. A., Hassan, M. M., Mohammad, L. N., Rupnow, T. (2016). "Characterization of Self-Healing Processes Induced by Calcium Nitrate Microcapsules in Cement Mortar." *J. Mater. Civ. Eng.*, 29(1), 04016189.
- Bello, M. A., & Gonzalez, A. G. (1996). Determination of phosphate in cola beverages using nonsuppressed ion chromatography: an experiment introducing ion chromatography for quantitative analysis. *Journal of chemical education*, 73(12), 1174.
- Bénard, P., Coumes, C. C. D., Garrault, S., Nonat, A., & Courtois, S. (2008). Dimensional stability under wet curing of mortars containing high amounts of nitrates and phosphates. *Cement and Concrete Research*, 38(10), 1181-1189.
- Bénard, P., Garrault, S., Nonat, A., & Cau-Dit-Coumes, C. (2005). Hydration process and rheological properties of cement pastes modified by orthophosphate addition. *Journal of the European Ceramic Society*, 25(11), 1877-1883.
- Blaiszik, B. J., Kramer, S. L., Olugebefola, S. C., Moore, J. S., Sottos, N. R., & White, S. R. (2010). Self-healing polymers and composites. *Annual review of materials research*, 40, 179-211.
- British Standard BS EN 12504-4 (2004). Testing concrete. Determination of ultrasonic pulse velocity.
- Bui VK, Geiker MR, Shah SP (2003) Rheology of fiber-reinforced cementitious materials. In: Conference of High performance fiber-reinforced cement composites (HPFRCC4), Springer, Netherlands, pp 221–231 27.
- Bundur, Z. B., Amiri, A., Ersan, Y. C., Boon, N., De Belie, N. (2017). "Impact of Air Entraining Admixtures on Biogenic Calcium Carbonate Precipitation and Bacterial Viability." *Cem. Concr. Res.*, 98, 44-49.
- Bundur, Z. B., Kirisits, M. J., Ferron, R. D. (2017). "Use of Pre-Wetted Lightweight Fine Expanded Shale Aggregates as Internal Nutrient Reservoirs for Microorganisms in Bio-Mineralized Mortar." *Cement and Concrete Composites*, 84, 167-174.
- Bundur, Z., Bae, S., Kirisits, M. J., Ferron, R. D. (2017). "Biom mineralization in Self-Healing Cement-Based Materials: Investigating the Temporal Evolution of Microbial Metabolic State and Material Porosity." *J. Mater. Civ. Eng.*, 29(8), 04017079.
- Cailieux, E., & Pollet, V. (2009, June). Investigations on the development of self-healing properties in protective coatings for concrete and repair mortars. In *Proceedings of the 2nd International Conference on Self-Healing Materials*, Chicago, IL, USA (Vol. 28).
- Choi, H., Choi, H., Inoue, M., & Sengoku, R. (2017). Control of the polymorphism of calcium carbonate produced by self-healing in the cracked part of cementitious materials. *Applied Sciences*, 7(6), 546.
- Choi, H., Inoue, M., Kwon, S., Choi, H., & Lim, M. (2016). Effective crack control of concrete by self-healing of cementitious composites using synthetic fiber. *Materials*, 9(4), 248.
- Choi, J. W., Lee, M. J., Oh, S. H., & Kim, K. M. (2019). Changes in the physical properties and color stability of aesthetic restorative materials caused by various beverages. *Dental materials journal*, 38(1), 33-40.
- Collepardi, M. (2003). A state-of-the-art review on delayed ettringite attack on concrete. *Cement and Concrete Composites*, 25(4-5), 401-407.
- Cuenca, E., & Ferrara, L. (2017). Self-healing capacity of fiber reinforced cementitious composites. State of the art and perspectives. *KSCE Journal of Civil Engineering*, 1-13.

Da Silva, F. B., De Belie, N., Boon, N., & Verstraete, W. (2015). Production of non-axenic ureolytic spores for self-healing concrete applications. *Construction and Building Materials*, 93, 1034-1041.

Danner, T., Hjorth Jakobsen, U., & Geiker, M. R. (2019). Mineralogical sequence of self-healing products in cracked marine concrete. *Minerals*, 9(5), 284.

Darquennes, A., K. Olivier, F. Benboudjema, and R. Gagné. 2016. "Selfhealing at early-age, a way to improve the chloride resistance of blast-furnace slag cementitious materials." *Constr. Build. Mater.* 113: 1017–1028.

De Koster, S., Mors, R., Nugteren, H., Jonkers, H., Meesters, G., Van Ommen, J. (2015). "Geopolymer Coating of Bacteria-Containing Granules for use in Self-Healing Concrete." *Procedia Engineering*, 102, 475-484.

De Muynck, W., Cox, K., De Belie, N., & Verstraete, W. (2008). Bacterial carbonate precipitation as an alternative surface treatment for concrete. *Construction and Building Materials*, 22(5), 875-885.

De Rooij, M., Van Tittelboom, K., De Belie, N., & Schlangen, E. (Eds.). (2013). Self-healing phenomena in cement-Based materials: state-of-the-art report of RILEM technical committee 221-SHC: self-Healing phenomena in cement-Based materials (Vol. 11). Springer Science & Business Media.

Divet, L., & Randriambololona, R. (1998). Delayed ettringite formation: The effect of temperature and basicity on the interaction of sulphate and CSH phase. *Cement and Concrete Research*, 28(3), 357-363.

Dong, B., Fang, G., Wang, Y., Liu, Y., Hong, S., Zhang, J., Lin, S., Xing, F. (2017a). "Performance Recovery Concerning the Permeability of Concrete by Means of a Microcapsule Based Self-Healing System." *Cement and Concrete Composites*, 78, 84-96.

Dong, B., Wang, Y., Fang, G., Han, N., Xing, F., & Lu, Y. (2015). Smart releasing behavior of a chemical self-healing microcapsule in the stimulated concrete pore solution. *Cement and Concrete Composites*, 56, 46-50.

Dry, C. M. (2000). Three designs for the internal release of sealants, adhesives, and waterproofing chemicals into concrete to reduce permeability. *Cement and Concrete Research*, 30(12), 1969-1977.

Dry, C., & McMillan, W. (1996). Three-part methylmethacrylate adhesive system as an internal delivery system for smart responsive concrete. *Smart Materials and Structures*, 5(3), 297.

Edvardsen, C. (1999). Water permeability and autogenous healing of cracks in concrete. *ACI Materials Journal-American Concrete Institute*, 96(4), 448-454.

Elkhadiri, I., Palacios, M., & Puertas, F. (2009). Effect of curing temperature on cement hydration. *Ceram Silik*, 53(2), 65-75.

Escalante-Garcia, J. I., & Sharp, J. H. (1998). Effect of temperature on the hydration of the main clinker phases in portland cements: Part I, neat cements. *Cement and Concrete Research*, 28(9), 1245-1257.

Ferrara, L., Krelani, V., & Carsana, M. (2014). A "fracture testing" based approach to assess crack healing of concrete with and without crystalline admixtures. *Construction and Building Materials*, 68, 535-551.

Ferrara, L., Krelani, V., Moretti, F. (2016a). "On the use of Crystalline Admixtures in Cement Based Construction Materials: From Porosity Reducers to Promoters of Self Healing." *Smart Mater. Struct.*, 25(8), 084002.

Ferrara, L., Krelani, V., Moretti, F. (2016b). "Autogenous Healing on the Recovery of Mechanical Performance of High Performance Fibre Reinforced Cementitious Composites (HPFRCCs): Part 2– Correlation between Healing of Mechanical Performance and Crack Sealing." *Cement and Concrete Composites*, 73, 299-315.

Ferrara, L., Krelani, V., Moretti, F., Flores, M. R., Ros, P. S. (2017). "Effects of Autogenous Healing on the Recovery of Mechanical Performance of High Performance Fibre Reinforced Cementitious Composites (HPFRCCs): Part 1." *Cement and Concrete Composites*, 83, 76-100.

Gagné, R., & Argouges, M. (2012). A study of the natural self-healing of mortars using air-flow measurements. *Materials and structures*, 45(11), 1625-1638.

Gallucci, E., Mathur, P., & Scrivener, K. (2010). Microstructural development of early age hydration shells around cement grains. *Cement and Concrete Research*, 40(1), 4-13.

- Gartner, E. (2004). Industrially interesting approaches to “low-CO₂” cements. *Cement and Concrete research*, 34(9), 1489-1498.
- Giannaros, P., Kanellopoulos, A., Al-Tabbaa, A. (2016). "Sealing of Cracks in Cement using Microencapsulated Sodium Silicate." *Smart Mater. Struct.*, 25(8), 084005.
- Gilford III, J., Hassan, M.M., Rupnow, T., Barbato, M., Okeil, A. and Asadi, S., 2013. Dicyclopentadiene and sodium silicate microencapsulation for self-healing of concrete. *Journal of Materials in Civil Engineering*, 26(5), 886-896.
- Gollapudi, U. K., Knutson, C. L., Bang, S. S., & Islam, M. R. (1995). A new method for controlling leaching through permeable channels. *Chemosphere*, 30(4), 695-705.
- Gonzalez, M. A., & Irassar, E. F. (1997). Ettringite formation in low C3A Portland cement exposed to sodium sulfate solution. *Cement and Concrete Research*, 27(7), 1061-1071.
- Granger, S., Loukili, A., Pijaudier-Cabot, G., Chanvillard, G. (2007). "Experimental Characterization of the Self-Healing of Cracks in an Ultra High Performance Cementitious Material: Mechanical Tests and Acoustic Emission Analysis." *Cem. Concr. Res.*, 37(4), 519-527.
- Gray, R. J. (1984). Autogenous healing of fibre/matrix interfacial bond in fibre-reinforced mortar. *Cement and Concrete Research*, 14(3), 315-317.
- Gruyaert, E., Debbaut, B., Kaasgaard, M., Erndahl Sorensen, H., Pelto, J., Branco, V., ... & De Belie, N. (2017). Evaluation of the performance of self-healing concrete at small and large scale under laboratory conditions. In 14th International Conference on Durability of Building Materials and Components (XIV DBMC) (pp. 1-12). RILEM Publications.
- Gruyaert, E., K. Van Tittelboom, H. Rahier, and N. D. Belie. 2015. "Activation of pozzolanic and latent-hydraulic reactions by alkalis in order to repair concrete cracks." *J. Mater. Civ. Eng.* 27 (7): 04014208.
- Guan, W., Ji, F., Chen, Q., Yan, P., & Zhang, Q. (2013). Preparation and phosphorus recovery performance of porous calcium–silicate–hydrate. *Ceramics International*, 39(2), 1385-1391.
- Han, N. X., & King, F. (2016). A Comprehensive Review of the Study and Development of Microcapsule Based Self-Resilience Systems for Concrete Structures at Shenzhen University. *Materials*, 10(1), 2.
- Hearn, N. (1998). Self-sealing, autogenous healing and continued hydration: What is the difference?. *Materials and Structures*, 31(8), 563-567.
- Hearn, N., & Morley, C. T. (1997). Self-sealing property of concrete – experimental evidence. *Materials and structures*, 30(7), 404-411.
- Herbert, E. N., and Li, V. C. (2013). "Self-Healing of Microcracks in Engineered Cementitious Composites (ECC) Under a Natural Environment." *Materials*, 6(7), 2831-2845.
- Herbert, E., and Li, V. (2012). "Self-healing of engineered cementitious composites in the natural environment." *Proc., High Performance Fiber Reinforced Cement Composites*, Springer, , 155-162.
- Hilloulin, B., Van Tittelboom, K., Gruyaert, E., De Belie, N., & Loukili, A. (2015). Design of polymeric capsules for self-healing concrete. *Cement and Concrete Composites*, 55, 298-307.
- Homma, D., Mihashi, H., Nishiwaki, T. (2009). "Self-Healing Capability of Fibre Reinforced Cementitious Composites." *Journal of Advanced Concrete Technology*, 7(2), 217-228.
- Huang, H., & Ye, G. (2015). Self-healing of cracks in cement paste affected by additional Ca²⁺ ions in the healing agent. *Journal of Intelligent Material Systems and Structures*, 26(3), 309-320.
- Huang, H., G. Ye, C. Qian, and E. Schlangen. 2016b. "Self-healing in cementitious materials: Materials, methods and service conditions." *Mater. Des.* 92: 499–511.
- Huang, H., Ye, G., & Damidot, D. (2013). Characterization and quantification of self-healing behaviors of microcracks due to further hydration in cement paste. *Cement and Concrete Research*, 52, 71-81.
- Huang, H., Ye, G., & Damidot, D. (2014). Effect of blast furnace slag on self-healing of microcracks in cementitious materials. *Cement and Concrete Research*, 60, 68-82.
- Huang, H.; Ye, G.; Damidot, D. Characterization and quantification of self-healing behaviors of microcracks due to further hydration in cement paste. *Cem. Concr. Res.* 2013, 52, 71-81.

- Hung, C., and Su, Y. (2016). "Medium-Term Self-Healing Evaluation of Engineered Cementitious Composites with Varying Amounts of Fly Ash and Exposure Durations." *Constr. Build. Mater.*, 118, 194-203.
- Hung, C., Su, Y., Su, Y. (2018). "Mechanical Properties and Self-Healing Evaluation of Strain-Hardening Cementitious Composites with High Volumes of Hybrid Pozzolan Materials." *Composites Part B: Engineering*, 133, 15-25.
- Jacobsen, S., Marchand, J., & Hornain, H. (1995). SEM observations of the microstructure of frost deteriorated and self-healed concretes. *Cement and Concrete Research*, 25(8), 1781-1790.
- Jiang, Z., Li, W., & Yuan, Z. (2015). Influence of mineral additives and environmental conditions on the self-healing capabilities of cementitious materials. *Cement and Concrete Composites*, 57, 116-127.
- Jiang, Z., Li, W., Yuan, Z., & Yang, Z. (2014). Self-healing of cracks in concrete with various crystalline mineral additives in underground environment. *Journal of Wuhan University of Technology-Mater.Sci.Ed.*, 29(5), 938-944.
- Jo, B. W., Sikandar, M. A., Balochb, Z., Khan, R. A. (2015). "Effect of Incorporation of Self Healing Admixture (SHA) on Physical and Mechanical Properties of Mortars." *Journal of Ceramic Processing Research*, 16, 138-143.
- Jonkers, H. M. (2007). Self-healing concrete: a biological approach. In *Self-Healing Materials* (pp. 195-204). Springer Netherlands.
- Jonkers, H. M. (2011). Bacteria-based self-healing concrete. *Heron*, 56(1/2), 1-12.
- Jonkers, H. M., & Schlangen, E. (2007). Self-healing of cracked concrete: a bacterial approach. *Proceedings of FRACOS6: fracture mechanics of concrete and concrete structures*. Catania, Italy, 1821-1826.
- Joseph, C., Jefferson, A. D., & Cantoni, M. B. (2007, April). Issues relating to the autonomic healing of cementitious materials. In *Proceedings of the 1st International Conference on Self-Healing Materials*, Noordwijk, the Netherlands. CD-ROM.
- Kalina, L., Bílek, V., Novotný, R., Mončeková, M., Másilko, J., & Koplík, J. (2016). Effect of Na₃PO₄ on the hydration process of alkali-activated blast furnace slag. *Materials*, 9(5), 395.
- Kan, L. L., Shi, H. S., Sakulich, A. R., & Li, V. C. (2010). Self-Healing Characterization of Engineered Cementitious Composite Materials. *ACI Materials Journal*, 107(6).
- Kan, L., & Shi, H. (2012). Investigation of self-healing behavior of engineered cementitious composites (ECC) materials. *Construction and Building Materials*, 29, 348-356.
- Kan, L., Shi, H., Sakulich, A. R., Li, V. C. (2010). "Self-Healing Characterization of Engineered Cementitious Composite Materials." *ACI Mater. J.*, 107(6).
- Kanellopoulos, A., Giannaros, P., & Al-Tabbaa, A. (2016). The effect of varying volume fraction of microcapsules on fresh, mechanical and self-healing properties of mortars. *Construction and Building Materials*, 122, 577-593.
- Kanellopoulos, A., Giannaros, P., Palmer, D., Kerr, A., Al-Tabbaa, A. (2017). "Polymeric Microcapsules with Switchable Mechanical Properties for Self-Healing Concrete: Synthesis, Characterisation and Proof of Concept." *Smart Mater. Struct.*, 26(4), 045025.
- Kanellopoulos, A., Qureshi, T. S., & Al-Tabbaa, A. (2015). Glass encapsulated minerals for self-healing in cement based composites. *Construction and Building Materials*, 98, 780-791.
- Karageorgiou, K., Paschalis, M., & Anastassakis, G. N. (2007). Removal of phosphate species from solution by adsorption onto calcite used as natural adsorbent. *Journal of Hazardous Materials*, 139(3), 447-452.
- Keskin, S. B., Keskin, O. K., Anil, O., Şahmaran, M., Alyousif, A., Lachemi, M., ... & Ashour, A. F. (2016). Self-healing capability of large-scale engineered cementitious composites beams. *Composites Part B: Engineering*, 101, 1-13.
- Khaliq, W., & Ehsan, M. B. (2016). Crack healing in concrete using various bio influenced self-healing techniques. *Construction and Building Materials*, 102, 349-357.

- Kim, H. G., A. Qudoos, and J. S. Ryou. 2018. "Self-healing performance of GGBFS based cementitious mortar with granulated activators exposed to a seawater environment." *Constr. Build. Mater.* 188: 569–582.
- Kim, J. D., Kang, H. S., Ahn, T. (2014). "Mechanical Characterization of High-Performance Steel-Fiber Reinforced Cement Composites with Self-Healing Effect." *Materials*, 7(1).
- Kirov, G. K., Vesselinov, I., & Cherneva, Z. (1972). Conditions of formation of calcite crystals of tabular and acute rhombohedral habits. *Kristall Und Technik*, 7(5), 497-509.
- Kjellsen, K. O., Detwiler, R. J., & Gjrv, O. E. (1991). Development of microstructures in plain cement pastes hydrated at different temperatures. *Cement and Concrete Research*, 21(1), 179-189.
- Kuder KG, Ozyurt N, Mu EB, Shah SP (2007) Rheology of fiber-reinforced cementitious composites. *Cem Concr Res* 37:191–199
- Kwon, S. J., & Wang, X. Y. (2019). Optimization of the Mixture Design of Low-CO₂ High-Strength Concrete Containing Silica Fume. *Advances in Civil Engineering*, 2019.
- Lee, H., Wong, H., Buenfeld, N. (2016). "Self-Sealing of Cracks in Concrete using Superabsorbent Polymers." *Cem. Concr. Res.*, 79, 194-208.
- Li, M., & Li, V. C. (2013). Rheology, fiber dispersion, and robust properties of engineered cementitious composites. *Materials and structures*, 46(3), 405-420.
- Li, V. C. (2012). Tailoring ECC for special attributes: A review. *International Journal of Concrete Structures and Materials*, 6(3), 135-144.
- Li, V. C., Wang, S., & Wu, C. (2001). Tensile strain-hardening behavior of polyvinyl alcohol engineered cementitious composite (PVA-ECC). *ACI Materials Journal-American Concrete Institute*, 98(6), 483-492.
- Li, V., C. (1998). (1998). Engineered Cementitious Composites (ECC) – tailored composites through micromechanical modelling. *Micromechanical*, T. C. T.
- Lin, R. S., Wang, X. Y., & Zhang, G. Y. (2018). Effects of quartz powder on the microstructure and key properties of cement paste. *Sustainability*, 10(10), 3369.
- Liu, H., Zhang, Q., Gu, C., Su, H., Li, V. (2017). "Self-Healing of Microcracks in Engineered Cementitious Composites Under Sulfate and Chloride Environment." *Constr. Build. Mater.*, 153, 948-956.
- Liu, Z., Jiao, W., Sha, A., Gao, J., Han, Z., & Xu, W. (2017). Portland cement hydration behavior at low temperatures: Views from calculation and experimental study. *Advances in Materials Science and Engineering*, 2017
- Luo, M., and Qian, C. (2016b). "Influences of Bacteria-Based Self-Healing Agents on Cementitious Materials Hydration Kinetics and Compressive Strength." *Constr. Build. Mater.*, 121, 659-663.
- Luo, M., and Qian, C. X. (2016a). "Performance of Two Bacteria-Based Additives used for Self-Healing Concrete." *J. Mater. Civ. Eng.*, 28(12), 04016151.
- Luo, M., Qian, C. X., & Li, R. Y. (2015). Factors affecting crack repairing capacity of bacteria-based self-healing concrete. *Construction and Building materials*, 87, 1-7.
- Lv, L., Schlangen, E., Yang, Z., & Xing, F. (2016). Micromechanical Properties of a New Polymeric Microcapsule for Self-Healing Cementitious Materials. *Materials*, 9(12), 1025.
- Lv, L., Yang, Z., Chen, G., Zhu, G., Han, N., Schlangen, E., Xing, F. (2016). "Synthesis and Characterization of a New Polymeric Microcapsule and Feasibility Investigation in Self-Healing Cementitious Materials." *Constr. Build. Mater.*, 105, 487-495.
- Ma, H., Qian, S., & Zhang, Z. (2014). Effect of self-healing on water permeability and mechanical property of medium-early-strength engineered cementitious composites. *Construction and Building Materials*, 68, 92-101.
- Maeda, H., Yokota, S., & Kasuga, T. (2018). Structural changes in calcium silicate hydrate gel and resulting improvement in phosphate species removal properties after mechanochemical treatment. *Royal Society Open Science*, 5(12), 181403.
- Matschei, T., & Glasser, F. P. (2010). Temperature dependence, 0 to 40 C, of the mineralogy of portland cement paste in the presence of calcium carbonate. *Cement and Concrete Research*, 40(5), 763-777.

- Mauludin, L. M., and C. Oucif. 2018a. "Interaction between matrix crack and circular capsule under uniaxial tension in encapsulation-based selfhealing concrete." *Underground Space* 3 (3): 181–189.
- Mauludin, L. M., and C. Oucif. 2018b. "The effects of interfacial strength on fractured microcapsule." *Front. Struct. Civ. Eng.* 13 (2): 1–11.
- Mehdipour, I., R. Zoughi, and K. H. Khayat. 2018. "Feasibility of using near-field microwave reflectometry for monitoring autogenous crack healing in cementitious materials." *Cem. Concr. Compos.* 85: 161–173.
- Mekmene, O., Quillard, S., Rouillon, T., Bouler, J., Piot, M., & Gaucheron, F. (2009). Effects of pH and ca/P molar ratio on the quantity and crystalline structure of calcium phosphates obtained from aqueous solutions. *Dairy Science & Technology*, 89(3-4), 301-316.
- Meyer, J. L., & Weatherall, C. C. (1982). Amorphous to crystalline calcium phosphate phase transformation at elevated pH. *Journal of Colloid and Interface Science*, 89(1), 257-267.
- Mignon, A., Snoeck, D., Schaubroeck, D., Luickx, N., Dubruel, P., Van Vlierberghe, S., De Belie, N. (2015). "pH-Responsive Superabsorbent Polymers: A Pathway to Self-Healing of Mortar." *React Funct Polym*, 93, 68-76.
- Mignon, A., Vermeulen, J., Snoeck, D., Dubruel, P., Van Vlierberghe, S., De Belie, N. (2017). "Mechanical and Self-Healing Properties of Cementitious Materials with pH-Responsive Semi-Synthetic Superabsorbent Polymers." *Mater. Struct.*, 50(6), 238.
- Mors, R. M., & Jonkers, H. M. (2017). Feasibility of lactate derivative based agent as additive for concrete for regain of crack water tightness by bacterial metabolism. *Industrial crops and products*, 106, 97-104.
- Mostavi, E., Asadi, S., Hassan, M. M., & Alansari, M. (2015). Evaluation of self-healing mechanisms in concrete with double-walled sodium silicate microcapsules. *Journal of Materials in Civil Engineering*, 27(12), 04015035.
- Na, S. H., Hama, Y., Taniguchi, M., Katsura, O., Sagawa, T., Zakaria, M. (2012). "Experimental Investigation on Reaction Rate and Self-Healing Ability in Fly Ash Blended Cement Mixtures." *Journal of Advanced Concrete Technology*, 10(7), 240-253.
- Naus, D. J., Mattus, C. H., & Dole, L. R. (2007). No title. *Assessment of Potential Phosphate Ion-Cementitious Materials Interactions*,
- Nishiwaki, T., Koda, M., Yamada, M., Mihashi, H., Kikuta, T. (2012). "Experimental Study on Self-Healing Capability of FRCC using Different Types of Synthetic Fibers." *Journal of Advanced Concrete Technology*, 10(6), 195-206.
- Nishiwaki, T., Kwon, S., Homma, D., Yamada, M., Mihashi, H. (2014). "Self-Healing Capability of Fiber-Reinforced Cementitious Composites for Recovery of Watertightness and Mechanical Properties." *Materials*, 7(3), 2141-2154.
- Nishiwaki, T., Sasaki, H., & Sukmin, K. (2015). Experimental study on self-healing effect of FRCC with PVA fibers and additives. *J. Ceram. Process. Res*, 16(1), 89-94.
- Olivier, K., A. Darquennes, F. Benboudjema, and R. Gagné. 2016. "Early age self-healing of cementitious materials containing ground granulated blast-furnace slag under water curing." *J. Adv. Concr. Technol.* 14 (11): 717–727.
- Orial, G., Vieweger, T., & Loubiere, J. F. (2002). *Les mortiers biologiques: une solution pour la conservation de la sculpture monumentale en pierre*. Art Biology and Conservation, Metropolitan Museum New York.
- Paine, K. (2016) Bacteria-based self-healing concrete: Effects of environment, exposure and crack size. In: *RILEM Conference on Microorganisms-Cementitious Materials Interactions*, 2016-06-23.
- Palin, D., Wiktor, V., & Jonkers, H. M. (2015). Autogenous healing of marine exposed concrete: Characterization and quantification through visual crack closure. *Cement and Concrete Research*, 73, 17-24.
- Palin, D., Wiktor, V., & Jonkers, H. M. (2016). A bacteria-based bead for possible self-healing marine concrete applications. *Smart Materials and Structures*, 25(8), 084008.
- Palin, D., Wiktor, V., Jonkers, H. M. (2017). "A Bacteria-Based Self-Healing Cementitious Composite for Application in Low-Temperature Marine Environments." *Biomimetics*, 2(3), 13.

- Pei, B., Wang, W., Dunne, N., & Li, X. (2019). Applications of Carbon Nanotubes in Bone Tissue Regeneration and Engineering: Superiority, Concerns, Current Advancements, and Prospects. *Nanomaterials*, 9(10), 1501.
- Perez, G., Erkizia, E., Gaitero, J. J., Kaltzakorta, I., Jimenez, I., & Guerrero, A. (2015). Synthesis and characterization of epoxy encapsulating silica microcapsules and amine functionalized silica nanoparticles for development of an innovative self-healing concrete. *Materials Chemistry and Physics*, 165, 39-48.
- Qian, S. Z., Zhou, J., & Schlangen, E. (2010). Influence of curing condition and precracking time on the self-healing behavior of engineered cementitious composites. *Cement and Concrete Composites*, 32(9), 686-693.
- Qian, S., Zhou, J., De Rooij, M. R., Schlangen, E., Ye, G., & Van Breugel, K. (2009). Self-healing behavior of strain hardening cementitious composites incorporating local waste materials. *Cement and Concrete Composites*, 31(9), 613-621.
- Qiu, J., Tan, H. S., & Yang, E. (2016). Coupled effects of crack width, slag content, and conditioning alkalinity on autogenous healing of engineered cementitious composites. *Cement and Concrete Composites*, 73, 203-212.
- Qureshi, T. S., Kanellopoulos, A., & Al-Tabbaa, A. (2016). Encapsulation of expansive powder minerals within a concentric glass capsule system for self-healing concrete. *Construction and Building Materials*, 121, 629-643.
- Qureshi, T., and Al-Tabbaa, A. (2016). "Self-Healing of Drying Shrinkage Cracks in Cement-Based Materials Incorporating Reactive MgO." *Smart Mater. Struct.*, 25(8), 084004.
- Rajczakowska, M., Habermehl-Cwirzen, K., Hedlund, H., & Cwirzen, A. (2019a). Autogenous Self-Healing: A Better Solution for Concrete. *Journal of Materials in Civil Engineering*, 31(9), 03119001.
- Rajczakowska, M., Habermehl-Cwirzen, K., Hedlund, H., & Cwirzen, A. (2019c). The Effect of Exposure on the Autogenous Self-Healing of Ordinary Portland Cement Mortars. Submitted.
- Rajczakowska, M., Nilsson, L., Habermehl-Cwirzen, K., Hedlund, H., & Cwirzen, A. (2019b). Does a High Amount of Unhydrated Portland Cement Ensure an Effective Autogenous Self-Healing of Mortar?. *Materials*, 12(20), 3298.
- Ramakrishnan, V., Panchalan, R. K., Bang, S. S., & Khokhlova, A. (2013, May). 4843-Improvement of concrete durability by bacterial mineral precipitation. In ICF11, Italy 2005.
- Randl, N., Steiner, T., Ofner, S., Baumgartner, E., & Mészöly, T. (2014). Development of UHPC mixtures from an ecological point of view. *Construction and Building Materials*, 67, 373-378.
- Reinhardt, H. W., & Jooss, M. (2003). Permeability and self-healing of cracked concrete as a function of temperature and crack width. *Cement and Concrete Research*, 33(7), 981-985.
- Roig-Flores, M., Moscato, S., Serna, P., & Ferrara, L. (2015). Self-healing capability of concrete with crystalline admixtures in different environments. *Construction and Building Materials*, 86, 1-11.
- Roig-Flores, M., Pirritano, F., Serna, P., & Ferrara, L. (2016). Effect of crystalline admixtures on the self-healing capability of early-age concrete studied by means of permeability and crack closing tests. *Construction and Building Materials*, 114, 447-457.
- Ryou, J., Ha, S., Ahn, T., Bang, S., Shim, K. B. (2015). "Effects of Air-Cooled Blast Furnace Slag Fine Aggregate in Mortar with Self-Healing Capability Exposed to Sulfuric Acid Attack." *J.Ceram.Process.Res*, 16, 45-49.
- Şahmaran, M., Christianto, H. A., & Yaman, İ. Ö. (2006). The effect of chemical admixtures and mineral additives on the properties of self-compacting mortars. *Cement and concrete composites*, 28(5), 432-440.
- Şahmaran, M., Keskin, S. B., Ozerkan, G., Yaman, I. O. (2008). "Self-Healing of Mechanically-Loaded Self Consolidating Concretes with High Volumes of Fly Ash." *Cement and Concrete Composites*, 30(10), 872-879.
- Sahmaran, M., Yildirim, G., & Erdem, T. K. (2013). Self-healing capability of cementitious composites incorporating different supplementary cementitious materials. *Cement and Concrete Composites*, 35(1), 89-101.

Şahmaran, M., Yildirim, G., Noori, R., Ozbay, E., Lachemi, M. (2015). "Repeatability and Pervasiveness of Self-Healing in Engineered Cementitious Composites." *Materials Journal*, 112(4), 513-522.

Sanjuan, M. A., Andrade, C., & Bentur, A. (1997). Effect of crack control in mortars containing polypropylene fibers on the corrosion of steel in a cementitious matrix. *ACI Materials Journal*, 94(2), 134-141.

Schlangen, E., Ter Heide, N., Van Breugel, K. (2006). "Crack Healing of Early Age Cracks in Concrete." *Measuring, Monitoring and Modeling Concrete Properties*, Springer, 273-284.

Schneider, C. A., Rasband, W. S., & Eliceiri, K. W. (2012). NIH image to ImageJ: 25 years of image analysis. *Nature Methods*, 9(7), 671.

Seifan, M., Samani, A. K., & Berenjian, A. (2017). New insights into the role of pH and aeration in the bacterial production of calcium carbonate (CaCO₃). *Applied Microbiology and Biotechnology*, 1-12.

Sherir, M. A., Hossain, K. M., Lachemi, M. (2016). "Self-Healing and Expansion Characteristics of Cementitious Composites with High Volume Fly Ash and MgO-Type Expansive Agent." *Constr. Build. Mater.*, 127, 80-92.

Sherir, M. A., Hossain, K. M., Lachemi, M. (2017a). "The Influence of MgO-Type Expansive Agent Incorporated in Self-Healing System of Engineered Cementitious Composites." *Constr. Build. Mater.*, 149, 164-185.

Sherir, M. A., Hossain, K. M., Lachemi, M. (2017b). "Development and Recovery of Mechanical Properties of Self-Healing Cementitious Composites with MgO Expansive Agent." *Constr. Build. Mater.*, 148, 789-810.

Siad, H., Alyousif, A., Keskin, O. K., Keskin, S. B., Lachemi, M., Şahmaran, M., Hossain, K. M. A. (2015). "Influence of Limestone Powder on Mechanical, Physical and Self-Healing Behavior of Engineered Cementitious Composites." *Constr. Build. Mater.*, 99, 1-10.

Siad, H., Lachemi, M., Şahmaran, M., Hossain, K. M. A. (2017). "Mechanical, Physical, and Self-Healing Behaviors of Engineered Cementitious Composites with Glass Powder." *J. Mater. Civ. Eng.*, 29(6), 04017016.

Sisomphon, K., Copuroglu, O., & Fraaij, A. (2011). Application of encapsulated lightweight aggregate impregnated with sodium monofluorophosphate as a self-healing agent in blast furnace slag mortar. *Heron*, 56(1/2), 13-32.

Sisomphon, K., Copuroglu, O., & Koenders, E. A. B. (2012). Self-healing of surface cracks in mortars with expansive additive and crystalline additive. *Cement and Concrete Composites*, 34(4), 566-574.

Sisomphon, K., Copuroglu, O., Koenders, E. (2013). "Effect of Exposure Conditions on Self Healing Behavior of Strain Hardening Cementitious Composites Incorporating various Cementitious Materials." *Constr. Build. Mater.*, 42, 217-224.

Snoeck, D. Self-healing and microstructure of cementitious materials with microfibres and superabsorbent polymers. Doctoral dissertation. Ghent University. 2015.

Snoeck, D., and De Belie, N. (2012). "Mechanical and Self-Healing Properties of Cementitious Composites Reinforced with Flax and Cottonised Flax, and Compared with Polyvinyl Alcohol Fibres." *Biosystems Engineering*, 111(4), 325-335.

Snoeck, D., and De Belie, N. (2015). "Repeated Autogenous Healing in Strain-Hardening Cementitious Composites by using Superabsorbent Polymers." *J. Mater. Civ. Eng.*, 28(1), 04015086.

Snoeck, D., Van Tittelboom, K., Steuperaert, S., Dubruel, P., De Belie, N. (2014). "Self-Healing Cementitious Materials by the Combination of Microfibres and Superabsorbent Polymers." *J Intel Mater Syst Struct*, 25(1), 13-24.

Suleiman, A. R., & Nehdi, M. L. (2018). Effect of environmental exposure on autogenous self-healing of cracked cement-based materials. *Cement and Concrete Research*, 111, 197-208.

Suryanto, B., Buckman, J., Thompson, P., Bolbol, M., McCarter, W. (2016). "Monitoring Micro-Crack Healing in an Engineered Cementitious Composite using the Environmental Scanning Electron Microscope." *Mater Charact*, 119, 175-185.

- Swamy RN, Mangat PS (1974) Influence of fiber-aggregate interaction on some properties of steel fiber reinforced concrete. *Mater Struct* 7(41):307–314
- Tan, N. P. B., Keung, L. H., Choi, W. H., Lam, W. C., & Leung, H. N. (2016). Silica-based self-healing microcapsules for self-repair in concrete. *Journal of Applied Polymer Science*, 133(12).
- Termkhajornkit, P., Nawa, T., Yamashiro, Y., Saito, T. (2009). "Self-Healing Ability of Fly Ash–cement Systems." *Cement and Concrete Composites*, 31(3), 195-203.
- Thakur, V. K., & Kessler, M. R. (2015). Self-healing polymer nanocomposite materials: A review. *Polymer*, 69, 369-383.
- Tole, I., Habermehl-Cwirzen, K., Rajczakowska, M., & Cwirzen, A. (2018). Activation of a raw clay by Mechanochemical process—effects of various parameters on the process efficiency and cementitious properties. *Materials*, 11(10), 1860.
- Van Kemenade, M., & De Bruyn, P. L. (1987). A kinetic study of precipitation from supersaturated calcium phosphate solutions. *Journal of Colloid and Interface Science*, 118(2), 564-585.
- Van Tittelboom, K., De Belie, N., De Muynck, W., & Verstraete, W. (2010). Use of bacteria to repair cracks in concrete. *Cement and Concrete Research*, 40(1), 157-166.
- Van Tittelboom, K., De Belie, N., Van Loo, D., & Jacobs, P. (2011). Self-healing efficiency of cementitious materials containing tubular capsules filled with healing agent. *Cement and Concrete Composites*, 33(4), 497-505.
- Van Tittelboom, K., Gruyaert, E., Rahier, H., De Belie, N. (2012). "Influence of Mix Composition on the Extent of Autogenous Crack Healing by Continued Hydration Or Calcium Carbonate Formation." *Constr. Build. Mater.*, 37, 349-359.
- Van Tittelboom, K., Tsangouri, E., Van Hemelrijck, D., De Belie, N. (2015). "The Efficiency of Self-Healing Concrete using Alternative Manufacturing Procedures and More Realistic Crack Patterns." *Cement and Concrete Composites*, 57, 142-152.
- Van Tittelboom, K., Wang, J., Araújo, M., Snoeck, D., Gruyaert, E., Debbaut, B., ... & De Belie, N. (2016). Comparison of different approaches for self-healing concrete in a large-scale lab test. *Construction and building materials*, 107, 125-137.
- Wang, C., Yang, C., Liu, F., Wan, C., & Pu, X. (2012). Preparation of ultra-high performance concrete with common technology and materials. *Cement and concrete composites*, 34(4), 538-544.
- Wang, D., Shi, C., Wu, Z., Xiao, J., Huang, Z., & Fang, Z. (2015). A review on ultra high performance concrete: Part II. Hydration, microstructure and properties. *Construction and Building Materials*, 96, 368-377.
- Wang, J. Y., De Belie, N., & Verstraete, W. (2012). Diatomaceous earth as a protective vehicle for bacteria applied for self-healing concrete. *Journal of industrial microbiology & biotechnology*, 39(4), 567-577.
- Wang, J. Y., Snoeck, D., Van Vlierberghe, S., Verstraete, W., & De Belie, N. (2014). Application of hydrogel encapsulated carbonate precipitating bacteria for approaching a realistic self-healing in concrete. *Construction and building materials*, 68, 110-119.
- Wang, J. Y., Soens, H., Verstraete, W., De Belie, N. (2014). "Self-Healing Concrete by use of Microencapsulated Bacterial Spores." *Cement and Concrete Research*, 56, 139-152.
- Wang, J., Van Tittelboom, K., De Belie, N., & Verstraete, W. (2011). Use of silica gel or polyurethane immobilized bacteria for self-healing concrete. *Construction and building materials*, 26(1), 532-540.
- Wang, X., Sun, P., Han, N., & Xing, F. (2017). Experimental Study on Mechanical Properties and Porosity of Organic Microcapsules Based Self-Healing Cementitious Composite. *Materials*, 10(1), 20.
- White, S. R., Sottos, N. R., Geubelle, P. H., Moore, J. S., Kessler, M., Sriram, S. R., ... & Viswanathan, S. (2001). Autonomic healing of polymer composites. *Nature*, 409(6822), 794.
- Williams, S. L., Kirisits, M. J., & Ferron, R. D. (2016). Influence of concrete-related environmental stressors on biomineralizing bacteria used in self-healing concrete. *Construction and Building Materials*.

- Wu, M., Johannesson, B., & Geiker, M. (2012). A review: Self-healing in cementitious materials and engineered cementitious composite as a self-healing material. *Construction and Building Materials*, 28(1), 571-583.
- Xiong, W., Tang, J., Zhu, G., Han, N., Schlangen, E., Dong, B., ... & Xing, F. (2015). A novel capsule-based self-recovery system with a chloride ion trigger. *Scientific reports*, 5, 10866.
- Xu, J., and Yao, W. (2014). "Multiscale Mechanical Quantification of Self-Healing Concrete Incorporating Non-Ureolytic Bacteria-Based Healing Agent." *Cem. Concr. Res.*, 64, 1-10.
- Xu, L., Wang, P., & Zhang, G. (2012). Formation of ettringite in portland cement/calcium aluminate cement/calcium sulfate ternary system hydrates at lower temperatures. *Construction and Building Materials*, 31, 347-352.
- Yang, E. H., Yang, Y., & Li, V. C. (2007). Use of high volumes of fly ash to improve ECC mechanical properties and material greenness. *ACI materials journal*, 104(6), 620.
- Yang, K. H., Jung, Y. B., Cho, M. S., & Tae, S. H. (2015). Effect of supplementary cementitious materials on reduction of CO₂ emissions from concrete. *Journal of Cleaner Production*, 103, 774-783.
- Yang, Y., Lepech, M. D., Yang, E., & Li, V. C. (2009). Autogenous healing of engineered cementitious composites under wet-dry cycles. *Cement and Concrete Research*, 39(5), 382-390.
- Yang, Y., Yang, E., & Li, V. C. (2011). Autogenous healing of engineered cementitious composites at early age. *Cement and Concrete Research*, 41(2), 176-183.
- Yang, Z., Hollar, J., He, X., & Shi, X. (2011). A self-healing cementitious composite using oil core/silica gel shell microcapsules. *Cement and Concrete Composites*, 33(4), 506-512.
- Yildirim, G., Şahmaran, M., Ahmed, H. U. (2014). "Influence of Hydrated Lime Addition on the Self-Healing Capability of High-Volume Fly Ash Incorporated Cementitious Composites." *J. Mater. Civ. Eng.*, 27(6), 04014187.
- Yu, J. H., Chen, W., Yu, M. X., Hua, Y. E. (2010). "The Microstructure of Self-Healed PVA ECC Under Wet and Dry Cycles." *Materials Research*, 13(2), 225-231.
- Yu, K., Li, L., Yu, J., Wang, Y., Ye, J., & Xu, Q. (2018). Direct tensile properties of engineered cementitious composites: A review. *Construction and Building Materials*, 165, 346-362.
- Zhang, J. L., Wang, C. G., Wang, Q. L., Feng, J. L., Pan, W., Zheng, X. C., ... & Deng, X. (2016). A binary concrete crack self-healing system containing oxygen-releasing tablet and bacteria and its Ca²⁺-precipitation performance. *Applied microbiology and biotechnology*, 100(24), 10295-10306.
- Zhang, J., Mai, B., Cai, T., Luo, J., Wu, W., Liu, B., ... & Deng, X. (2017). Optimization of a Binary Concrete Crack Self-Healing System Containing Bacteria and Oxygen. *Materials*, 10(2), 116.
- Zhang, L., Catalan, L. J., Balc, R. J., Larsen, A. C., Esmaili, H. H., & Kinrade, S. D. (2010). Effects of saccharide set retarders on the hydration of ordinary Portland cement and pure tricalcium silicate. *Journal of the American ceramic society*, 93(1), 279-287.
- Zhang, Z., and Zhang, Q. (2017). "Self-Healing Ability of Engineered Cementitious Composites (ECC) Under Different Exposure Environments." *Constr. Build. Mater.*, 156, 142-151.
- Zheng, P., & McCarthy, T. J. (2012). A surprise from 1954: siloxane equilibration is a simple, robust, and obvious polymer self-healing mechanism. *Journal of the American Chemical Society*, 134(4), 2024-2027.
- Zhu, Y., Yang, Y., & Yao, Y. (2012). Autogenous self-healing of engineered cementitious composites under freeze-thaw cycles. *Construction and Building Materials*, 34, 522-530.
- Zhu, Y., Zhang, Z. C., Yao, Y., Guan, X. M., Yang, Y. Z. (2016). "Analysis of Crack Microstructure, Self-Healing Products, and Degree of Self-Healing in Engineered Cementitious Composites." *J. Mater. Civ. Eng.*, 28(6), 04016017.
- Özbay, E., Şahmaran, M., Lachemi, M., Yücel, H. E. (2013). "Self-Healing of Microcracks in High-Volume Fly-Ash-Incorporated Engineered Cementitious Composites." *ACI Mater. J.*, 110(1).
- Özbay, E., Şahmaran, M., Yücel, H. E., Erdem, T. K., Lachemi, M., Li, V. C. (2013). "Effect of Sustained Flexural Loading on Self-Healing of Engineered Cementitious Composites." *Journal of Advanced Concrete Technology*, 11(5), 167-179.

Department of Civil, Environmental and Natural Resources Engineering

ISSN 1402-1757

ISBN 978-91-7790-490-8 (print)

ISBN 978-91-7790-491-5 (pdf)

Luleå University of Technology 2019